

**UNIVERSITY OF CRETE
CHEMISTRY DEPARTMENT
LABORATORY OF ANALYTICAL CHEMISTRY**

PhD THESIS

**DEVELOPMENT OF OPTICAL AND
ELECTROCHEMICAL BIOSENSORS
BASED ON Au MNPs AND CdSe/ZnS
QUANTUM DOTS**

RALUCA BUICULESCU

HERAKLION 2011

ΠΑΝΕΠΙΣΤΗΜΙΟ ΚΡΗΤΗΣ
ΤΜΗΜΑ ΧΗΜΕΙΑΣ
ΕΡΓΑΣΤΗΡΙΟ ΑΝΑΛΥΤΙΚΗΣ ΧΗΜΕΙΑΣ

ΔΙΔΑΚΤΟΡΙΚΗ ΔΙΑΤΡΙΒΗ

ΑΝΑΠΤΥΞΗ ΟΠΤΙΚΩΝ ΚΑΙ
ΗΛΕΚΤΡΟΧΗΜΙΚΩΝ ΒΙΟΑΙΣΘΗΤΗΡΩΝ
ΒΑΣΙΣΜΕΝΩΝ ΣΕ ΜΕΤΑΛΛΙΚΑ
ΝΑΝΟΣΩΜΑΤΙΔΙΑ Au ΚΑΙ ΚΒΑΝΤΙΚΕΣ
ΗΜΙΑΓΩΓΙΜΕΣ ΤΕΛΕΙΕΣ CdSe/ZnS

RALUCA BUICULESCU

ΗΡΑΚΛΕΙΟ 2011

EXAMINING COMMITTEE

CHANIOTAKIS NIKOLAOS (SUPERVISOR)

Professor of the Chemistry Department, University of Crete

GHANOTAKIS DIMITRIOS

Professor of the Chemistry Department, University of Crete

KONSTANTINIDIS GEORGE

Senior Scientist, Microelectronics Research Group, Institute of Electronic Structure and Laser, Foundation for Research and Technology Hellas

KATERINOPOULOS CHARALAMPOS

Professor of the Chemistry Department, University of Crete

SAVVIDIS PAVLOS

Assistant Professor of the Department of Materials Science and Technology, University of Crete

MICHALOPOULOS NIKOLAOS

Professor of the Chemistry Department, University of Crete

MILIOS KONSTANTINOS

Assistant Professor of the Chemistry Department, University of Crete

TABLE OF CONTENTS

1. ABSTRACT	1
ΠΕΡΙΛΗΨΗ	4
2. BIOSENSORS	7
2.1. Principle of operation	8
2.1.1. The biological recognition element	8
2.1.1.1. <i>Biocatalytic receptors</i>	8
<i>Enzymes</i>	9
2.1.1.2. <i>Bioaffinity receptors</i>	11
2.1.1.3. <i>Hybrid receptors</i>	12
<i>Principles of DNA</i>	12
2.1.2. The signal transducer element	15
2.1.2.1. <i>Optical biosensors</i>	15
2.1.2.2. <i>Electrochemical biosensors</i>	16
2.1.2.3. <i>Thermal biosensors</i>	16
2.1.2.4. <i>Piezoelectric biosensors</i>	17
2.2. Optical biosensors	17
2.3. Amperometric biosensors	19
2.4. Performance factors of a biosensor	21
2.4.1. <i>Calibration curve</i>	21
2.4.2. <i>Linear range</i>	22
2.4.3. <i>Sensitivity</i>	22
2.4.4. <i>Limit of detection</i>	22
2.4.5. <i>Selectivity</i>	23
2.4.6. <i>Stability – life time</i>	23
2.4.7. <i>Reproducibility – repeatability</i>	23
2.4.8. <i>Response time – recovery time</i>	23
3 NANOMATERIAL-BASED BIOSENSORS	26
3.1. Addressing the stability problem	26
3.1.1. <i>DNA denaturation process</i>	26

3.1.2. <i>Enzyme denaturation process</i>	27
3.1.3. <i>Enzyme stabilization platforms</i>	28
3.2. Why nanomaterials?	30
3.3. Immobilization onto nanomaterials	31
3.4. Quantum dots	34
3.4.1. <i>Quantum dot properties</i>	34
3.4.2. <i>Quantum dot sensing applications</i>	36
3.5. Gold nanoparticles	38
3.5.1. <i>Gold nanoparticles properties</i>	38
3.5.2. <i>Gold nanoparticles sensing applications</i>	40
3.6. Biosilica	41
3.6.1. <i>Biosilica properties</i>	41
3.6.2. <i>Biosilica applications</i>	43
4. HYBRIDIZATION OF OLIGONUCLEOTIDES ON PHOTOLUMINESCENT SEMICONDUCTOR QUANTUM DOTS	50
Mycobacterium tuberculosis	50
<i>Water solubilisation procedures of CdSe quantum dots</i>	52
<i>Water solubilisation procedures of CdSe/ZnS quantum dots</i>	54
<i>Preparation of QD – oligonucleotide conjugates</i>	55
<i>Hybridization with target oligonucleotides experiment</i>	56
Conclusions	59
5. A PHOTOLUMINESCENT ACETYLCHOLINESTERASE-BASED BIOSENSOR	62
Acetylcholinesterase (AChE)	64
<i>Detection method and assay conditions</i>	67
<i>Preparation of QD/AChE conjugates</i>	69
<i>Preparation of poly-L-lysine templated QD/AChE/PLL/silica nanocomposites</i>	69
<i>Verification of successful conjugation and biosilicification by fluorescence measurements</i>	71
<i>Determination of the QD/AChE/PLL/silica nanocomposite’s morphology</i>	71
<i>Verification of successful biosilicification by ATR-FT-IR measurements</i>	72
<i>QD/AChE/PLL/silica based fluorescence assay</i>	75

<i>Storage stability assay</i>	76
Conclusions	76
6. COLORIMETRIC DETECTION OF OLIGONUCLEOTIDES USING GOLD NANOPARTICLES	83
<i>Synthesis of colloidal gold nanoparticles</i>	84
<i>Determination of Au NPs extinction coefficient</i>	84
<i>Conjugation of gold nanoparticles with oligonucleotides, using a thiol-group-linker</i>	87
<i>Conjugation of gold nanoparticles with thiol-modified oligonucleotides</i>	88
<i>Confirmation of conjugation by ATR-FT-IR spectroscopy</i>	90
<i>Effect of oligonucleotide conjugation onto gold nanoparticles absorbance</i>	91
<i>Hybridization of Au-thiol-oligo pairs with targets</i>	92
<i>Confirmation of hybridization by ATR-FT-IR spectroscopy</i>	93
<i>Effect of DNA double strand formation onto gold nanoparticles absorbance</i>	94
<i>Storage stability of Au NPs – oligonucleotide conjugates</i>	96
Conclusions	97
7. GOLD NANOPARTICLES AS BUILDING BLOCKS IN THE DEVELOPMENT OF ENZYMATIC BIOSENSORS	100
<i>Preparation of Au NPs – AChE conjugates</i>	101
<i>Verification of successful conjugation by absorbance measurements</i>	102
<i>Confirmation of successful conjugation by infrared spectrometry</i>	102
<i>Preparation of poly-L-lysine templated Au NPs – AChE – silica nanocomposites</i>	103
<i>Confirmation of successful biosilicification by infrared spectrometry</i>	104
<i>Determination of the Au NPs – AChE – PLL - silica nanocomposite’s morphology</i>	106
<i>Electrochemical assay conditions</i>	107
<i>Monitoring of the system’s electrochemical response and storage stability study</i>	108
Conclusions	110
PROSPECTIVE WORK	114
ACKNOWLEDGMENTS	115
CURRICULUM VITAE	116

CHAPTER 1 – ABSTRACT

The combination of biotechnology and nanotechnology has led to a tremendous development of hybrid nanomaterials that combine the unique recognition, catalytic, and inhibition properties of biomolecules, such as DNA/RNA, protein/enzyme, antigen/antibody, whole cells, with the unique electronic, photonic, and catalytic properties of the nanoparticles, nanowires or nanorods. Conjugation of biomolecules to nanoparticles has offered infinite application possibilities to the field of nano-bio-technology.

The interest in nanomaterials comes from the fact that new properties are acquired at this length scale and, equally important, that these properties change with their size or shape.

Nanomaterials are structures with at least one of their dimensions in the nanometer scale (smaller than 100 nm), their physico-chemical properties differing substantially from their bulk counterparts. A wide variety of nanoscale materials of different shapes, sizes and compositions are now available, the huge interest in nanomaterials being driven by their many desirable properties. In particular, the ability to tailor the size and structure and as a follow up, the properties of nanomaterials, offers excellent perspectives for designing sensing systems and enhancing the performance of the bioanalytical assay by providing an immobilization platform and a stabilization matrix for biomolecules (proteins, enzymes, antibodies, nucleic acids, etc.). No matter their composition (metallic nanoparticles, carbon based nanomaterials or semiconductor quantum dots), shape (particles, rods, tubes, wires) or surface functionalization (physical, chemical or biological), they have attracted the interest of numerous research groups.

On the other hand, biomolecules are fascinating molecular structures that bring new recognition, catalytic, transport and inhibition properties. Nanomaterials exhibit similar dimensions to those of biomolecules, like proteins, enzymes, antibodies or DNA which usually possess dimensions in the 2-20 nm range, rendering these two classes of materials structurally compatible. The marriage of nanomaterials, like nanoparticles, with biomolecules could provide different transduction mechanisms of biological phenomena for the development of novel biosensors.

There are many fundamental features that render biomolecules suitable for conjugation to nanomaterials. First and most important, their specificity for certain substrates allows for self-assembly upon recognition. Many biomolecules possess more than one binding site allowing for a three-dimensional assembly of nano-structures. They can be synthesized

bearing a wide range of functionalities or even engineered genetically. Another very important feature is that enzymes catalyze reactions without being consumed in the process thus offering a reusable biosensing tool. And so on and so forth.

Aim of the work

Biosensors are fast and selective detection systems of low operational cost with potential applications in areas where rapid detection, high sensitivity and specificity are important. They could play an important role in the development and improvement of public health, however, their use is not as wide spread as expected. The reasons are various and focus mainly on the poor biosensor stability during storage or continuous operation, as well as the reproducibility of their construction. Among these parameters, the one that influences most the analytical characteristics of biosensors is their stability, which in turn depends on the life time and the rate of deactivation of the biomolecule used. The past decade, nanomaterials have been proposed for using in biosensing systems due to the fact that they can act as immobilizing platforms for the biomolecules and thus improve their stability.

The purpose of the present work was to develop new nanomaterial-based biosensor systems that would take advantage of the excellent properties they possess in offering sensitive and reliable optical and electrochemical transducing systems and biomolecule immobilization matrices. In order to achieve this purpose, semiconductor quantum dots and gold nanoparticles, in combination with oligonucleotide strands and enzymes have been used.

The excellent photoluminescent properties of semiconductor CdSe/ZnS core/shell quantum dots (QDs) have been used in order to construct detection systems for mutations in oligonucleotide strands obtained from bacteria of the *Mycobacterium* class, a particularly dangerous class of bacteria since it's the causative agent of most cases of tuberculosis and have recently been linked also to sarcoidosis and Crohn disease. The probe oligonucleotide has been conjugated to the surface of the QDs and their photoluminescent signal has been followed upon conjugation with the target oligonucleotide and with mismatched oligonucleotides.

The same semiconductor core/shell CdSe/ZnS QDs have been used for the construction of a new optical biosensor system for the detection of the enzymatic activity of acetylcholinesterase (AChE). This enzyme plays a fundamental role in the correct function of the nervous system by controlling and regulating the neural responses, its gradual loss being related to a number of serious diseases like Alzheimer's disease. The QDs have been

conjugated to AChE obtained from *Drosophila melanogaster* flies and further entrapped into bio-inspired silica matrix as means of offering a higher degree of stabilization for the enzyme. The highly luminescent QDs offer an excellent optical transduction platform for the development of the enzymatic reaction and prove to be suitable for monitoring low substrate concentrations in solution.

The same biomolecules (*Mycobacterium* specific oligonucleotides and the enzyme AChE) have been used in the construction of biosensors based on the excellent optical and electrochemical properties of colloidal gold nanoparticles (Au NPs). Different sizes of Au NPs have been tested for the construction of optical biosensors, based on their surface Plasmon resonance properties that are dependent on size and inter-particle distance. Their conjugation to probe oligonucleotides and hybridization with target was the basis for obtaining a simple and easy-to-use optical method in detecting hybridization events.

Finally, gold nanoparticles have been tested for their ability to transfer electrons from the biological molecule, in this case AChE from *Electric Eel*, to the surface of electrodes, in the construction of an amperometric biosensor, but also as stabilizing platforms for the biomolecule. The enzyme has been conjugated to the surface of the Au NPs and further subjected to biosilicification as an additional stabilization step. The proposed biosensor system was found able to provide electron transfer from the enzyme to the electrode, sensitive to very small substrate concentrations, being very stable over time. It is also shown that the immobilization of the AChE onto the Au doped biosilica nano-composite provides better signal mediation and significant enzyme stabilization when compared with the existing AChE biosensors.

ΠΕΡΙΛΗΨΗ

Ο συνδυασμός της βιοτεχνολογίας και της νανοτεχνολογίας έχει οδηγήσει σε θεαματική ανάπτυξη υβριδικών νανοϋλικών που συνδυάζουν τις μοναδικές ιδιότητες χημικής αναγνώρισης και κατάλυσης βιομορίων όπως τα DNA, RNA, πρωτεΐνες, ένζυμα, αντιγόνα, αντισώματα, αλλά και ολόκληρα κύτταρα, με τις μοναδικές ηλεκτρονικές, καταλυτικές και οπτικές ιδιότητες των νανοσωματιδίων, νανοκαλωδίων και νανοράβδων. Η σύζευξη των βιομορίων και των νανοϋλικών δίνει τη δυνατότητα πολλών εφαρμογών στον τομέα της νανο-βιο-τεχνολογίας.

Το συνεχώς αυξανόμενο ενδιαφέρον για τα νανοϋλικά οφείλεται στο γεγονός ότι απαιτούνται νέες ιδιότητες σ' αυτήν την κλίμακα και ότι οι ιδιότητες αυτές πρέπει να μεταβάλλονται ανάλογα με το μέγεθος ή το σχήμα.

Τα νανοϋλικά έχουν τουλάχιστον μια διάσταση μικρότερη από 100 nm και οι φυσικοχημικές τους ιδιότητες διαφέρουν σημαντικά από τα αντίστοιχα κυρίως υλικά. Σήμερα υπάρχουν διαθέσιμα διάφορα νανοϋλικά σε ποικιλία σχημάτων, μεγεθών και σύστασης, ενώ το μεγάλο ενδιαφέρον για τα νανοϋλικά οφείλεται στις πολλές επιθυμητές ιδιότητές τους. Συγκεκριμένα, η δυνατότητα ελέγχου του μεγέθους και της δομής και ως αποτέλεσμα των ιδιοτήτων των νανοϋλικών, παρέχει εξαιρετικές προοπτικές στο σχεδιασμό συστημάτων αισθητήρων και βελτιώνει τα αναλυτικά χαρακτηριστικά των βιοαναλυτικών συστημάτων, με δεδομένο ότι τα νανοϋλικά αποτελούν το υλικό ακινητοποίησης των βιομορίων (πρωτεΐνες, ένζυμα, αντισώματα, νουκλεϊκά οξέα, κλπ). Ανεξάρτητα από τη σύστασή τους (μεταλλικά νανοσωματίδια, ανθρακικά νανοϋλικά ή ημιαγώγιμες κβαντικές τελείες), το σχήμα τους (σωματίδια, ράβδοι, σωλήνες, καλώδια, κλπ) ή την τροποποίηση της επιφάνειάς τους (φυσική, χημική ή βιολογική), τα νανοϋλικά έχουν προσελκύσει το ενδιαφέρον πολλών ερευνητικών ομάδων.

Εξάλλου, τα βιομόρια αποτελούν εντυπωσιακές μακρομοριακές δομές που έχουν μοναδικές ιδιότητες χημικής αναγνώρισης, κατάλυσης, μεταφοράς ή αναστολής. Τα νανοϋλικά έχουν παρόμοιες διαστάσεις με αυτές των βιομορίων, όπως πρωτεΐνες, ένζυμα, αντισώματα, ή DNA τα οποία έχουν συνήθως διαστάσεις στην κλίμακα 2-20 nm, καθιστώντας αυτές τις δύο κατηγορίες δομών συμβατές. Η σύζευξη των νανοϋλικών με τα βιομόρια μπορεί να παρέχει διαφορετικούς μηχανισμούς μετάλλαξης του σήματος που προέρχεται από βιολογικά φαινόμενα, συντελώντας στην ανάπτυξη νέων βιοαισθητήρων.

Υπάρχουν πολλές χαρακτηριστικές ιδιότητες που καθιστούν τα βιομόρια κατάλληλα για σύζευξη με τα νανοϋλικά. Πρώτον και σημαντικότερο, η ειδική αναγνώριση ενός συγκεκριμένου μορίου επιτρέπει την αυτοσυγκρότηση κατά τη χημική αναγνώριση. Πολλά βιομόρια έχουν περισσότερες από μια θέσεις δέσμησης επιτρέποντας την τρισδιάστατη συγκρότηση των νανοδομών. Τα βιομόρια μπορούν να συντεθούν έχοντας ποικιλία δραστικών ομάδων ή να τροποποιηθούν γενετικά. Μια άλλη πολύ σημαντική ιδιότητα είναι ότι τα ένζυμα καταλύουν αντιδράσεις χωρίς να καταναλώνονται οπότε δίνουν τη δυνατότητα επαναχρησιμοποίησης του βιοαισθητήρα.

Στόχος του έργου

Οι βιοαισθητήρες αποτελούν γρήγορα και ευαίσθητα συστήματα ανίχνευσης με μικρό κόστος λειτουργίας, που θα μπορούσαν να βρουν εφαρμογή σε τομείς όπου η γρήγορη ανίχνευση, η υψηλή ευαισθησία και επιλεκτικότητα είναι σημαντικές. Οι βιοαισθητήρες θα μπορούσαν να έχουν σημαντικό ρόλο στην ανάπτυξη και βελτίωση της δημόσιας υγείας, ωστόσο η χρήση τους δεν είναι ακόμα ευρέως διαδεδομένη. Υπάρχουν πολλοί λόγοι για αυτό με κυριότερους τη μικρή σταθερότητα κατά την αποθήκευση και λειτουργία, καθώς επίσης και τη μικρή αναπαραγωγιμότητα της κατασκευής τους. Μεταξύ αυτών των παραμέτρων, η σταθερότητα των βιοαισθητήρων επηρεάζει περισσότερο τα αναλυτικά χαρακτηριστικά τους. Η σταθερότητα εξαρτάται από τον χρόνο ζωής και το ρυθμό απενεργοποίησης του βιομορίου που χρησιμοποιείται. Την τελευταία δεκαετία, τα νανοϋλικά χρησιμοποιούνται σε συστήματα βιοαισθητήρων λόγω του ότι αποτελούν υλικά κατάλληλα για την ακινητοποίηση των βιομορίων βελτιώνοντας τη σταθερότητά τους.

Σκοπός της παρούσας εργασίας ήταν η ανάπτυξη νέων συστημάτων βιοαισθητήρων βασισμένων σε νανοϋλικά, τα οποία λόγω των εξαιρετικών ιδιοτήτων τους αποτελούν ευαίσθητους και αξιόπιστους οπτικούς ή ηλεκτροχημικούς μεταλλάκτες σήματος, καθώς και υλικά ακινητοποίησης των βιομορίων. Για το σκοπό αυτό, χρησιμοποιήθηκαν ημιαγώγιμες κβαντικές τελείες και νανοσωματίδια χρυσού σε συνδυασμό με αλυσίδες ολιγονουκλεοτιδίων και ένζυμα.

Η φωταύγεια των ημιαγώγιμων κβαντικών τελειών (QDs) CdSe/ZnS αποτελεί τη βάση για την κατασκευή συστημάτων ανίχνευσης μεταλλάξεων στις αλυσίδες ολιγονουκλεοτιδίων που προέρχονται από βακτήρια του γένους *Mycobacterium*, ένα ιδιαίτερα επικίνδυνο γένος βακτηρίων που αποτελούν την αιτία των περισσότερων περιπτώσεων φυματίωσης και πρόσφατα έχουν συνδεθεί με τη σαρκοείδωση και τη νόσο του Crohn. Το

ολιγονουκλεοτίδιο ανίχνευσης συνδέθηκε στην επιφάνεια των κβαντικών τελειών και μετρήθηκε η φωταύγεια κατά τη σύζευξη με το συμπληρωματικό ολιγονουκλεοτίδιο-στόχο και με μη συμπληρωματικά ολιγονουκλεοτίδια.

Οι ίδιες ημιαγώγιμες κβαντικές τελείες CdSe/ZnS χρησιμοποιήθηκαν για την κατασκευή ενός νέου οπτικού βιοαισθητήρα για την ανίχνευση της ενζυμικής δραστηριότητας της ακετυλοχολινεστεράσης (AChE). Αυτό το ένζυμο έχει βασικό ρόλο στη σωστή λειτουργία του νευρικού συστήματος ελέγχοντας και ρυθμίζοντας τις αντιδράσεις των νευρών, ενώ η απουσία του σχετίζεται με μια σειρά σοβαρών ασθενειών όπως η νόσος Alzheimer. Οι κβαντικές τελείες συνδέθηκαν σε AChE από μύγες *Drosophila melanogaster* και στη συνέχεια παγιδεύτηκαν σε βιομιμητικά παραγόμενο διοξείδιο του πυριτίου για την περαιτέρω σταθεροποίηση του ενζύμου. Η υψηλή φωταύγεια των κβαντικών τελειών αποτελεί εξαιρετικό τρόπο μετάλλαξης του σήματος κατά την ενζυμική αντίδραση και αποδεικνύεται κατάλληλη για την παρακολούθηση χαμηλών συγκεντρώσεων υποστρώματος στο διάλυμα.

Τα ίδια βιομόρια (ολιγονουκλεοτίδια ειδικά σε *Mycobacterium* και το ένζυμο ακετυλοχολινεστεράση) χρησιμοποιήθηκαν στην κατασκευή βιοαισθητήρων βασισμένων στις εξαιρετικές οπτικές και ηλεκτροχημικές ιδιότητες κολλοειδών νανοσωματιδίων χρυσού (Au NPs). Στην κατασκευή των οπτικών βιοαισθητήρων χρησιμοποιήθηκαν νανοσωματίδια χρυσού διαφορετικού μεγέθους, εκμεταλλευόμενοι τον επιφανειακό συντονισμό πλάσματος των σωματιδίων που εξαρτάται από το μέγεθος και την απόσταση μεταξύ τους.

Τέλος, τα νανοσωματίδια χρυσού εξετάστηκαν ως προς την ικανότητά τους να μεταφέρουν ηλεκτρόνια από το βιομόριο, σ' αυτή την περίπτωση ακετυλοχολινεστεράση από *Electric Eel*, στην επιφάνεια του ηλεκτροδίου σε ένα αμπερομετρικό βιοαισθητήρα, αλλά και ως υποστρώματα σταθεροποίησης των βιομορίων. Το ένζυμο συνδέθηκε στην επιφάνεια των Au NPs και στη συνέχεια ακολούθησε παγίδευση σε βιομιμητικά παραγόμενο διοξείδιο του πυριτίου για την περαιτέρω σταθεροποίηση. Ο προτεινόμενος βιοαισθητήρας παρείχε εξαιρετική μεταφορά ηλεκτρονίων από το ένζυμο στο ηλεκτρόδιο, μεγάλη ευαισθησία σε μικρές συγκεντρώσεις υποστρώματος και μεγάλη σταθερότητα στο χρόνο. Επίσης αποδείχθηκε ότι η ακινητοποίηση της AChE στις δομές Au-βιομιμητικά παραγόμενου διοξειδίου του πυριτίου παρέχει τόσο μεταφορά του σήματος, αλλά και σημαντική σταθεροποίηση του ενζύμου σε σχέση με τους ήδη υπάρχοντες βιοαισθητήρες.

CHAPTER 2 – BIOSENSORS

For the past 40 years, biosensors are the “hot subject” of the research community, with the last two decades witnessing an extraordinary growth in research on sensors in general and on chemical and biochemical sensors in particular. Since the first mentioning of the word ‘biosensor’ by Clark and Lyons in 1962 [1], research activities for development of biosensors have increased exponentially. Exciting biosensor designs have been proposed in several reports during past few decades and numerous approaches for effective sensor systems have been demonstrated in laboratories. The distinctiveness of a biosensor system is the marriage of a chemical’s system sensitivity with the selectivity of a biological recognition mechanism.

The fact that biosensors are a blend of several disciplines like chemistry, biochemistry, physics, biotechnology, health, environment, materials science or electrochemistry, lead to confusion in finding a satisfying definition of the field. In 1999, an international group of researchers published a technical report for the International Union of Pure and Applied Chemistry (IUPAC), defining the biosensor as “an integrated receptor-transducer device, which is capable of providing selective quantitative or semi-quantitative analytical information using a biological recognition element (biochemical receptor)” [2]. The high specificity of biomolecules and biological systems can be successfully exploited in constructing biosensor devices only if there is a highly efficient coupling between the biological and transducer components. The biological molecule interacts with the solution to be analyzed and the selective biological reaction produces the analytical signal.

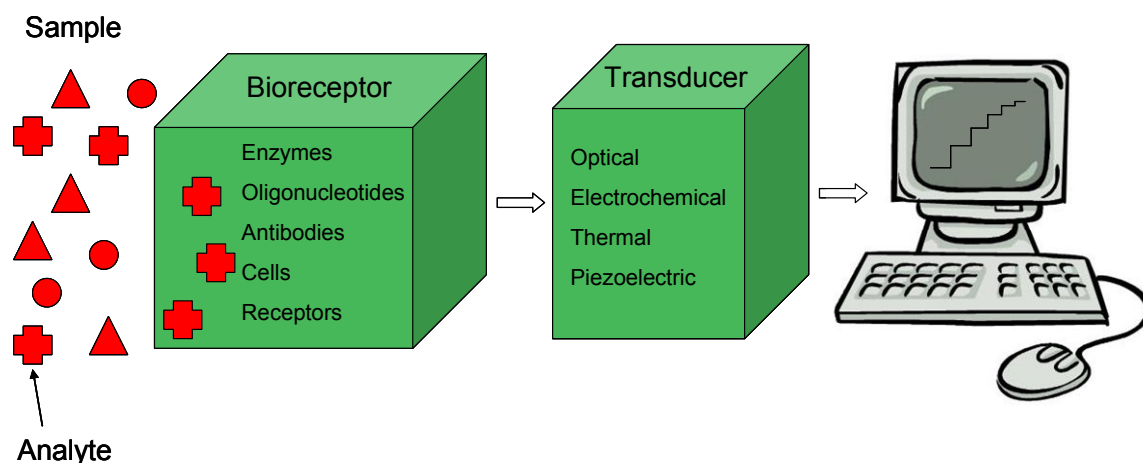


Figure 2.1. Schematic diagram of a biosensor system

2.1. Principle of operation

The biosensors are composed of two distinct parts, the biological recognition element (the biochemical receptor) and the signal transducer element. A schematic of the biosensor system can be observed in Figure 2.1.

2.1.1. *The biological recognition element*

For a biosensor, the biological recognition element represents its most important component. The biological reaction takes place at the interface of the biosensor with the sample to be analyzed, with the biological molecule interacting specifically only with the substance to be analyzed without being influenced by the presence of interfering substances [2]. Biomolecules and biological systems of relevance to biosensor research may be divided into the following main groups:

- Enzymes - proteins which catalyze specific biochemical transformations. They accelerate the rate of reaction of a particular chemical (the substrate) without being consumed in the process.
- Antibodies - globular serum proteins (known as immunoglobulins, Ig) which form an important part of a much wider biological group, namely the binding proteins. Antibodies bind a particular substance (the corresponding antigen) with high specificity and affinity.
- Whole cells - intact biological structural units which contain a wide range of biomolecules and which respond to many types of substances.
- Receptors - protein systems which interact with specific chemicals such as hormones with a resultant conformational change.

According to the biomolecule - analyte interaction, biosensors are divided into three categories: biocatalytic biosensors, bioaffinity biosensors and hybrid biosensors.

2.1.1.1. *Biocatalytic receptors*

In this case, the biosensor is based on a reaction catalyzed by macromolecules, which are present in their original biological environment, have been previously isolated or synthesized. Thus, a continuous consumption of substrate(s) is achieved by the immobilized biocatalyst incorporated into the sensor. Three types of biocatalysts are commonly used: enzymes, whole cells/cell organelles or cell particles and tissues (plant or animal tissues). The

biocatalytic based biosensors are the best known and studied and have been the most frequently applied to biological matrices since the pioneering work of Clark and Lyons [1]. One or more analytes, usually named substrates S and S₀, react in the presence of enzyme(s), whole cells or tissue culture and yield one or several products, P and P₀, according to the general reaction scheme:



From these biological recognition elements, the most frequently used in biosensor construction are the enzymes.

Enzymes

Enzymes are biological catalysts which convert a specific substrate into one or more products without being consumed during the course of this reaction. They accelerate the rate of chemical reactions by stabilizing the transition state of the reaction, hence lowering the activation energy barrier to product formation [3]. The catalytic power of enzymes facilitates life processes in essentially all life forms from viruses to humans. Enzyme-catalyzed reactions have very high reaction rates, typically 10⁶-10¹² times greater than uncatalyzed reactions [3]. The enhancement of the biological reaction is accomplished due to the decrease of the transition levels' energy. In other words, the enzyme helps the substrate to take an appropriate spatial structure that will provoke it's transformation into products.

Enzymes display a range of specificities [4,5]. Some enzymes react only with a single substrate, this being called absolute specificity, other enzymes reacting with a variety of substrates. Most of the enzymes retain their catalytic potential after extraction from the living organisms and it did not take long for mankind to recognize and exploit the catalytic power of enzymes for commercial purposes [3].

Enzymes are made up of amino acids bound together by peptide bonds. The sequence of amino acids makes up the *primary structure* of an enzyme. Depending on the formed patterns by the hydrogen bonds between the backbone amide and carboxyl groups, enzymes can have different structures, the most common being the α -helix and β -sheets. These make up the *secondary structure*. The *tertiary structure* of an enzyme refers to its three-dimensional structure which is due to the molecule arranging itself as to minimize non-favourable thermodynamic interactions with its environment. In many cases, the enzymes consist of more than one subunit, subunits that may or may not be identical. The combination and spatial

arrangement of such units into functional, active complex is known as the *quaternary structure* [4,5].

The kinetics of the enzymatic reactions was best described by Leonor Michaelis and Maud Menten in what is now known as the Michaelis-Menten model [6,7]. According to this model, the enzymatic catalysis is portrayed by the following equation:



The enzyme E reacts with the substrate S and forms the unstable complex [ES]. This reaction is characterized by the kinetic constant k_1 . The [ES] complex can either dissociate back into enzyme and substrate (with the kinetic constant k_{-1}), either release the product P, the enzyme returning to its initial state. The formation of the product is characterized by the kinetic constant k_2 . The catalysis velocity, V, is given in equation 2.3:

$$V = \frac{V_{\max} \cdot [S]}{K_M + [S]} \quad (\text{Eq. 2.3})$$

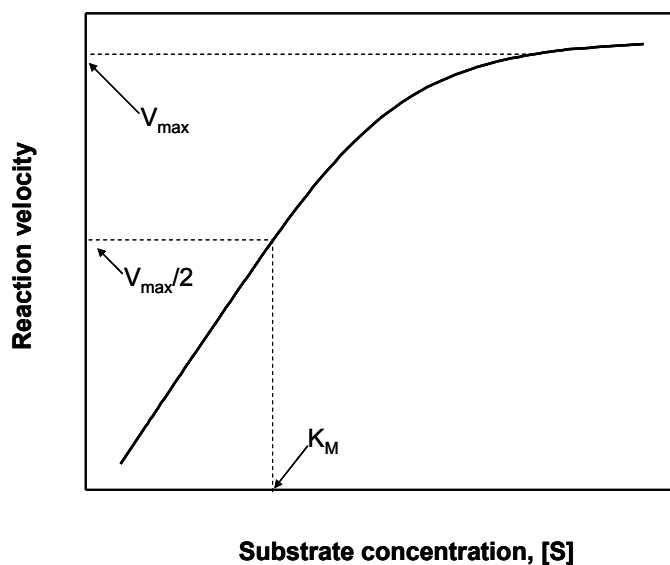


Figure 2.2. A typical Michaelis-Menten plot

The maximum value of the reaction velocity, V_{\max} , is observed when the enzyme is saturated with the substrate concentration, and K_M , the Michaelis-Menten constant, is calculated as the ratio $(k_{-1} + k_2)/k_1$. This equation defines a rectangular hyperbola and describes the curve of the experimental velocity versus the substrate concentration. A plot representing the Michaelis-Menten equation is presented in Figure 2.2.

The basis for the vast majority of enzyme biosensors reported to date is, as mentioned above, the fact that the enzymatic reaction converts the substrate into products that are easily detectable due to a quantifiable property. Depending on this property, different types of enzyme biosensors have been reported in literature. Electrons produced by redox-active enzymes can be detected through their electro-activity with the aid of electrochemical sensors. A number of enzymes produce or consume heat during the enzymatic reaction they catalyze, the heat being related to the analyte concentration by enzyme thermistors. There are also enzymes whose activity is blocked by inhibitors. This is the basis for inhibited enzyme biosensors, where the analyte inhibits the enzymatic reaction which results in a modification of the electrochemical or optical signal. Finally, novel types of enzyme optrodes have been constructed. They are based on collecting the optical signal originating either from the enzyme itself, either from an optical associated marker (like a co-factor).

2.1.1.2. Bioaffinity receptors

The biosensor operation is based on the interaction of the analyte with macromolecules or organized molecular assemblies that have either been isolated from their original biological environment or engineered [8]. The biological molecules most commonly used in this case are antibodies, nucleic acids and receptors. Equilibrium is usually reached and there is no further net consumption of the analyte by the immobilized biocomplexing agent. These equilibrium responses are monitored by the integrated detector. In some cases, this biocomplexing reaction is itself monitored using a complementary biocatalytic reaction. The drawback of bioaffinity biosensors is the fact that, being based on equilibrium reactions, they generally present a very narrow linear operating range of concentration and are often unable to monitor continuously the analyte concentration. Furthermore, some of these biosensors may be difficult to operate in a biological matrix because their sensing layer has to be in direct contact with the sample, and because it may not be possible to incorporate an outer membrane to separate the sensing element from the sample matrix.

2.1.1.3. Hybrid receptors

The hybrid receptors, such as DNA and RNA probes, are based on the principle of selective detection of a unique sequence of nucleic acid bases through hybridization. The nucleic acid structure is a double helix conformation of two polynucleotide strands, each strand being constituted of bases. These bases are complementary two by two through hydrogen bonds. This base-pairing property gives the ability of one single strand to recognize its complementary strand to form a duplex. A DNA probe is added to DNA or RNA strand from an unknown sample. If hybridization occurs with the unknown nucleic acid due to pairing of complementary bases, detection and identification are possible. DNA-based analytical methods seem to be the only method for detecting genetic modifications and are the most sensitive approaches for detecting microorganisms [2].

Principles of DNA

The nucleic acids are responsible for storing and transmitting information in cells. They instruct the cells as to which proteins to synthesize and in what amounts [4-6]. Deoxyribonucleic acid (DNA) and ribonucleic acid (RNA) are the building blocks of genetics, DNA making up the genes of all animal and bacterial cells and some viruses, while RNA is the genetic component of some other viruses.

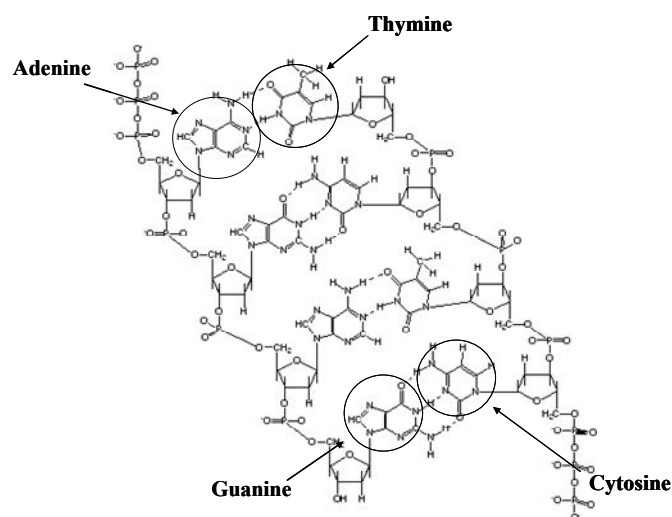


Figure 2.3. The DNA structure

[http://en.wikipedia.org/wiki/File:DNA_chemical_structure.svg (accessed on 18.05.2011)]

The DNA techniques, including hybridization, amplification, and recombination, are all based on the double helix structure of the DNA, nucleic acid hybridization being the

underlying principle of DNA biosensors. DNA is a polymer, consisting of a chain of deoxyribonucleotide molecules joined together. A deoxyribonucleotide is composed of a sugar molecule (deoxyribose in the case of RNA, lacking an oxygen atom), one phosphate group and one of four repeating nucleotides (sometimes called nucleotide bases or simply bases): adenine (A), guanine (G), cytosine (C), and thymine (T). Sugar molecules are joined together by phosphate groups to form the “backbone” of DNA, through phosphodiester bonds, in which the 3'-hydroxyl group of one sugar is linked to the 5'-hydroxyl of the next one. The 5' and 3' ends of a DNA chain (also known as oligonucleotide chain) are free, conferring polarity. By convention, the succession of bases in one oligonucleotide chain is written from the 5' to the 3' end [5,6].

In 1954, James Watson and Francis Crick were the first ones to present to the public the three-dimensional structure of DNA. Thus, its molecule is composed of two right-handed helices bound to each other through hydrogen bonds, and that have a common axis, forming the double-stranded DNA, or dsDNA. The two chains are antiparallel, running in opposite directions: one from 5' to 3' and the second one from 3' to 5'. The backbone described earlier is positioned at the outside of the double helix, the bases forming the inside. These bases pair specifically, A with T and G with C (in RNA, the nucleotide base uracil (U) replaces thymine and pairs with adenine), through hydrogen bonds, more specifically, two hydrogen bonds for the A-T pair and three for the G-C one. The double helix has a diameter of 20 Å, with one turn containing 10 bases and having a height of 3.4 nm. This form of DNA is called B-DNA and is the type present in almost all cells under physiological conditions [4-6].

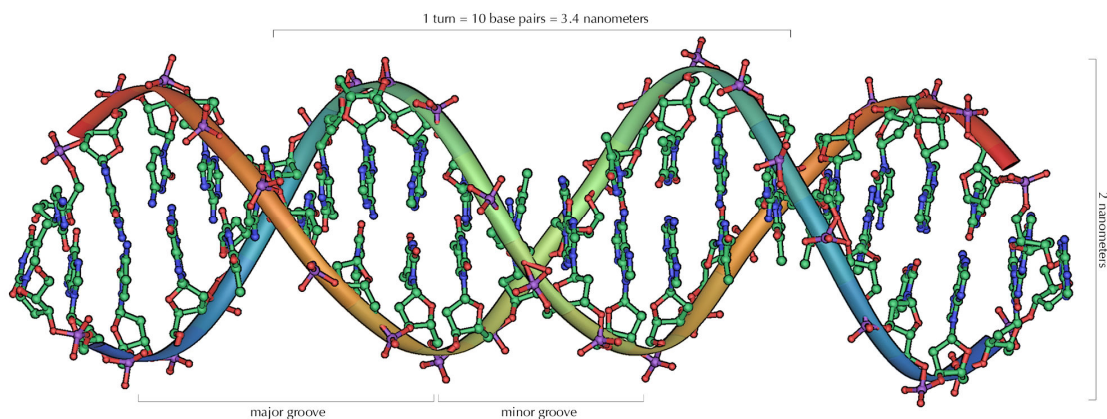


Figure 2.4. The dimensions of a DNA double strand

[http://el.wikipedia.org/wiki/%CE%91%CF%81%CF%87%CE%B5%CE%AF%CE%BF:DNA_Overview.png, (accessed on 18.05.2011)]

The hydrogen bonds connecting the two oligonucleotide strands can be broken by heat or in solutions with extreme pH values, causing the denaturation of the DNA molecule. Each DNA molecule has a distinctive melting temperature (T_m), defined as the temperature at which half of the double helix is unwound. The T_m of each DNA chain depends on its base sequence, a large number of G-C pairs increasing the melting temperature. This is due to the higher number of hydrogen bonds that need to be broken [5,6]. The single stranded DNA (ssDNA) is relatively stable, but on removal of the heat source or of the extreme pH, the DNA molecule will reanneal into the double stranded configuration. This is called hybridization. The stability of the hybridization depends on the nucleotide sequences of both strands. A perfect match in the sequence of nucleotides produces very stable dsDNA, whereas the presence of one or more base mismatches causes instability that can lead to weak hybridization.

In the cells of higher life forms, DNA is present in the form of chromosomes. The DNA in these chromosomes is bound to a group of small proteins called histones, which account for up to 50% of the mass of the chromosome. Most of the DNA is wrapped around histones, forming the units called nucleosomes. Yeast cells contain 12-18 chromosomes, whereas human cells have two sets of 23 chromosomes. Most of the cells in the organism are diploid, containing two sets of each chromosome, except for ovary and sperm cells which are haploid, containing only one copy of the genetic information.

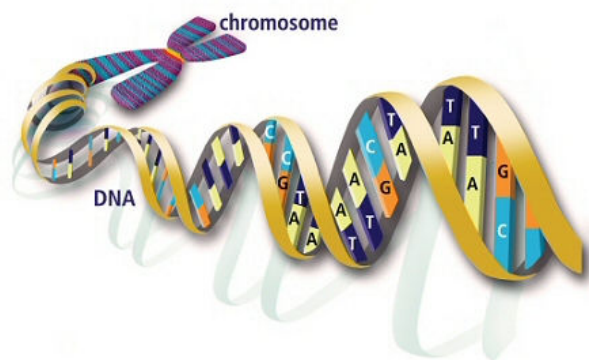


Figure 2.5. DNA organization into chromosomes in the cells of higher life forms
[<http://www.odec.ca/projects/2006/bach6k2/background.htm>, (accessed on 18.05.2011)]

The property of base complementarity presented by the DNA makes possible the construction of DNA probes that can be then used in analytical techniques. Knowing the base sequence of a ssDNA, the complementary strand can be synthesized. This sequence is known

as probe. The probe can be labelled and further used in hybridization experiments in order to recognize and bind, through annealing, to a certain target sequence.

DNA sensors are usually in the form of electrodes, chips, and in solution, solution hybridization being much more rapid than hybridization on solid-supports.

One application of DNA probes is in the diagnosis of hereditary diseases. Each disease is characterized by a specific mutation of the DNA base sequence. Through annealing with the synthesized complementary strand, the disease can be diagnosed. Another application can be found in detection of viral infections. Viruses act by injecting their genetic material into the host cell, “hijacking” the cell’s ribosomes and making them produce the viral proteins. Analytic methods using DNA probes can facilitate early diagnosis.

2.1.2. The signal transducer element

The transducer of a biosensor system represents the part that transforms the changes created by the interaction between the biological recognition element and the analyte into a signal that further undergoes a proper work-out process resulting in the analytical information. The selection of a proper transducer element is dependent on the signal that arises from the biological process and on the character of the changes that appear in the system. According to the signal transducer, the biosensors can be divided into four classes: optical, electrochemical, thermal and piezoelectric.

2.1.2.1. Optical biosensors

Biosensors with optical transducers are receiving considerable attention nowadays, offering new developing opportunities for optical fibers and laser technology. These sensors help extending the limits of application of the spectrophotometric methods in analytical chemistry, especially for use in miniaturized systems.

One of the major advantages of optical sensors is their ability to probe surfaces and films in a non-destructive manner. Additionally, they offer advantages in speed, safety, sensitivity and robustness, as well as permitting *in situ* sensing and real time measurements [9]. Other attractive features of optical sensors include their suitability to component miniaturization, remote sensing and multi-analyte sensing capabilities. After amperometric and potentiometric devices, optical devices are the next most commonly used transducers.

The optical biosensors are based on methods such as UV–Vis absorption, bio- and chemiluminescence, fluorescence and phosphorescence, reflectance, scattering and refraction.

Optical sensors have been initially developed for oxygen, carbon dioxide and pH detecting systems using acid-base indicators [10]. Later, they have been extended for the construction of fluorescent and luminescent optodes. Optodes are constructed with an immobilized selective biocomponent at one end of an optical fibre, with both the excitation and detection components located at the other end.

2.1.2.2. *Electrochemical biosensors*

Electrochemical biosensors are the most commonly used class of biosensors [11]. They are based on the fact that during a bio-interaction process, electrochemical species such as electrons are consumed or generated producing an electrochemical signal which can in turn be measured by an electrochemical detector. These biosensors can be operated in turbid media, have comparable instrumental sensitivity and are more amenable to miniaturization [12].

Depending on the electrochemical property to be measured by a detector system, electrochemical biosensors may further be divided into conductometric, potentiometric and amperometric biosensors. *Conductometric* biosensors measure the changes caused in the conductance between a pair of metal electrodes as response to the presence of the biomolecule. *Potentiometric* biosensors measure the potentials at the working electrode with respect to the reference electrode. They function under equilibrium conditions and monitor the accumulation of charge, at zero current, created by selective binding at the electrode surface. *Amperometric* biosensors measure the change of the current at the working electrode as a response to the direct oxidation or reduction of the products of a biochemical reaction. It is usually performed by maintaining a constant potential at a Pt-, Au- or C-based working electrode or an array of electrodes with respect to a reference electrode, which may also serve as the auxiliary electrode, if current is low (10^{-9} to 10^{-6} Å) [2]. The resulting current is directly correlated to the bulk concentration of the electroactive species or its production or consumption rate within the adjacent biocatalytic layer.

2.1.2.3. *Thermal biosensors*

Biosensors with thermal transducers are based on the monitoring over time of the heat produced or consumed during a chemical reaction catalyzed by enzymes or microorganisms [13]. However, the heat cannot be perfectly confined in an adiabatic system and always

presents a loss of information since the produced heat is partly wasted by irradiation, conduction or convection. The thermal biosensors can be based on thermistors or stacks.

2.1.2.4. Piezoelectric biosensors

The piezoelectric transducers (surface acoustic wave) are more applied in immunosensors. In these devices, an antigen or antibody is immobilized on the surface of a crystal [14]. The interaction of these elements with the analyte can be monitored through the oscillation of the immersed crystal in a liquid, which will produce a modification of mass in the crystal. This modification is perceptible by means of its frequency of oscillation [15].

The biosensors used in this work are based on optical and electrochemical transduction systems, and for this they will be described in more detail further down.

2.2. Optical biosensors

The first optical sensors were conceived for remote sensing in medical applications. Fiber optical devices were designed to achieve some degree of miniaturization and ruggedness within the biological matrix, and also to measure backscattered light by luminescence techniques [16]. This approach competed with the work of Clark and Lyons on small, miniaturized electrochemical devices.

Optical techniques for chemical analysis are now well established. Biosensors based on these techniques are now attracting considerable attention due to their importance in applications such as environmental monitoring or biomedical sensing [4].

Optical biosensors are based on tracing the changes that appear in the optical properties of the analyzed species, of a product of the biological reaction or of a label or marker introduced for this purpose to the system. Most optical biosensors are based on spectroscopic techniques such as measurement of absorbance or fluorescence, whereby the detected signal is used to deduce the concentration of the target analyte [17]. The sample is being irradiated by a source of light of intensity I_0 , yielding transmitted (I_T), reflected (I_R) or fluorescence (I_F) signals. This signal is emitted after interaction either directly with the analyte or with the indicator system [4]. Although a range of geometrical configurations can be used, the basic principles of interaction remain the same and are presented in Figure 2.6.

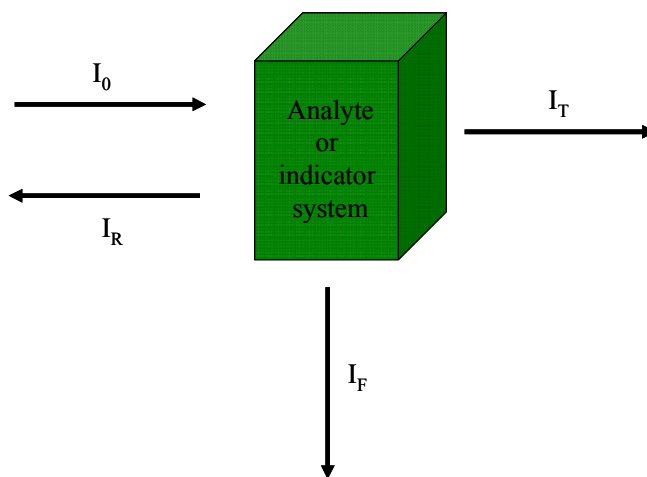


Figure 2.6. The principles of an optical sensing system

Absorption experiments are characterized by the Lambert-Beer law (usually referred to as Beer's law):

$$\text{Log} (I_T/I_0) = A = \varepsilon \cdot c \cdot l \quad (\text{Eq. 2.4})$$

with: I_0 = intensity of incident light

I_T = intensity of transmitted light

A = absorbance (usually measured directly by instrument)

ε = extinction coefficient

c = concentration of analyte

l = path length of light through solution (usually 1cm for common quartz cuvettes).

High concentrations of the absorbing species can result in measurement errors, the optical characteristics of the adsorbing material differing significantly from those observed at low concentrations. The Lambert-Beer law is thus applied for concentrations below the unity.

Fluorescence represents the radiative deexcitation of a molecule following absorption of a photon [4]. In general, the emitted photon is of lower energy than the absorbed one resulting in emission peaks at higher wavelengths than the absorption peak. The wavelength separation between these peaks is called the Stokes shift.

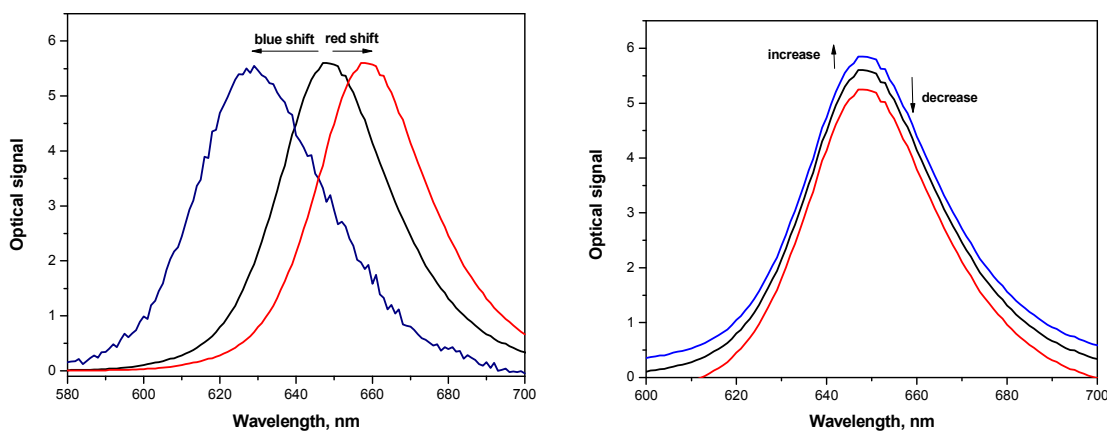


Figure 2.7. The changes followed through the course of an optical experiment

Usually, a change in the absorption or emission wavelength (shift towards higher or lower wavenumbers) or a modification of the absorption or fluorescence peaks' intensity is followed (Figure 2.7).

2.3. Amperometric biosensors

An amperometric biosensor is based on the principle that when a species is oxidized or reduced at an electrode, the current produced is directly related to the concentration of the species in solution [4]. The amperometric biosensor is fast, sensitive, precise, and accurate and the response is a linear function of the concentration of the analyte [15]. However, the selectivity of the amperometric devices is only governed by the redox potential of the electroactive species present. Consequently, the current measured by the instrument can include the contributions of several chemical species.

The first amperometric biosensor reported by Updike & Hicks in 1967 [18], was employed for glucose analysis. It was using the enzyme glucose oxidase with the Clark oxygen electrode and was based on the monitoring of the oxygen consumption. The formation of the product or consumption of reagent can be monitored to measure the analyte concentration. These biosensors are referred to as *first generation biosensors*. Amperometric biosensors modified with mediators are referred to as *second generation biosensors*. Mediators are redox substances that facilitate the electron transfer between the enzyme and electrode. The biosensors using the direct enzyme-electrode coupling, without the use of mediators, are based on direct electron transfer mechanisms and called *third generation*

biosensors. In this case, the electron is directly transferred from the enzyme to the electrode [15].

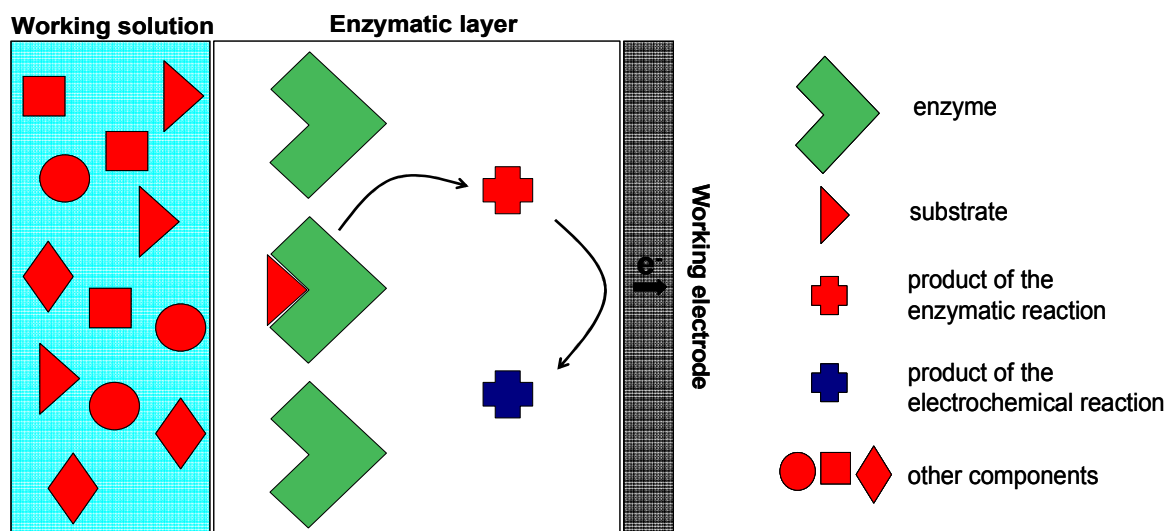


Figure 2.8. The principle of operation of an amperometric biosensor

The usual configuration for amperometric circuits is composed of three electrodes: the working electrode (W), the reference electrode (R) and the counter electrode (C). A potentiostat is used to apply a constant potential to the working with respect to the reference electrode and at the same time force any current to flow through the counter electrode [4]. The value of the applied potential is chosen such to allow the electron active species to be oxidized or reduced at the working electrode. The produced current leaks into the circuit with the help of the counter electrode, and as mentioned before, it is proportional to the concentration of the analyzed species in solution.

A normal amperometric biosensor based on an enzymatic reaction is composed of two elements: the biological recognition element (in this case, the enzyme layer) and the signal transducer element (in this case, the working electrode).

The substrate, present in the working solution, reaches the immobilized enzyme where it is transformed into products. The products are either oxidized or reduced at the working electrode surface, producing electrons, and thus producing current. The produced current decreases as the substrate is used up and reaches an approx. steady state [19] after a certain time. The current has become effectively independent of time, as indicated by the Cottrell equation:

$$i = n \cdot F \cdot A \cdot D \cdot C_{ox} / \delta \quad (\text{Eq. 2.5})$$

where: δ = a constant related to the diffusion layer thickness,

n = the number of electrons that participate in the redox reaction

F = the Faraday number

A = the active surface of the working electrode

D = the diffusion coefficient (a constant characteristic of the analyte)

C = the species concentration

As we can see, the rate of reaction is a diffusion controlled phenomenon where external membranes are used, therefore the current produced is proportional to the analyte concentration and independent of both the enzyme and electrochemical kinetics [12].

The majority of the amperometric biosensors are using oxidases. Amperometric electrodes and oxidases have shown good results due to the facility in measurements associated with high sensitivity of the enzymes' reaction with their substrates. Among these biosensors, transducers that are based on the monitoring of hydrogen peroxide present a higher sensitivity than those with detection of the oxygen consumption [15]. However, these are more suitable when the biological components are microbial cells, vegetables or animal tissues.

2.4. Performance factors of a biosensor

Each technique is characterized by a number of performance parameters which need to be established from the beginning. These parameters allow for the evaluation and comparison between different results [15,20]. The main parameters that characterize the analytical performance of a biosensor are described further down:

2.4.1. Calibration curve

It is the graphic representation of the measured signal as a function of the analytes' concentration [20]. The calibration curve of a biosensor is obtained through two methods: either by adding known quantities of the analyte, or by using solutions of known concentrations. A representative calibration curve and its parameters is presented in Figure 2.9. The biosensor response is measured after the system has reached steady state, meaning

when the analyte found close to the surface of the electrode has been almost completely converted.

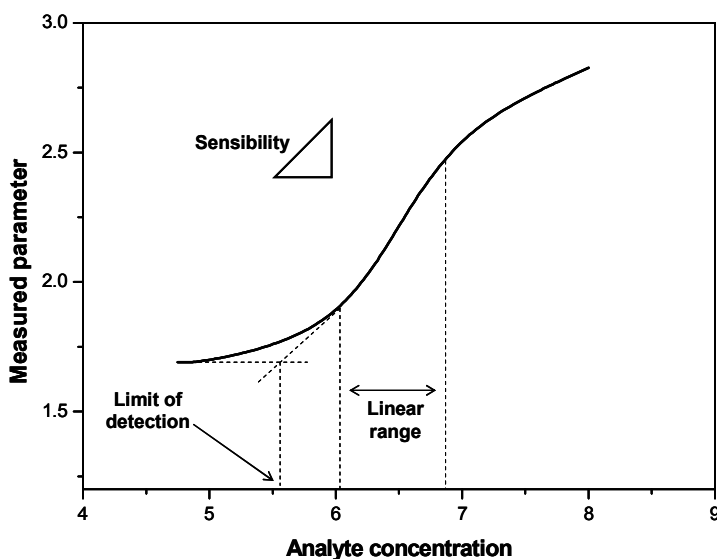


Figure 2.9. A representative calibration curve

2.4.2. Linear range

Represents the concentration range over which the response of the measured analytical parameter is linear. For trustworthy measurements, a linear range bigger than two orders of magnitude is required. If the linear range is small, then more complicated analysis methods are required in order to obtain the requested analytical information.

2.4.3. Sensitivity

It is defined as the ratio of conversion of the measured species as respect to the concentration of the analyte and is calculated from the slope of the calibration curve at its linear range [20].

2.4.4. Limit of detection

The detection limit is defined by IUPAC as the concentration of the analyte at which the extrapolated linear portion of the calibration graph intersects the baseline – a horizontal line corresponding to zero change in response over several decades of concentration change [15]. Nevertheless, the limit of detection is usually defined as the concentration at which the analyte gives a threefold signal as respect to the noise ($S/N = 3$).

2.4.5. Selectivity

It represents the measure of the biosensors' capacity to respond to the analyte even in the presence of other interfering compounds (of defined concentration). Usually the response of the biosensor to the analyte is measured and then compared with the corresponding response to the interfering substances. The selectivity of a biosensor reflects the maximum allowed concentration of possible interfering compounds or the concentration ratio between the obstructive and the analyte giving defined error (usually 5%). The selectivity mainly depends on the biological component, but many times it is influenced also by the used transducer.

2.4.6. Stability – life time

The stability of a biosensor depends mainly on the life time of the biological component. All the parameters that could lead to the deactivation of the biological molecule (like temperature, extreme pH values, inhibition, etc) influence the stability of the biosensor. It is defined as the time interval needed to decrease its sensibility to 50% of the initial. The stability of a biosensor during storage (storage stability) and continuous operation (operational stability) are two of its most important characteristics.

2.4.7. Reproducibility – repeatability

Reproducibility is defined as the relative standard deviation (RSD) between the measurements of the same biosensor. Reproducibility relates to the agreement of test results with different operators, test apparatus, and laboratory locations.

Repeatability is defined as the RSD between several measurements of the same biosensor or between construction characteristics (sensitivity, response to specific analyte concentration, etc) of different biosensors, obtained by one person.

An analytical method or an analytical instrument is considered reliable if the RSD is smaller than 10%.

2.4.8. Response time – recovery time

It is defined as the necessary time for the measured analytical parameter to reach 90% of its final value. For biosensors, response times can vary from a few seconds up to several minutes. Up to 5 minutes is probably acceptable, but if the time exceeds 10 minutes, it is considered to be too long. Related to the response time is the recovery time, which is defined as the time before a biosensor is ready to be used for the next sample.

The mentioned characteristics, and the details of measurements, are important to be checked when the results of the development of a new biosensor are reported, together with the details of the measurements. Unfortunately, this is not always possible, due to omissions or because they are part of a patent. The outcomes of these are the difficulties encountered in comparing the results of different laboratories.

References

1. L.C. Clark Jr. and C. Lyons, Electrode systems for continuous monitoring in cardiovascular surgery, *Ann. N.Y. Acad. Sci.*, 1962, 102, 29-45
2. D.R. Thevenot, K. Toth, R.A. Durst, G.S. Wilson, Electrochemical biosensors: recommended definitions and classifications, *Pure Appl. Chem.*, 1999, 71(12), 2333-2348
3. R.A Copeland, *Enzymes, A practical introduction to structure, mechanism and data analysis*, Wiley-VCH, 1996
4. D. Diamond, *Principles of Chemical and Biological Sensors*, John Wiley & Sons, New York, 1998
5. A.L. Lehninger, *Biochemistry, Second Edition*, Worth Publishers, Inc. 1975
6. C.K. Mathews and K.E. van Holde, *Biochemistry, Second Edition*, The Benjamin/Cummings Publishing Company, Inc., 1996
7. T. Keleti, *Basic Enzyme Kinetic*, Akademiai Kiado, 1986
8. M. Aizawa. Principles and applications of electrochemical and optical biosensors, *Anal. Chim. Acta*, 1991, 250, 249-256
9. A F Collings and F. Caruso, Biosensors: recent advances, *Rep. Prog. Phys.*, 1997, 60, 1397–1445
10. W.R. Seitz, Chemical sensors based on immobilized indicators and fiber optics, *CRC Crit. Rev. Anal. Chem.*, 1988, 19, 135–173
11. Μ. Προδρομίδης, Ηλεκτροχημικοί αισθητήρες και βιοαισθητήρες, Πανεπιστημιακό Τυπογραφείο Ιωαννινών, 2010
12. A. Chaubey and B.D. Malhotra, Mediated biosensors, *Biosens. Bioelectron.*, 2002, 17, 441–456
13. *Biosensors, a practical approach*, Edited by A.E.G. Cass, Oxford University Press, 1990
14. C.K. O’Sullivan, R. Vaughan, G.G. Guilbault, Piezoelectric immunosensors-theory and applications, *Anal. Lett.*, 1999, 32(12), 2353–2377
15. L.D. Mello and L.T. Kubota, Review of the use of biosensors as analytical tools in the food and drink industries, *Food Chem.*, 2002, 77, 237–256
16. U.E. Spichiger-Keller, *Chemical sensors and biosensors for medical and biological applications*, Wiley-VCH, 1998
17. J.J. Ramsden, Optical biosensors, *J. Mol. Recogn.*, 1997, 10(3), 109-120
18. S.J. Updike and G.P. Hicks, Enzyme electrode, *Nature*, 1967, 214(5092), 986-988
19. B. Egging, *Biosensors an intruduction*, John Wiley & Sons, New York, 1997
20. H.H. Willard, L.L. Merritt Jr., J.A. Dean, F.A. Settle Jr, *Instrumental methods of analysis*, Sixth edition, Litton Educational Publishing, Inc., 1981

CHAPTER 3 – NANOMATERIAL-BASED BIOSENSORS

3.1. Addressing the stability problem

Biosensors play an important role in the development and improvement of public health by finding applications in areas where rapid detection, high sensitivity and specificity are important [1]. Unfortunately, commercialization of biosensor technologies has continued to lag behind the research by several years. The reasons are various and focus mainly on the biosensor stability during storage or continuous operation, on their sensitivity and on the reproducibility of their construction [1,2]. Among these parameters, the one that influences most the analytical characteristics of biosensors is their stability, which in turn depends on the life time and the rate of deactivation of the biological element used. There are many factors that can shorten the life time or even lead to deactivation of the biological molecule. During the construction of the biosensor, extreme pH values, high salt concentrations, temperatures outside the accepted range for that specific molecule or organic solvents, can have this effect. This does not mean that the biosensor is completely safe during measurements. The application of high potentials during electrochemical measurements, or even irradiation with different light sources, can have the same destructive results.

In the present work, two different biological transduction elements have been used, oligonucleotides and enzymes, and for this, emphasis will be given further down on the existing ways to improve the stability of the biological recognition element, and especially of the enzymes.

3.1.1. DNA denaturation process

The DNA double-structure is very stable, being possible to recover fragments of DNA even from ancient fossils [3]. Even so, there are a few parameters that can lead to its denaturation.

Due to its huge length in relation to its diameter and due to the rigidity of the double-helix structure, even very diluted solutions of double stranded DNA are highly viscous. When viscosity decreases, denaturation takes place. Denaturation, though, does not lead to breaking of covalent bonds but to unwinding and separation of the two DNA strands [3,4].

Factors that can lead to DNA denaturation include extreme pH values, heat, and presence of enzymes or exposure to amides, urea and similar solutes, these factors being discussed further down.

pH

As discussed earlier in Chapter 2, the DNA molecule is constituted of two complementary oligonucleotide strands that bind to each other through hydrogen bonds. Due to their phosphate groups, the nucleotides are quite strong acids having a rather low pK and thus being fully ionized at pH above 4 [4]. The hydrogen bonds that connect two bases depend thus on the pH, the double-stranded DNA being stable between pH 4 and 11, and becoming unstable and unwinding outside this range.

Heat

The temperature at which the double stranded DNA unwinds is dependent on the purine and pyrimidine bases sequence, a large number of G-C base pairs conferring increased stability due to the three hydrogen bonds they form, as an opposite to the two hydrogen bonds formed by the A-T pair. Upon removing of the heat source, the separated strands quickly hybridize to reform the double stranded DNA.

Enzymes

The phosphodiester bonds in both DNA and RNA are susceptible to hydrolysis in the presence of enzymes called *nucleases*. Under uncatalyzed conditions, the hydrolysis of these bonds is exceedingly slow. In the presence of nucleases, though, the process takes place rapidly. In order to avoid DNA or RNA break-down due to nucleases, extremely care should be taken when constructing DNA or RNA – based biosensors not to contaminate the media used.

3.1.2. Enzyme denaturation process

The term *stability* refers to the persistence of a proteins' molecular integrity or biological function in the face of adverse influences [5]. During production, storage and experimental workup, enzymes undergo a variety of denaturation reactions, denaturation meaning the unfolding of the enzyme tertiary structure to a disordered polypeptide in which key residues are no longer aligned closely enough for continued participation in functional or structure stabilizing interactions [6]. Denaturation can be reversed if the denaturing influence

is removed. A protein is also subject to chemical changes leading to an irreversible loss of activity or inactivation particularly following unfolding [5].

These molecular phenomena have led to defining two distinct *in vitro* protein stability parameters: thermodynamic (or conformational) stability and long-term (or kinetic) stability [6]. Thermodynamic stability describes the resistance of the folded protein conformation (native enzyme structure, N) to denature to the unfolded structure (U), while long-term stability measures the resistance to irreversible inactivation (I) (i.e., persistence of biological activity). Both types are represented in the following equation:



N \longrightarrow U corresponds to thermodynamic (conformational) stability

N \longrightarrow I corresponds to kinetic (long-term) stability

The enzymes normally exist in their native active state. This state is in equilibrium with the partially denatured, enzymatically inactive U state, at high temperatures the enzyme tending to unfold. The temperature at which N = U is called melting temperature (T_m) of the enzyme. Understanding the mechanism of enzyme inactivation and the reversibility or irreversibility of the reactions involved, helps us better characterize its stability and thus enables us to better control the deactivation process [6]

3.1.3. Enzyme stabilization platforms

Enzymes can be stabilized against denaturation or inactivation through a series of methods like protein engineering, chemical modification, use of additives or immobilization.

Protein engineering

This method presumes the substitution of particular amino acids of the protein (by site specific mutagenesis) so as to increase stabilizing interactions like hydrogen bonds or van der Waals forces, or to remove destabilizing ones [5,7].

Chemical modification

The amino acids present in the structure of a protein (with the exception of glycine) have side chains that are chemically active. These groups can react under mild conditions with quite specific reagents to yield chemically modified protein derivatives, often with altered properties [7].

Additives

Additives are usually low molecular weight substances that introduced at quite high concentrations (~ 1 M or greater) can result in an increased stability of proteins [5].

Immobilization

More and more, the immobilization of the biological part onto solid substrates has become the preferred stabilization method. This method brings huge advantage to the biosensor area since enzymes can now be immobilized directly onto the transduction element and thus not requiring an extra stabilization step. The choice of immobilization method used, depends on the biocomponent to be immobilized, the nature of the solid surface and the transducing mechanism [8]. Whatever immobilization method is eventually chosen, careful consideration should be given in order to preserve the activity of the enzyme, not to reduce its specificity, to ensure that nonspecific binding does not occur and that the enzymes' active centre can be easily reached by the substrate [9].

The main immobilization methods employed are as follows:

- *Adsorption* - It represents the simplest method of immobilization and requires minimal preparation. Many substances adsorb enzymes on their surfaces, as for example alumina, charcoal, clay, cellulose, silica gel, glass or collagen. Adsorption can be roughly divided into two classes: physical adsorption and chemical adsorption. Physical adsorption is usually weak, occurring via van der Waals forces and occasionally with hydrogen bonds. Chemical adsorption is much stronger and involves the formation of covalent bonds.
- *Microencapsulation* - This was the method used in early biosensors [10]. An inert membrane is used to trap the enzyme, allowing for a close contact between the biological part and the transducer. Membranes are usually produced from polyurethane, polytetrafluoroethylene (Teflon) or nylon. It is adaptable, does not interfere with the reliability of the enzyme, and limits contamination and biodegradation. It is also stable towards temperature, pH, ionic strength or chemical composition changes and is usually permeable to small molecules and electrons.
- *Entrapment* - The enzyme is mixed together with a monomer solution and upon polymerization a gel matrix is formed trapping the enzyme. Polyacrylamide is the most used in entrapment experiments, but starch gels and nylon have also been used. Unfortunately, there are some disadvantages to this method since the gel matrix can be unstable and it may result in loss of enzyme through pores in the gel.

- *Cross linking* – Enzymes can be cross-linked together using small-molecule cross linkers, like glutaraldehyde. In most cases, bifunctional reagents are used. The enzyme molecules are linked to one another and a final proteic web is being formed. There are some diffusion limitations to this method that can cause damage to the enzyme.
- *Covalent bonding* - In this method, the enzyme is chemically bonded to solid supports or to other supporting materials. This can be done with the help of functional groups present on the enzyme that are not part of the active centre or are not essential for the catalytic activity of the enzyme. This method uses nucleophilic groups for coupling such as, -NH₂, -COOH, -OH, -SH, and others. Reactions need to be performed under mild temperature, ionic strength and pH conditions. The advantage is that the enzyme will not be released during use of the biosensor.

Immobilization of enzymes on the surface of solid substrates presents the advantage of succeeding to restrain the deactivation of enzymes, but the resulting degree of stabilization is still highly dependent on the enzyme and substrate used.

The methods described for immobilization of enzymes present also a number of disadvantages. Either the enzymes are not bound to the substrate strongly enough, or they are inactivated during work up. Furthermore, the enforcement of the immobilization methods in biosensing systems is difficult, due to the fact that most methods require more than one step, thus arising problems in the sensor-to-sensor reproducibility. Nevertheless, the developments that nanotechnology has seen the past decade offer new perspectives and possibilities for the stabilization of enzymes through a large variety of nanomaterials.

3.2. Why nanomaterials?

The buzzword “nanotechnology” is now around us everywhere. Nanotechnology has recently become one of the most exciting forefront fields in analytical chemistry [11]. We can define nanotechnology as the science that creates functional materials, devices and systems by controlling the matter at the sub-100 nm scale. At this point, a wide variety of nanometer-scale materials of different sizes, shapes and compositions are available, the huge interest they present coming from their many desirable properties that can be used for designing novel sensing systems and enhancing the performance of the bioanalytical assay.

Nanomaterials, such as metal or semiconductor nanoparticles, nanorods, carbon materials, nanotubes, nanowires, etc., exhibit similar dimensions to those of biomolecules,

such as proteins, enzymes, antibodies, whole cells, receptors or DNA. Combining the unique electronic, photonic, and catalytic properties of the nanomaterials with the unique recognition, catalytic, and inhibition properties of biomaterials, could bring the scientific community the advantage of novel hybrid nanobiomaterials of synergetic properties and functions. The conjugation of nanomaterials, like nanoparticles, with biomolecules could provide electronic or optical transduction of biological phenomena for the development of novel biosensors [12-14]. Enzymes, antibodies, biomolecular receptors and DNA possess dimensions in the range of 2–20 nm, similar to those of nanoparticles, thus the two classes of materials are structurally compatible [15].

3.3. Immobilization onto nanomaterials

Recent breakthroughs in nanotechnology have made various nanostructured materials more affordable for a broad range of applications. Although we are still at the beginning of exploring the use of these materials, a large number of nanostructures have been examined as immobilization matrices, e.g. for proteins, enzymes, oligonucleotides, antibodies, through different approaches [16].

The interest in nanomaterials comes from the fact that new properties are acquired at this length scale and, equally important, that these properties change with their size or shape. The change in the properties at this length scale is not a result of scaling factors but it is determined by different factors in different materials [17]. These will not be discussed here, since they are not the force that drove this work.

Nanomaterials are structures with at least one of their dimensions in the nanometer scale (smaller than 100 nm), their physico-chemical properties differing substantially from their bulk counterparts. A wide variety of nanoscale materials of different shapes, sizes and compositions are now available, the huge interest in nanomaterials being driven by their many desirable properties. In particular, the ability to tailor the size and structure and as a follow up, the properties of nanomaterials, offers excellent prospects for designing sensing systems and enhancing the performance of the bioanalytical assay by providing an immobilization platform and a stabilization matrix for biomolecules (proteins, enzymes, antibodies, nucleic acids, etc.). No matter their composition (metallic nanoparticles, carbon based nanomaterials or semiconductor quantum dots), shape (particles, rods, tubes, wires, etc) or surface functionalization (physical, chemical or biological), they have attracted the interest of numerous research groups.

One-dimensional (nanotubes, nanofibers) and two-dimensional carbon nanomaterials (graphene) have high surface-to-volume ratio, increased catalytic activity, facile electron transfer properties, and can be modified to bare different functional groups, finding applications as signal transduction platforms and immobilization matrices for biomolecules [18,19]. A recently published study combined the excellent electron transfer properties of carbon nanofibers with the ability to act as immobilizing platform for enzymes, due to the large number of induced surface functional moieties, and constructed a new, very sensitive and stable, electrochemical biosensor system [20].

Another group of nanomaterials with great potential for biosensing applications, is the one of semiconducting quantum dots. They possess fascinating optoelectronic properties due to quantum-confinement effects, including broad excitation and narrow size-tunable emission spectrum, negligible photobleaching, and high photochemical stability [21]. In addition, their surface can be modified by conjugation with a wide range of functional molecules (e.g., small biomolecules, ions, nucleic acids or proteins) thus expanding their use in a wide variety of optical sensing experiments [22]. Their sensitivity to environmental pH proposed them for use in the detection of acetylcholinesterase inhibitors and of glucose, or for following biological processes in living cells [23,24]. They can function as nanoscaffolds, to participate in energy transfer events and to provide multiplexed analysis. Due to the fact that, upon excitation with a light source, they can act as energy donors and therefore excite acceptors found in their proximity, semiconductor QDs have been used in fluorescence resonance energy transfer (FRET) experiments with high success [25]. At the same time, QDs have attracted considerable interest and have been utilized for the development of electrochemical sensors and biosensors.

Metallic nanomaterials, such as nanoparticles, nanorods or nanowires, and more specific gold nanoparticles, are attracting much interest due to their main characteristic of absorbing light in the visible spectrum, also known as surface Plasmon resonance (SPR). The ability to manipulate the topography of these structures in a controllable manner, thereby altering their optical properties, finds important applications in a number of technological fields including localized surface Plasmon resonance and surface-enhanced Raman scattering, useful in chemical and biomedical detection and analysis [26]. Like this, colloidal gold nanoparticles have constituted the basis for detecting aqueous mercuric (Hg^{2+}), silver (Ag^+), and lead (Pb^{2+}) ions in a number of reports [27-29]. Another factor motivating the use of Au nanoparticles is their facile bioconjugation and biomodification [30]. The Au nanoparticle surface has a strong binding affinity towards thiols, disulfides, and amines and led to the application of Au NPs as immobilization platforms for biological molecules like

oligonucleotide strands or enzymes. Results have shown that the bio-conjugation not only avoided the inactivation of the biological part, but rather provided enhanced activity and stability to the biomolecules as compared to their free form [31]. Another advantage of gold nanoparticles is that they are good electricity conductors, property which opened the door for their use in electrochemistry experiments as electron transducers from the analyzed species to the electrode. Electrochemical nanosensors have been fabricated using colloidal gold on one hand to enhance the amount of immobilized biomolecules and on the other to catalyze biochemical reactions and to improve the biosensor response [32]. This ability may be especially useful in the development of amperometric or electroluminescence-based biosensors. They can also act as label for most biological molecules, participating in affinity assays that can be monitored by the electrochemical signal of the metal NPs.

The purpose of the present work was to develop new nanomaterial-based biosensor systems that would take advantage of the excellent properties they possess in offering sensitive and reliable optical and electrochemical transducing systems and biomolecule immobilization matrices. In order to achieve this purpose, semiconductor quantum dots and gold nanoparticles, in combination with oligonucleotide strands and enzymes have been used. We have taken advantage of the excellent photoluminescent properties of semiconductor CdSe/ZnS core/shell quantum dots in order to construct detection systems for mutations in oligonucleotide strands obtained from bacteria of the *Mycobacterium* class. This is a particularly dangerous class of bacteria since it's the causative agent of most cases of tuberculosis and has recently been linked to sarcoidosis and Crohn disease. Acetylcholinesterase, an enzyme that plays a fundamental role in the correct function of the nervous system by controlling and regulating the neural responses, has also been used.

The same biomolecules have been used in the construction of biosensors based on the excellent optical and electrochemical properties of colloidal gold nanoparticles. Different sizes of Au NPs have been tested for the construction of optical biosensors. The size proven to be the most suitable, was further used in the construction of optical and amperometric biosensors, this leading to new detection systems for oligonucleotide identification and enzymatic activity.

Further down, emphasis will be given to the properties that distinguish the chosen nanomaterials and to their important applications found to date.

3.4. Quantum dots

3.4.1. Quantum dot properties

Quantum dots (QDs) are colloidal semiconductor nanocrystals, with sizes in the range of nanometers, whose size and shape can be precisely controlled by the duration, temperature and ligand molecules used in the synthesis. These quantum dots possess unique properties due to quantum confinement effects. QDs have high quantum yields and very broad continuous absorption spectra, which cover a wide wavelengths range extending from the ultraviolet to the visible (e.g., CdSe can emit in the 450-650 nm range, CdTe in the 500-700 nm range, while InAs or PbSe can emit above 800 nm), depending on the particle size [33] (Figure 3.1).

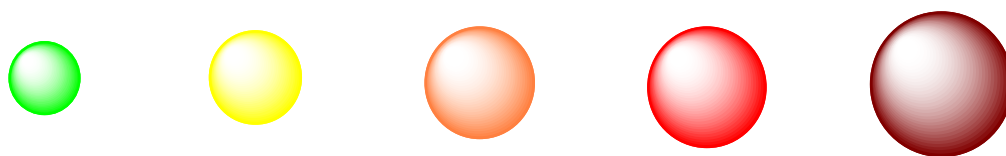
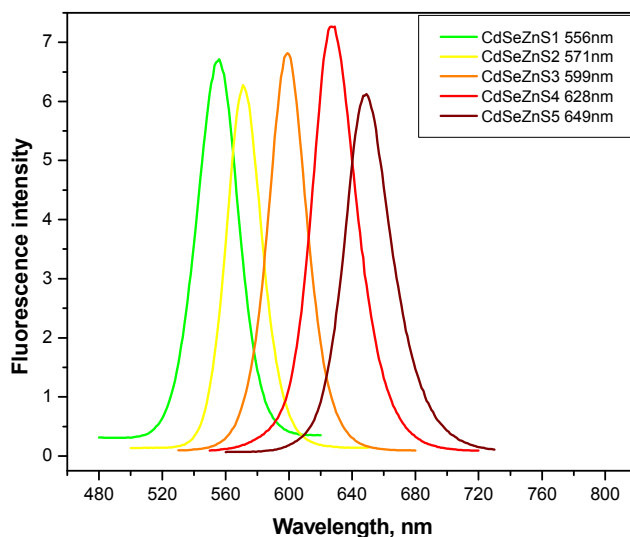


Figure 3.1. Size dependent emission spectra of CdSe/ZnS quantum dots

Their possibility to be excited over a broad wavelength range (they can be excited with any wavelength shorter than the wavelength of fluorescence), narrow and symmetric size-tunable emission spectra (usually 20-40 nm full width at half maximum intensity) that do not exhibit a red tail, resistance to photobleaching and chemical degradation and high photochemical stability [34,35] opened the way for their use in a large number of bioanalytical applications.

Semiconductor QDs exhibit atom-like size-dependent energy states due to the confinement of charge carriers (electrons and holes) in three dimensions. As a consequence, their bandgap energies vary as a function of size (the higher the size of the QD, the lower the energy of the bandgap). The bandgap energy can be defined as the minimum energy that must be supplied to an electron in order to move it from the valence to the conduction band, leaving a hole behind. The removed electron can recombine immediately with the produced hole and produce during this process heat or emit fluorescence light with energy equal to the bandgap energy. Nevertheless, it is more likely that trap states within the material trap either the electron or the hole (Figure 3.2).

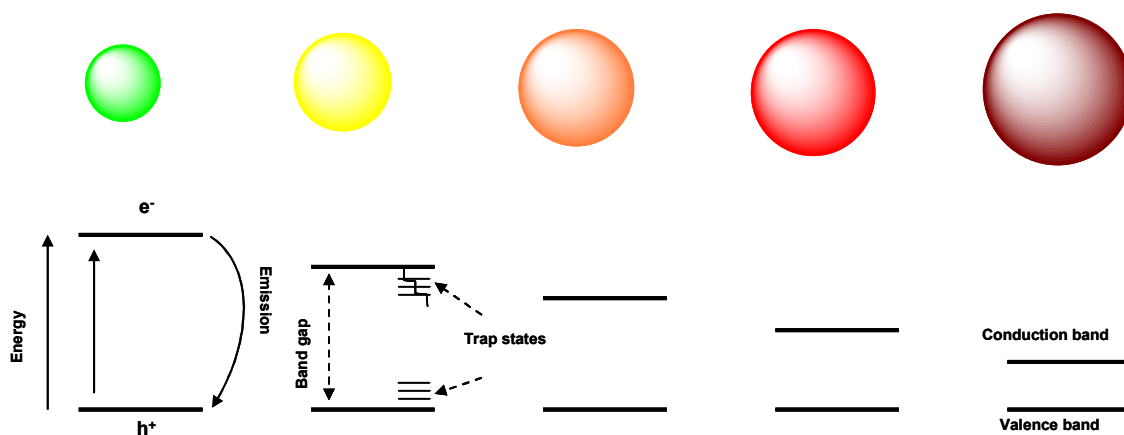


Figure 3.2. The photoexcitative creation of an electron-hole pair and the following radiative relaxation through trap states

Structural defects in the QD crystal structure, such as atomic vacancies, local lattice mismatches, dangling bonds, or adsorbates at the surface [36], can act as temporary “traps” for the electron or hole and influence critically the photoluminescence of the QDs preventing their radiative recombination. The alternation of trapping and untrapping events results in intermittent fluorescence, also called blinking [37]. Blinking causes a drop in the quantum yield (the ratio of emitted to absorbed photons). In order to eliminate defects and consequently decrease the possibility of charge carriers to be kept in trap states, surface passivation by coating with semiconductor materials of wider bandgaps has been achieved [38]. Surface passivation increases the photostability of the QDs core, and subsequently their quantum yield, resulting in core-shell structures that are more robust and favourable for fluorescence-based applications [39].

Due to the availability of precursors and the simplicity of crystallization, Cd-chalcogenide nanocrystals have been the most studied colloidal QDs [21]. A literature search reveals a variety of approaches to synthesize monodisperse nanocrystals [40-42]. Usually, QDs are synthesized using a coordinating solvent, most common one being trioctylphosphine, TOPO/TOP, that provides charged surfaces preventing their aggregation and renders them soluble in organic solvents. Since biological processes are typically taking place in an aqueous environment, a hydrophilic nanocrystal surface is desired for reactions with biological molecules. This is why several water-solubilisation methods [43] have been developed. Most of them rely on the exchange of the hydrophobic surfactant cations with ligand molecules that carry functional groups reactive towards the nanocrystal surface at one end, and hydrophilic groups that ensure water solubility at the other end. Other methods include the growth of a hydrophilic silica shell through surface silanization, the use of amphiphilic polymers or incorporation into micelles [21]. Although there is yet no optimum protocol available that includes all the advantages of individual procedures, state of the art semiconductor quantum dots have reached a degree of performance regarding water solubility that is sufficient for biological experiments.

3.4.2. Quantum dot sensing applications

Owing to the above mentioned fascinating optoelectronic properties, the number of applications that these nanomaterials are finding in biomedicine is in continuous expansion [44,45]. Water-soluble QDs possessing a wide range of surface functional groups (-COOH, -SH, -NH₂, etc) can be easily conjugated with different biomolecules (oligonucleotides, proteins, enzymes, antibodies, etc). The resulting structures combine the properties of both materials, for example, the fluorescence properties of the semiconductor quantum dots and the biological function of the surface-attached molecule.

Depending on the QD size, two types of conjugates can be obtained. If QDs with sizes considerably larger than that of the biomolecule are used, nano-bio-hybrids consisting of a single QD surrounded by a large number of biomolecules on its surface can be produced. In this case, since the QD offers an important number of surface attachment groups, different functionalities can be attached, resulting in multifunctional probes. If small sized QDs are used, nano-bio-hybrids consisting of a biological molecule surrounded by a number of QDs can be produced [46]. If this is the case, a strong fluorescent signal resulting from the nano-bio-hybrid can be registered, and the biomolecule easily tracked.

In theory, the ligands' molecular orientation on the QDs surface, and the QD-ligand molar ratios could be obtained, but for the moment, QD probes with precisely controlled ligand orientations and molar ratios are still not available.

Semiconductor QDs have been successfully used in detecting metal ions. A very recent study reported the functionalization of CdSe QDs with a cation-selective carrier, tetrapyrrolyl-substituted porphyrin. The porphyrin ion carrier coordinates to Cd atoms of the CdSe quantum dots through the Lewis basic pyridyl groups. Upon addition of zinc ions, they coordinate with the porphyrin capping of the QDs and it is shown that this interaction strongly contributes to the increase in the fluorescence efficiency of CdSe. Thus, a highly fluorescent and selective nanosensor for the detection of Zn ions from organic media has been designed [47].

The research work published in 1998 by Chan and Nie [35] pioneered the conjugation of semiconducting QDs to biological molecules for use in biological detection. Their method involved conjugation of CdSe/ZnS QDs to transferrin. Receptor-mediated endocytosis events resulting in the transport of the bioconjugates inside the cell occurred and fluorescence of the cells could be observed. In another work, CdSe QDs have been conjugated to antibodies and used to detect specific antigens (in this case proteins) in fixed cells and cell lysates. The bioconjugates proved to be appropriate for application in flow cytometric and western blot analyses [48].

There have been reports of systems using semiconducting QDs to transfer electronic excitation energy to a nearby acceptor species in a process called fluorescence resonance energy transfer or FRET [25]. Single- and multi-colour assays have been mentioned [49], the latter being the base for identification of oligonucleotide hybridization events. The dynamics of DNA replication and telomerisation have also been reported [50]. Oligonucleotide-modified QDs were incubated with a mixture of deoxyribonucleotides with an organic dye in the presence of telomerase or polymerase. As the telomerization or replication advanced, decrease of the QDs fluorescence and a concomitant increase of the dye's emission were observed due to FRET mechanisms.

Electrochemical applications using semiconducting quantum dots have also been reported. Recently, the assembly of nucleotide-crosslinked CdS QDs arrays on surfaces was mentioned [51]. The specific hydrogen-bonding between nucleotides was used for bridging the layers, the resulting structures proving to be highly stable. The specific G-C and A-T bonding generated photocurrents that increased linearly with the number of aggregated layers, providing an efficient tunneling interface for transporting conduction-band electrons to the electrode.

3.5. Gold nanoparticles

3.5.1. Gold nanoparticles properties

Nanoparticles in the diameter range 1-100 nm (intermediate between the size of small molecules and that of bulk metal) display physical properties that are neither those of bulk metal nor those of molecular compounds. The properties of these nano-sized particles strongly depend on the particle size, inter-particle distance, nature of the protecting organic shell, and shape of the nanoparticles [52].

Today, the potential of gold nanoparticles (Au NPs) is recognized to spring from their interesting optical properties via spectroscopic and photonic techniques [30]. While Faraday was the first one to attribute the red colour to colloidal Au NPs, Mie explained the origin of the phenomenon in 1908. For spherical nanoparticles with diameters much smaller than the wavelength of light ($d \ll \lambda$), an electromagnetic field at a certain frequency (ν) induces a resonant, coherent oscillation of the metal free electrons across the particle [30]. This oscillation is known as the Surface Plasmon Resonance, or SPR. For Au NPs, this resonance lies at visible frequencies. This surface Plasmon oscillation results in a strong enhancement of absorption and scattering of electromagnetic radiation in resonance with the SPR frequency giving the Au NPs their intense red colour and interesting optical properties. The SPR of metal nanoparticles depends on their composition, nanoparticle size and shape, dielectric properties of the surrounding medium and the presence of inter-particle interactions [30]. Highly dispersed nanoparticles in solution exhibit a single peak that is size dependent. When inter-particle spacing is higher than twice their diameter, classical single particle theory should apply. When inter-particle spacing is smaller than twice their diameter, gold nanoparticles tend to aggregate and the surface Plasmon band shifts to higher wavelengths emitting a colour that is different than the one of the initial colloidal solution (Figure 3.3).

Gold nanoparticles and semiconductor quantum dots have in common the fact that the control of their size and the prevention of their agglomeration and precipitation are realized via stabilization by molecules attached to their surface or by embedding in a solid matrix. This is done in order to avoid aggregation and the formation of the thermodynamically favoured bulk material. In the absence of any counteractive repulsive forces, the van der Waals forces between two nanoparticles would lead to coagulation [53]. This can be avoided by either electrostatic or steric stabilization [54]. Electrostatic stabilization is realized by synthesizing the Au NPs with negatively or positively charged ions at their surface that lead to repulsion forces between two particles. Steric stabilization in solution is achieved by covering the particle surface with polymers or surfactant molecules with long alkyl chains that

prevent the particles from coming in proximity to one another. Gold nanoparticles covered by organic thiols have been successfully synthesized, the gold-SH bond being well known to be particularly strong.

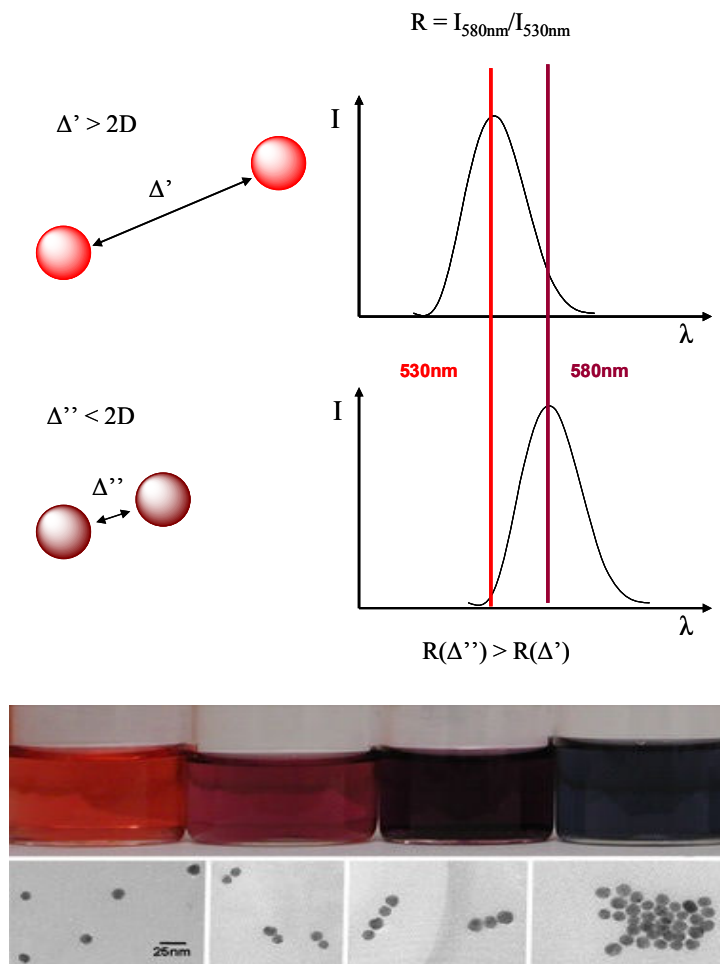


Figure 3.3. Colloidal gold nanoparticles solution colour as a function of inter-particle distance

Gold nanoparticles can be synthesized using a range of methods but the most widely used, and oldest method, is the reduction of the gold salt HAuCl_4 in water by reducing agents such as sodium citrate, phosphor or sodium borohydride [53]. Used in excess, sodium citrate serves also as a protective capping agent inducing negatively charged ligand shell surrounding the NPs. When using other reducing agents, polymers or surfactants have to be added before the salt reduction in order to stabilize the nanoparticles. The reduction with sodium citrate was introduced by Turkevich and co-workers in 1951 [55] and is still one of the preferred synthesis methods for spherical Au NPs. It produces nanoparticles with an average diameter of about 20 nm, very narrow size distribution and good reproducibility.

3.5.2. Gold nanoparticles sensing applications

Their uniformity, stability and size-related properties have made them ideal candidates for fields like catalysis, biosensors or drug delivery, many applications requiring aggregation-resistant, water soluble nanoparticles capable of surviving the complex *in vivo* environment.

Au nanoparticles are well known to enhance Raman signals thus being used in surface enhanced Raman scattering experiments. Their use enables the increase by a factor of 10^{14} – 10^{15} [56] of the Raman signal coming from biomolecules. The main purpose is to detect the weak Raman signal of molecules at low concentrations or having a low Raman scattering cross-section.

Mirkin and co-workers pioneered the research in the detection of DNA sequences with the help of Au NPs. They had conjugated Au NPs of different sizes with oligonucleotide linkers, and based in the oligonucleotides' property to bind to complementary targets, they have managed to build network materials comprising of two different-sized oligonucleotide-functionalized nanoparticles [57,58].

It is well known that Au NPs act as fluorescence quenchers. This was the basis on which Tang and co-workers created a glucose sensing system [59]. Fluorescent quantum dots have been conjugated to concavalin A while Au NPs are conjugated to β -cyclodextrins that bind specifically to the concavalin. Upon addition of glucose into the system, the Au NPs conjugates are displaced, resulting in the fluorescence recovery of the quenched QDs. The nanobiosensor was also used in normal adult human serum and provided satisfactory results.

The last decade, many reports that take advantage of Au NPs conductive properties for the construction of electrochemical biosensors have been materialized. In a very elegant work [60], 1.4 nm gold nanocrystals immobilized on the surface of a Au electrode have been functionalized with the cofactor flavin adenine dinucleotide. The redox apo-flavoenzyme, precisely apo-glucose oxidase, was then reconstructed on the Au NPs and electrochemical detection of glucose was possible. The Au NP acts as an electron relay or “electron nanoplug” for the alignment of the enzyme on the conductive support and for the electrical wiring of its redox-active center [60].

A more recent report [61] proposed another method for determining glucose by immobilizing glucose oxidase on Au NPs which had self-assembled on Au electrode modified with thiol-containing three dimensional network of silica gel. The Au NPs determined an improvement in the electron transfer from the analyte to the electrode surface and the enzyme demonstrated excellent catalytic activity. The biosensor constructed in this way exhibited fast amperometric response, high sensitivity, good reproducibility and long-time stability.

3.6. Biosilica

3.6.1. Biosilica properties

As described before, a wide range of protein stabilization and immobilization methods is available to the research community, with nanoparticles holding an important place in the market. We have seen that gold nanoparticles and semiconductor quantum dots present an advantageous platform for biomolecule immobilization by preventing inactivation of the biological part and enhanced activity and stability. However, weak binding between the enzymes and the support can lead to enzyme leaching upon changes in the local environment (e.g. pH, temperature, ionic strength).

In recent years, porous silica has proven to be a suitable alternative for enzyme stabilization since it is inert, has high specific surface area and controllable pore diameters that can be tailored to the dimensions of a specific enzyme [62]. According to the pore size, porous materials can be categorized as micropores (diameters below 2 nm), mesopores (diameters between 2 and 50 nm), and macropores (diameters above 50 nm). As most enzymes have diameters in the order of 3 - 6 nm, mesoporous silica is the most commonly used. Mesoporous materials possess high specific surface areas (up to ca. 1500 m²/g) and pore volumes (up to ca. 1.5 cm³/g). In addition, the synthesis of mesoporous silica can be tailored to encapsulate biomolecules (e.g. enzymes) since they possess a large number of functional groups, are water insoluble with a hydrophilic character, chemically and physically stable and non-toxic [63].

Sol-gel method has been proven versatile for mesoporous silica synthesis and sol-gel encapsulation has been demonstrated for a number of biomolecules [62]. Using a similar sol-gel technique, but based on a biological template, Luckarift et al. reported a biological silicification reaction that provides a biocompatible and simple method for enzyme encapsulation resulting in stable catalysts with enhanced mechanical stability and high volumetric activity [64]. The biomimetic silicification reaction produces silica nanospheres (biosilica) that physically entrap biomolecules. The method appears to limit negative interactions and allows high recoveries of enzyme activity and improved thermal stability [64].

Biological organisms are able to uptake, store and process soluble silicon (in an as yet unknown form) and mould it with great sophistication into ornate hierarchical patterned biosilicas [65]. Diatoms use biosilica in the formation of a cell wall which offers protection to the cell. In sponges, biosilica spicules provide mechanical support as well as protection from

predators. In plants, silicic acid or silica was found to be essential for plant growth, while at the same time it provides mechanical strength and resistance against attack by fungi and insects [65].

Synthetic preparation of silica typically requires acidic conditions (for the synthesis of gels) or moderately high pH (for the preparation of particulate silicas). Biosilicification on the other hand, presents the advantage of occurring at pHs in the mild acidic to neutral range [65]. The mild reaction conditions are compatible with enzyme immobilization and allow retention of high levels of enzyme activity. At the same time, when using biosilicification, great control over the process of silica formation can be achieved, as well as on the form of the biosilica generated, in contrast to synthetic silica preparations. Also, the silicification reaction imparts remarkable stability to the encapsulated enzyme in terms of both operational stability (reuse during catalysis) and inherent catalytic stability (resistance to denaturation) [62,64].

In order to reproduce biological silicification reactions, researchers have tried to unlock its secrets. In diatoms, cationic polypeptides named silaffins have been shown to precipitate silica from monosilicic acid at pH 5.5 [66]. Within the native peptide, many of the lysines have been modified to either ϵ -*N*-dimethyllysine, phosphorylated ϵ -*N*-trimethyl- δ -hydroxylysine, or long-chain polyamine moieties of *N*-methyl derivatives of polypropylenimine, while the serines have been post-translationally phosphorylated [67]. Functional analysis of native silaffins and isolated polyamines has shown that the peptides self-assemble into supramolecular structures, providing a template for silicic acid polycondensation by long-chain polyamine moieties.

The nonmodified peptide R5 (H₂N-SSKKSGSYSGSKGSKRRIL-COOH) has also been shown to produce silica. The peptide is a synthetic derivative of a naturally occurring silaffin protein, found in the silica skeleton of the marine diatom *Cylindrotheca fusiformis* [62]. While forming, the silica particles entrap the peptide and any other material that is contained within the reaction mixture. Experiments by Luckarift et al. [64] showed the successful encapsulation of biological (enzymes) and non-biological components (magnetic cobalt platinum, CdSe/ZnS QDs and iron oxide nanoparticles).

Despite the versatility of the synthetic peptide R5, subsequent studies demonstrated that silica-formation could also be catalyzed by a wide range of cationic amine-rich molecules including silica-binding peptides, polymers such as polyethyleneimine and poly-L-lysine (PLL), pentapropylenehexamine, cysteamine and proteins such as silicatein and lysozyme [68-71].

3.6.2. Biosilica applications

The applications of biosilica in biotechnology are numerous, the group of Luckarift being very active in this field. They have encapsulated enzymes like catalase and horseradish peroxidase [64], butyryl cholinesterase [72] or nitrobenzene nitroreductase [73] in R5 or polyethyleneimine templated biosilica, all composites proving enhanced enzyme stability. They have also managed the encapsulation of inorganic nanoparticles like magnetic cobalt platinum or streptavidin conjugated CdSe/ZnS quantum dots for further use in bioanalytic and biocatalytic experiments. The use of biosilica encapsulation of quantum dots increases their possible applications in biomedicine since it has been demonstrated that a biosilica shell protects the QDs from chemical degradation and leaching of the toxic core materials [74-76] thus decreasing their cytotoxic effects on living cells.

Electrochemical biosensors that used biosilicification processes have also been reported. Representative is the construction of amperometric acetylcholinesterase (AChE) biosensors [20,77]. A biosilica matrix was constructed around carbon nanofibers-immobilized AChE leading to the formation of a biocompatible electrochemically active nanocomposite structure with high enzyme loading level. The carbon nanofibers promoted the electron transfer from the enzyme to the electrode surface leading to biosensors of enhanced analytical characteristics

References

1. H.H. Weetall, Chemical sensors and biosensors, update, what, where, when and how, *Biosens. Bioelectron.*, 1999, 14, 237–242.
2. R. Gupta and N.K. Chaudhury, Entrapment of biomolecules in sol–gel matrix for applications in biosensors: Problems and future prospects, *Biosens. Bioelectron.*, 2007, 22, 2387–2399
3. C.K. Mathews and K.E. van Holde, *Biochemistry*, Second Edition, The Benjamin/Cummings Publishing Company, Inc., 1996
4. A.L. Lehninger, *Biochemistry*, Second Edition, Worth Publishers, Inc. 1975
5. C. O’Fagain, Understanding and increasing protein stability, *Biochim. Biophys. Acta*, 1995, 1252, 1-14
6. P.V. Iyer and L. Ananthanarayan, Enzyme stability and stabilization—Aqueous and non-aqueous environment, *Proc. Biochem.*, 2008, 43, 1019–1032
7. C. O’Fagain, Enzyme stabilization—recent experimental progress, *Enz. Microb. Tech.* 2003, 33, 137–149
8. D. Diamond, *Principles of chemical and biological sensors*, John Wiley & Sons, New York, 1998
9. Μ. Προδρομίδης, Ηλεκτροχημικοί αισθητήρες και βιοαισθητήρες, Πανεπιστημιακό Τυπογραφείο Ιωαννινών, 2010
10. B. Eggins, *Biosensors an Introduction*, John Wiley & Sons, New York, 1997
11. J. Wang, Nanomaterial-based electrochemical biosensors, *Analyst*, 2005, 130, 421–426
12. S.G. Penn, L. He, M.J. Natan, Nanoparticles for bioanalysis, *Curr. Opin. Chem. Biol.*, 2003, 7, 609 – 615
13. J.L. West and N.J. Halas, Engineered nanomaterials for biophotonics applications: improving sensing, imaging, and therapeutics, *Annu. Rev. Biomed. Eng.*, 2003, 5, 285 – 292
14. P. Alivisatos, The use of nanocrystals in biological detection, *Nat. Biotechnol.*, 2004, 22, 47 – 52
15. E. Katz and I. Willner, Integrated nanoparticle–biomolecule hybrid systems: synthesis, properties, and applications, *Angew. Chem. Int. Ed.*, 2004, 43, 6042 – 6108
16. J. Kim, J.W. Grate, P. Wang, Nanostructures for enzyme stabilization, *Chem. Eng. Sci.*, 2006, 61, 1017 – 1026
17. C. Burda, X. Chen, R. Narayanan, M.A. El-Sayed, Chemistry and properties of nanocrystals of different shapes, *Chem. Rev.*, 2005, 105, 1025-1102

18. V. Vamvakaki, M. Fouskaki, N. Chaniotakis, Electrochemical biosensing systems based on carbon nanotubes and carbon nanofibers, *Anal. Lett.*, 2007, 40, 2271-2287
19. G.A. Crespo, S. Macho, J. Bobacka, F.X. Rius, Transduction mechanism of carbon nanotubes in solid-contact ion-selective electrodes, *Anal. Chem.*, 2009, 81, 676-681
20. V. Vamvakaki, M. Hatzimarinaki, N. Chaniotakis, Biomimetically synthesized silica-carbon nanofiber architectures for the development of highly stable electrochemical biosensor systems, *Anal. Chem.*, 2008, 80, 5970-5975
21. M.F. Frasco and N. Chaniotakis, Semiconductor Quantum Dots in Chemical Sensors and Biosensors, *Sensors*, 2009, 9, 7266-7286
22. R. Gill, M. Zayats, I. Willner, Semiconductor quantum dots for bioanalysis, *Angew. Chem. Int. Ed.*, 2008, 47, 7602-7625
23. R. Gill, L. Bahshi, R. Freeman, I. Willner, Optical detection of glucose and acetylcholine esterase inhibitors by H₂O₂ sensitive CdSe/ZnS quantum dots, *Angew. Chem. Int. Ed.*, 2008, 47, 1676-1679
24. Y.S. Liu, Y. Sun, P.T. Vernier, C.H. Liang, S.Y.C. Chong, M.A. Gundersen, pH-sensitive photoluminescence of CdSe/ZnSe/ZnS quantum dots in human ovarian cancer cells, *J. Phys. Chem. C*, 2007, 111, 2872-2878
25. W.R. Algar and U.J. Krull, Adsorption and hybridization of oligonucleotides on mercaptoacetic acid-capped CdSe/ZnS quantum dots and quantum dot-oligonucleotide conjugates, *Langmuir*, 2006, 22, 11346-11352
26. J. Zhang and C. Noguez, Plasmonic optical properties and applications of metal nanostructures, *Plasmonics*, 2008, 3, 127-150
27. G.K. Darbha, A.K. Singh, U.S. Rai, E. Yu, H. Yu, P.C. Ray, Selective detection of mercury (II) ion using nonlinear optical properties of gold nanoparticles, *J. Am. Chem. Soc.*, 2008, 130, 8038-8043
28. Y.L. Hung, T.M. Hsiung, Y.Y. Chen, Y.F. Huang, C.C. Huang, Colorimetric detection of heavy metal ions using label-free gold nanoparticles and alkanethiols, *J. Phys. Chem. C*, 2010, 114, 16329-16334
29. C.Y. Lin, C.J. Yu, Y.H. Lin, W.L. Tseng, Colorimetric sensing of silver(I) and mercury(II) ions based on an assembly of tween 20-stabilized gold nanoparticles, *Anal. Chem.*, 2010, 82, 6830-6837
30. P.K. Jain, I.H. El-Sayed, M.A. El-Sayed, Au nanoparticles target cancer, *NanoToday*, 2007, 2(1), 18-29

31. P. Pandey, S.P. Singh, S.K. Arya, V. Gupta, M. Datta, S. Singh, B.D. Malhotra, Application of thiolated gold nanoparticles for the enhancement of glucose oxidase activity, *Langmuir*, 2007, 23, 3333-3337
32. I. Willner, B. Willner, E. Katz Biomolecule-nanoparticle hybrid systems for bioelectronic applications, *Bioelectrochem.*, 2007, 70, 2-11
33. X. Michalet, F.F. Pinaud, L.A. Bentolila, J.M. Tsay, S. Doose, J.J. Li, G. Sundaresan, A.M. Wu, S.S. Gambhir, S. Weiss, *Science*, 2005, 307, 538-544
34. M. Bruchez Jr., M. Moronne, P. Gin, S. Weiss, A.P. Alivisatos, Semiconductor nanocrystals as fluorescent biological labels, *Science*, 1998, 281, 2013-2016
35. W.C.W. Chan and S. Nie, Quantum dot bioconjugates for ultrasensitive nonisotopic detection, *Science*, 1998, 281, 2016-2018
36. C.J. Murphy, Optical sensing with quantum dots, *Anal. Chem.*, 2002, 74, 520A-526A
37. Nanomaterial for biosensors, Edited by C.S.S.R. Kumar, Wiley-VCH, 2007
38. B.O. Dabbousi, J. Rodriguez-Viejo, F.V. Mikulec, J.R. Heine, H. Mattoussi, R. Ober, K.F. Jensen, M.G. Bawendi, (CdSe)ZnS core-shell quantum dots: synthesis and characterization of a size series of highly luminescent nanocrystallites, *J. Phys. Chem. B*, 1997, 101, 9463-9475
39. J.K. Jaiswal, H. Mattoussi, J.M. Mauro, S.M. Simon, Long-term multiple color imaging of live cells using quantum dot bioconjugates, *Nat. Biotechnol.*, 2003, 21, 47-51
40. C.B. Murray, D.J. Norris, M.G. Bawendi, Synthesis and characterization of nearly monodisperse CdE (E = sulphur, selenium, tellurium) semiconductor nanocrystallites., *J. Am. Chem. Soc.*, 1993, 115, 8706-8715
41. J. Park, J. Joo, S.G. Kwon, Y. Jang, T. Hyeon, Synthesis of monodisperse spherical nanocrystals, *Angew. Chem. Int. Ed.*, 2007, 46, 4630-4660
42. P. Reiss, M. Protière, L. Li, Core/shell semiconductor nanocrystals, *Small*, 2009, 5, 154-168
43. A.M. Smith, G. Ruan, M.N. Rhyner, S. Nie, Engineering luminescent quantum dots for in vivo molecular and cellular imaging, *Ann. Biomed. Eng.*, 2006, 34, 3-14
44. T. Jamieson, R. Bakhshi, D. Petrova, R. Pockock, M. Imani, A.M. Seifalian, Biological applications of quantum dots, *Biomaterials*, 2007, 28, 4717-4732
45. J.B. Delehanty, H. Mattoussi, I.L. Medintz, Delivering quantum dots into cells: strategies, progress and remaining issues, *Anal. Bioanal. Chem.*, 2009, 393, 1091-1105
46. Z. Zhelev, H. Ohba, R. Bakalova, R. Jose, S. Fukuoka, T. Nagase, M. Ishikawa, Y. Baba, Fabrication of quantum dot-lectin conjugates as novel fluorescent probes for microscopic

- and flow cytometric identification of leukemia cells from normal lymphocytes, *Chem. Commun.*, 2005, 15, 1980-1982
47. M.F. Frasco, V. Vamvakaki, N. Chaniotakis, Porphyrin decorated CdSe quantum dots for direct fluorescent sensing of metal ions, *J. Nanopart. Res.*, 2010, 12, 1449–1458
 48. Z. Zhelev, R. Bakalova, H. Ohba, R. Jose, Y. Imai, Y. Baba, Uncoated, broad fluorescent, and size-homogeneous CdSe quantum dots for bioanalyses, *Anal. Chem.*, 2006, 78(1), 321–330
 49. W.R. Algar and U.J. Krull, Towards multi-colour strategies for the detection of oligonucleotide hybridization using quantum dots as energy donors in fluorescence resonance energy transfer (FRET), *Anal. Chim. Acta*, 2007, 581, 193-201
 50. F. Patolsky, R. Gill, Y. Weizmann, T. Mokari, U. Banin, I. Willner, Lighting-up the dynamics of telomerization and DNA replication by CdSe-ZnS quantum dots, *J. Am. Chem. Soc.*, 2003, 125, 13918-13919
 51. J.P. Xu, Y. Weizmann, N. Krikhely, R. Baron, I. Willner, Layered hydrogen-bonded nucleotide-functionalized CdS nanoparticles for photoelectrochemical applications, *Small*, 2006, 2(10), 1178-1182
 52. M.C. Daniel and D. Astruc, Gold Nanoparticles: Assembly, supramolecular chemistry, quantum-size-related properties, and applications toward biology, catalysis, and nanotechnology, *Chem. Rev.*, 2004, 104(1), 293-346
 53. S. Link and M.A.El-Sayed, Shape and size dependence of radiative, non-radiative and photothermal properties of gold nanocrystals, *Int. Rev. Phys. Chem.*, 2000, 19(3), 409 – 453
 54. G. Schmid, *Clusters and Colloids: From Theory to Application*, Weinheim VCH, 1994
 55. J. Turkevich, P.C. Stevenson, J Hillier, A study of the nucleation and growth processes in the synthesis of colloidal gold, *Discuss. Faraday Soc.*, 1951, 11, 55-75
 56. V. Biju, T. Itoh, A. Anas, A. Sujith, M. Ishikawa, Semiconductor quantum dots and metal nanoparticles: syntheses, optical properties, and biological applications, *Anal. Bioanal. Chem.*, 2008, 391, 2469–2495
 57. R.C. Mucic, J.J. Storhoff, C.A. Mirkin, R.L. Letsinger, DNA-directed synthesis of binary nanoparticle network materials, *J. Am. Chem. Soc.*, 1998, 120, 12674-12675;
 58. R.A. Reynolds, C.A. Mirkin, R.L. Letsinger, Homogenous, nanoparticle based quantitative colorimetric detection of oligonucleotides, *J. Am. Chem. Soc.*, 2000, 122, 3795-3796

59. B. Tang, L. Cao, K. Xu, L. Zhuo, J. Ge, Q. Li, L. Yu, A new biosensor system for glucose with high sensitivity and selectivity in serum based on FRET between CdTe quantum dots and Au nanoparticles, *Chem. Eur. J.*, 2008, 14, 3637-3644
60. Y. Xiao, F. Patolsky, E. Katz, J.F. Hainfeld, I. Willner, "Plugging into enzymes": nanowiring of redox enzymes by a gold nanoparticle, *Science*, 2003, 299, 1877-1881
61. S. Zhang, N. Wang, Y. Niu, C. Sun, Immobilization of glucose oxidase on gold nanoparticles modified Au electrode for the construction of biosensor, *Sens. Act. B.*, 2005, 109, 367-374
62. Luckarift H.R., Silica-Immobilized Enzyme Reactors, *J. Liq. Chromatogr. Rel. Techn.*, 2008, 31(11), 1568 – 1592
63. M. Hartmann, Ordered mesoporous materials for bioadsorption and biocatalysis, *Chem. Mater.*, 2005, 17(18), 4577-4593
64. R.R. Naik, M.M. Tomczak, H.R. Luckarift, J.C. Spain, M.O. Stone, Entrapment of enzymes and nanoparticles using biomimetically synthesized silica, *Chem. Commun.*, 2004, 15, 1684 – 1685
65. S.V. Patwardhan, S.J. Clarson, C.C. Perry, On the role(s) of additives in bioinspired silicification, *Chem. Commun.*, 2005, 9, 1113–1121
66. N. Kroger, R. Deutzmann, M. Sumper, Polycationic peptides from diatom biosilica that direct silica nanosphere formation, *Science*, 1999, 286, 1129-1132
67. N. Kroger, S. Lorenz, E. Brunner, M. Sumper, Self-assembly of highly phosphorylated silaffins and their function in biosilica morphogenesis, *Science*, 2002, 298, 584-586
68. S.V. Patwardhan, N. Mukherjee, S.J. Clarson, The use of poly-L-lysine to form novel silica morphologies and the role of polypeptides in biosilicification, *J. Inorg. Organomet. Polymers.*, 2001, 11, 193-198
69. F. Noll, M. Sumper, N. Hampp, Nanostructure of diatom silica surfaces and of biomimetic analogues, *Nano Lett.*, 2002, 2, 91-95
70. S.V. Patwardhan and S.J. Clarson, Silicification and biosilicification: Part 5 An investigation of the silica structures formed at weakly acidic pH and neutral pH as facilitated by cationically charged macromolecules, *Mater. Sci Eng. C*, 2003, 23, 495-499
71. E. Brunner, K. Lutz, M. Sumper, Biomimetic synthesis of silica nanospheres depends on the aggregation and phase separation of polyamines in aqueous solution, *Phys. Chem. Chem. Phys.*, 2004, 6, 854-857
72. H.R. Luckarift, J.C. Spain, R.R. Naik, M.O. Stone, Enzyme immobilization in a biomimetic silica support, *Nat. Biotechnol.*, 2004, 22, 211–213

73. C. Berne, L. Betancor, H.R. Luckarift, J.C. Spain, Application of a microfluidic reactor for screening cancer prodrug activation using silica-immobilized nitrobenzene nitroreductase, *Biomacromol.* 2006, 7, 2631–2636
74. S. Dembski, C. Graf, T. Kruger, U. Gbureck, A. Ewald, A. Bock, E. Ruhl, Photoactivation of CdSe/ZnS quantum dots embedded in silica colloids, *Small*, 2008, 4(9), 1516-1526
75. C. Kirchner, T. Liedl, S. Kudera, T. Pellegrino, A.M. Javier, H.E. Gaub, S. Stolzle, N. Fertig, W.J. Parak, Cytotoxicity of colloidal CdSe and CdSe/ZnS nanoparticles, *Nano Lett.*, 2005, 5, 331-338
76. T.J. Daou, L. Li, P. Reiss, V. Josserand, I. Texier, Effect of poly(ethylene glycol) length on the in vivo behavior of coated quantum dots, *Langmuir*, 2009, 25, 3040-3044
77. M. Hatzimarinaki, V. Vamvakaki, N. Chaniotakis, Spectro-electrochemical studies of acetylcholinesterase in carbon nanofiber-bioinspired silica nanocomposites for biosensor development, *J. Mater. Chem.*, 2009, 19, 428–433

CHAPTER 4 – HYBRIDIZATION OF OLIGONUCLEOTIDES ON PHOTOLUMINESCENT SEMICONDUCTOR QUANTUM DOTS

After the pioneering work of Chan and Nie [1] which reported that semiconductor quantum dots could be used as an alternative to organic fluorophores for the labelling of transferrin and IgG, a great number of publications have followed focusing on the marriage of these materials with other nanomaterials and biomolecules. QDs have been used as donors/acceptors in FRET processes [2-5], for fluorescent imaging of living cells [6], for the construction of pH sensors in solution [7,8] or enzyme biosensors [9,10]. They have also been conjugated to antibodies [11], cellular proteins [12] or receptors [13].

A field that is lately benefiting from using QD-based detection methods is the one of nucleic acid detection. The specificity of the hybridization event is the basis of many DNA sensing approaches using probe oligonucleotide linked through different strategies either to the surface of highly luminescent quantum dots, or to different substrates. In the latter case, recognition is obtained by hybridization with QD-conjugated target oligonucleotide.

The purpose of the present work was to use the quantum dots' excellent photoluminescence properties in developing a simple biosensing system for the detection of *Mycobacterium* specific oligonucleotides.

Mycobacterium tuberculosis

Mycobacterium tuberculosis (MTB) is a pathogenic bacterium and the causative agent of most cases of tuberculosis. *M. tuberculosis* has unusual high lipid content in its wall, which makes the cells impervious to Gram staining, so other detection techniques must be used instead.

Primarily a pathogen of the mammalian respiratory system, MTB usually infects the lungs, but it can also affect other parts of the body. It is spread through air by infected people through cough, sneeze or saliva transmission. It is believed that almost one third of the world's population is infected by these bacteria with new infections appearing every second, mostly in developing countries. The World Health Organization (WHO) reports that tuberculosis results to millions of deaths or disabilities each year, especially in poorer areas of

the planet. The problem is exacerbated by the AIDS epidemic that increases disease incidence in developed countries too. However, in addition to tuberculosis, exposure to *Mycobacteria* has also been linked to the pathogenesis of sarcoidosis and Crohn's disease that affect millions of people in Europe only.

Crohn's disease is an inflammatory disease that may affect any part of the gastrointestinal tract from mouth to anus, causing a wide variety of symptoms. Unfortunately, there is no known cure for Crohn's disease, treatment options being restricted to controlling the symptoms.

Sarcoidosis is a disease in which abnormal collections of chronic inflammatory cells (granulomas) form as nodules in a number of organs, most commonly in lungs or the lymph nodes, but virtually any organ can be affected. It commonly improves or clears up spontaneously.

Diagnostic investigation of mycobacterial infections is hampered by the difficulty to detect in a specific manner low populations of mycobacteria or the immunology markers associated with the infections they cause. This is why, new sensitive and specific detection systems for molecular and immunology diagnostic markers associated with infection caused by *M. tuberculosis* complex must be developed.

In order to achieve the proposed goal, core CdSe and core/shell CdSe/ZnS semiconducting quantum dots have been subjected to water solubilisation techniques. Then, oligonucleotides have been conjugated to the surface of highly luminescent quantum dots and further subjected to hybridization with complementary or mismatched target oligonucleotides. The semiconducting quantum dots have been chosen as a signal transducer due to their excellent photoluminescence efficiency and stability. Any modifications that hybridization experiments might cause to the QDs' properties have been followed by photoluminescent means.

Water solubilisation procedures of CdSe quantum dots

CdSe semiconductor quantum dots have been synthesized and supplied to us by our Laboratory's partners, Vinca Institute of Nuclear Sciences, Belgrade, Serbia. Briefly, CdO and tetradecylphosphonic acid (TDPA) were loaded into a three neck flask. At temperatures above 270 °C, the phosphonic acid complexes with the CdO forming a clear and colourless solution that contains cadmium phosphonate complexes. After the formation of the complex, TOP(trioctylphosphine):Se is injected into the flask and initiates the formation of the CdSe nanocrystals. These QDs present TOPO (trioctyl phosphine oxide) functional groups on their surface that render them soluble in organic solvents. The TOPO-covered QDs in hexane present an absorbance maximum at 553 nm (Figure 4.1).

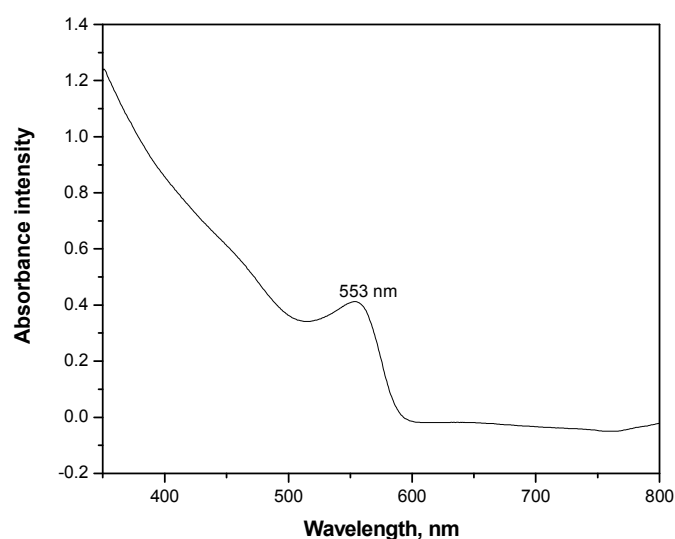


Figure 4.1. Absorption spectrum of the TOPO covered CdSe QDs, in hexane

In order to be able to conjugate the semiconducting QDs to any biological molecule (DNA, enzyme, etc), the TOPO functional groups present on their surface need to be exchanged with ligands that render the QDs water solubility. There are many research groups that have reported on successfully replacing the ligands on the CdSe surface with molecules that make them water soluble [6,14,15]. Preparation of water-soluble CdSe quantum dots (QDs) was experimented according to these methods or with modifications to these methods, using 11-mercaptoundecanoic acid (MUA) and 3-mercaptopropionic acid (MPA) that replace the trioctylphosphine oxide (TOPO) groups from the surface of the QDs and introduce carboxyl moieties.

According to the above mentioned reports, carboxyl-covered CdSe quantum dots are obtained and they can further be functionalized with biological molecules. Unfortunately, all

these methods were tried, without success in providing the necessary water soluble quantum dots. Water-soluble CdSe nanocrystals were finally obtained using mercaptosuccinic acid (MSA) as a surface-modifying agent, according to the procedure described by Zhelev et al. [11]. According to their method, MSA (stock solution in PBS) was added to a solution of QDs in chloroform. Both phases (aqueous and nonaqueous) were shaken intensively for 10 min until the aqueous phase became yellow indicating the replacement of the TOPO ligands from the surface of the QDs with MSA. The mixture was centrifuged for the two phases to separate and the aqueous phase containing water-soluble CdSe QDs was decanted carefully and subjected immediately to ultrafiltration to remove free (non-reacted) MSA. The water-soluble CdSe QDs were further washed with PBS on the same filter, by centrifugation at 3000g. The disadvantage of this method is that water soluble CdSe QDs obtained by this exchange method were not stable as can be seen from Figure 4.2. Figure 4.2a presents the QDs immediately after ligand exchange and water solubilisation, and is presented as a clear orange solution. Figure 4.2b presents the QDs 12 hours after ligand exchange and as it can be observed, a large portion of the QDs had precipitated to the bottom of the vial, rendering them unsuitable for further surface modifications experiments.

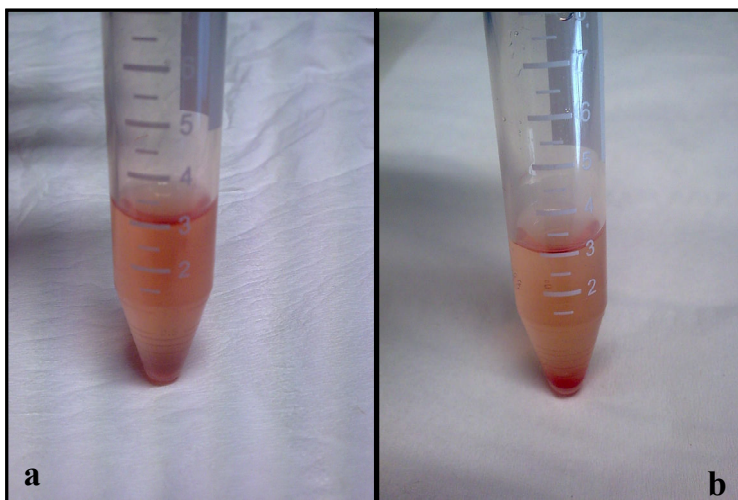


Figure 4.2. CdSe quantum dots: a – 0.5 hours after ligand exchange;
b – 12 hours after ligand exchange

The problem encountered with the prepared water soluble quantum dots was confirmed by photoluminescence measurements. The spectra presented in Figure 4.3 represent the photoluminescence spectra of TOPO-capped and MSA-capped CdSe. Upon water solubilisation by replacement of TOPO groups with MSA on the surface of the quantum

dots, the fluorescence spectrum registers a drastic decrease of the photoluminescence signal. Nevertheless, experiments were undertaken to conjugate amino-modified oligonucleotides and enzymes to the surface of the water soluble quantum dots, but in all cases the result was their complete precipitation from solution within a couple of hours.

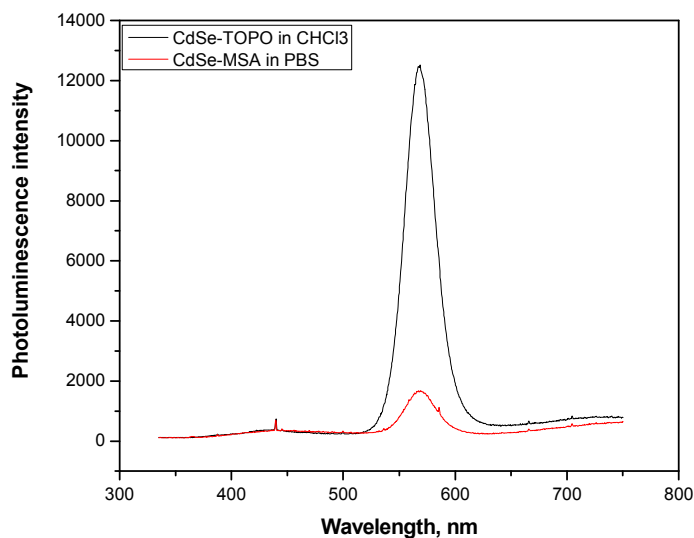


Figure 4.3. Photoluminescence spectra of TOPO-covered (in hexane) and MSA-capped (in PBS) CdSe QDs

Water solubilisation procedures of CdSe/ZnS quantum dots

We did then redirect our attention to core-shell quantum dots. These QDs are highly fluorescent in the visible spectrum and the passivating shell used to cover the CdSe core enhances their chemical- and photostability. CdSe/ZnS core/shell semiconductor quantum dots have been synthesized and supplied to us by our Serbian partner. Briefly, CdSe nanocrystals synthesized by TOP/TOPO method described above were isolated as powders and then redispersed in hexane. Equimolar amounts of Zn (diethylzinc – ZnEt_2) and S (hexamethyldisilathiane – $(\text{TMS})_2\text{S}$) precursors were dissolved in TOP inside a glove box, loaded into a syringe, and injected drop wise (over a period of 5–10 min) in the vigorously stirred reaction mixture placed in a heated flask. After addition, the mixture was cooled to 90°C and stirring was continued for several hours. Butanol was added to keep the TOPO from solidifying. The ZnS coated CdSe particles were stored in TOPO to ensure surface passivation.

Water solubilisation of CdSe/ZnS core/shell QDs has been experimented according to Choi et al. [16] and Pong et al. [17] with the same results as for CdSe QDs.

This led us to the decision to purchase water soluble QDs from an outside source. Water soluble CdSe/ZnS quantum dots linked on the surface with MUA units were purchased from Nanomaterials & Nanofabrication Laboratories (NN-Labs), for further experiments. A TEM micrograph of the mercaptoundecanoic acid capped CdSe/ZnS QDs is presented in Figure 4.4. We can observe that these QDs are well defined, mainly spherically shaped, and with a diameter of ~ 5 nm.

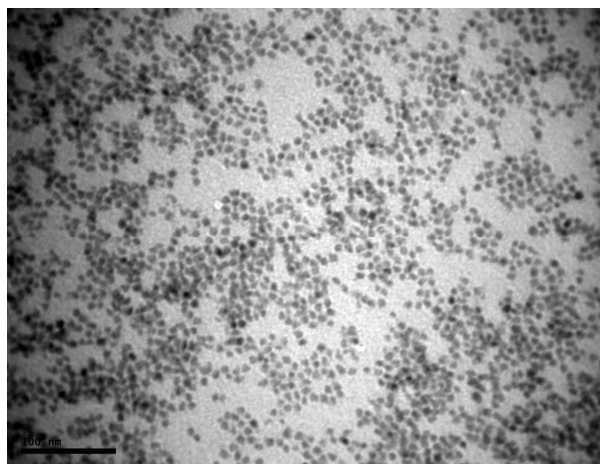


Figure 4.4. MUA-capped CdSe/ZnS QDs (bar 100nm)

Preparation of QD – oligonucleotide conjugates

CdSe/ZnS modified with oligonucleotides have been obtained by conjugating amino-terminated oligonucleotides with the carboxyl groups present on the surface of the QDs, through the coupling reaction of N-ethyl-N'-(3-dimethylaminopropyl) carbodiimide (EDC) and N-hydroxysulfosuccinimide (sulfo-NHS). EDC is one of the most used cross-linking agents to couple carboxyl groups to primary amines. It reacts with a carboxyl group to form an amine-reactive *O*-acylisourea intermediate that further, upon addition of sulfo-NHS, produces a semi-stable amine reactive NHS ester.

In a plastic tube, to 0.25 nmol of dark red QDs, stock solutions of EDC (1.5 mg/mL) and NHS (1.5 mg/mL) and TB buffer were added and left to react for 30 min. Then, 25 μ L of 100 pmole oligonucleotide stock solution were added and reacted for another 4 hours with gentle stirring. As a follow up, the QD-oligo conjugates were separated from any possible unbound oligonucleotide by 4 rounds of centrifugation/washing (5000 rpm, 60 min) with TB buffer (pH 7.4) on a Millipore Amicon Ultra filter with a molecular weight cutoff, MWCO, of 10,000. The first centrifugation step was also used to verify the success of the conjugation

procedure, since unconjugated CdSe/ZnS QDs are not stopped by the filter and they are found in the lower phase. The lower phase was subjected to fluorescence measurements and no signal was recorded. Oligonucleotide-modified QDs were used immediately for the hybridization experiment. The conjugates stock solution was stored at 4°C.

Table 4.1 presents the 30-bases oligonucleotide sequence used in these experiments, as well as the complementary and mismatched strands. Stock solutions were prepared in tris-boric acid buffer (TB buffer) to a concentration of 100 pmol/μL and kept in freezer.

Table 4.1. Oligonucleotide sequences (the mismatched bases are written in red)

Description	Name	Sequence
Amino-modified oligonucleotide		NH ₂ -5'-TCG AAC TCG AGG CTG CCT ACT ACG CTC AAC-3'
100% complementary	100%	5' – GTT GAG CGT AGT AGG CAG CCT CGA GTT CGA – 3'
1 mismatch	1m	5' – GTT GAG CGT AGT AGA CAG CCT CGA GTT CGA – 3'
2 mismatches	2m	5' – GTT GAG CGC AGT AGG CAG CCT CGG GTT CGA – 3'
6 mismatches	6m	5' – GTT GAG CGT AGT AGG CAG CCT CGA ACC TAC – 3'
12 mismatches	12m	5' - GTT GAG CGT AGT AGG CAG AAC TAG ACC TAC – 3'

Hybridization with target oligonucleotides experiment

In an Eppendorf tube, 20μL of QD-oligo, 275 μL of hybridization buffer and 5 μL of complementary sequence were mixed, heated to 95°C for 5 minutes and then left to slowly cool on the working bench. For fluorescence measurements, the solution was diluted to 1000 μL with TB buffer. Same procedure was followed for hybridization experiments with mismatched bases sequences. All experiments were performed in duplicate.

As reported by the group of Algar and Krull [18,19], oligonucleotides covalently attached or adsorbed to the surface of quantum dots have a conformation that lies along their surface. Figure 4.5 represents the schematic of the QD – oligonucleotide conjugation and of the hybridization with the targets in accordance with these reports.

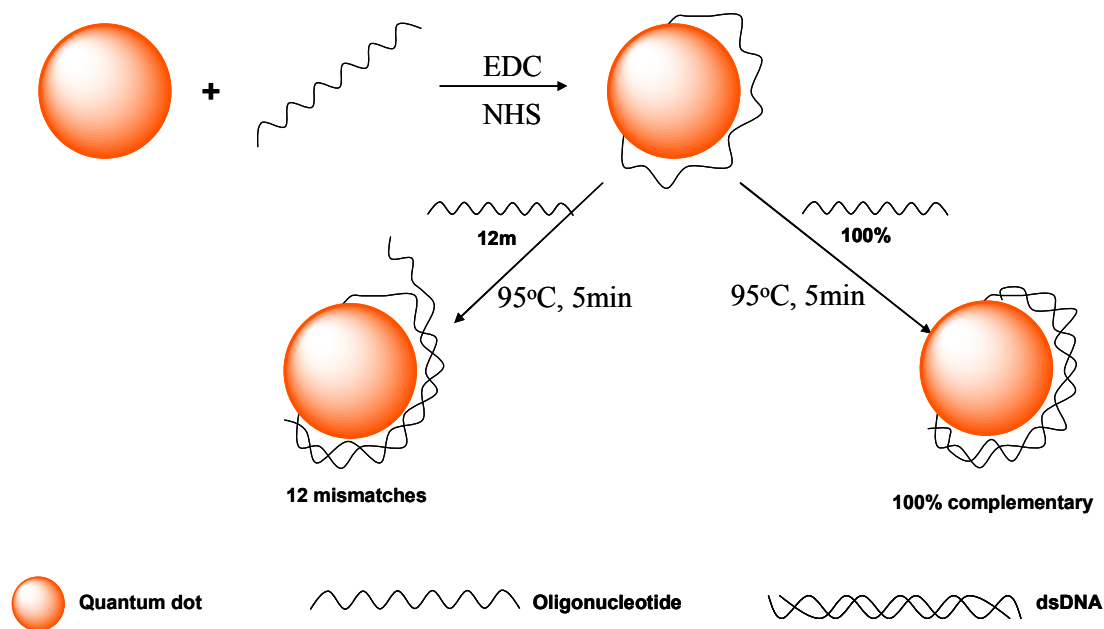


Figure 4.5. Schematic representation of the hybridization experiment

Figure 4.6 presents the fluorescence signal of the oligonucleotide-modified QDs before and after development of the hybridization experiment. Heating of the complexes to 95°C and the formation of the double stranded DNA sequence, results in an enhancement of the fluorescence fingerprint.

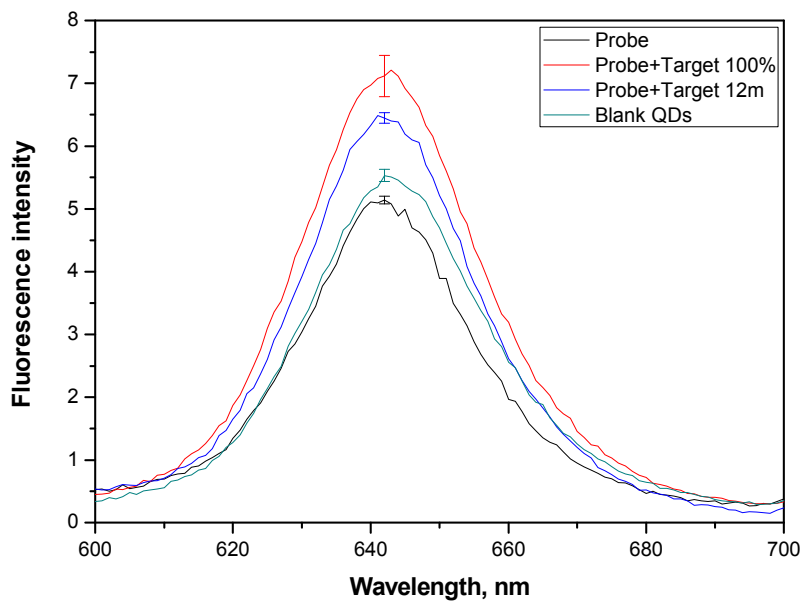


Figure 4.6. QD-oligonucleotide probe before (black line) and after hybridization with the 100% (red line) and 12m (blue line) targets, and QD blank (green line) after heating at 95°C for 5 min

The increase in the fluorescence signal intensity was obvious and of the same order of magnitude for the 100%, 1m, 2m and 6m target oligonucleotides. As far as the 12 mismatched base pairs is concerned, an increase of the fluorescence signal can also be observed, but to a smaller extent as compared to the other target oligonucleotides. As a next step, we wanted to check how the QDs react to the hybridization conditions (heating at 95°C for 5 minutes). For this we have subjected them to heating, and after cooling down we have recorded their fluorescence. We can observe from Figure 4.6 that heating results in an increase of the QDs fluorescence signal, but to a smaller extent than for the QDs conjugated to probe oligonucleotide and hybridized with targets.

The fact that an increase in the fluorescence signal was also recorded in the case of the bare QDs, lead us to conclude that it is due to modifications that appear in the QDs structure and not as a result of hybridization to oligonucleotides. As reported by a study published in 2009 [20], the photoluminescence of core/shell quantum dots is indeed temperature dependent. The authors attributed the increase in QDs fluorescence upon heating to delocalization of the carriers localized at the core – shell interface states induced by atom diffusion or lattice strain. Further experiments in collaboration with a team of physicists should be carried out in order to elucidate this phenomenon in the case of our QD-oligonucleotide conjugates.

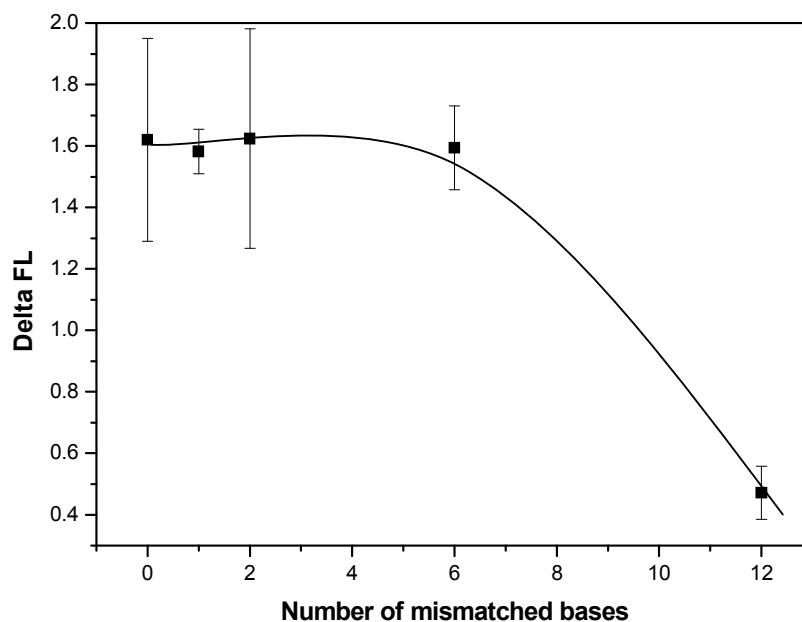


Figure 4.7. The relative increase in fluorescence as a function of mismatched base pairs

In order to make sure that the observed increase in fluorescence of our hybridized samples is due to DNA formation and not to the phenomenon observed for the bare QDs, we have subtracted the intensity of the QD-oligonucleotide peak, both before and after heating, from the values of the QD-DNA fluorescence peak, and plotted the obtained values as a function of number of mismatched base pairs (Figure 4.7).

Figure 4.7 confirms the observations presented earlier, proving that hybridization of the QD-oligonucleotide conjugates to different target oligonucleotides produces an increase in the fluorescence signal. There is no visible difference between the 100% complementary, 1 mismatch, 2 mismatches and 6 mismatches samples, all recording an obvious increase of the fluorescence signal after completion of the hybridization experiment. As far as the sample containing 12 mismatched base pairs is concerned, the increase recorded is far less impressive.

Conclusions

From the data presented we can conclude that oligonucleotide-modified core/shell CdSe/ZnS quantum dots are useful tools in detecting large sequences of mismatched bases through the hybridization process, thus finding possible applications in detecting mutations of DNA sequences. The mechanisms that lie behind this phenomenon are still not well understood. Further experiments will be undertaken leading to a better understanding of the phenomenon and improving of the method.

References

1. W.C.W. Chan and S. Nie, Quantum dot bioconjugates for ultrasensitive nonisotopic detection, *Science*, 1998, 281, 2016–2018
2. D.M. Willard, L.L. Carillo, J. Jung, A. Van Orden, CdSe-ZnS quantum dots as resonance energy transfer donors in a model protein–protein binding assay, *Nano Lett.*, 2001, 1(9), 469-474
3. F. Patolski, R. Gill, Y. Weizmann, T. Mokari, U. Banin, I. Willner, Lighting-up the dynamics of telomerization and DNA replication by CdSe-ZnS quantum dots, *J. Am. Chem. Soc.*, 2003, 125, 13918-13919
4. Clapp A.R., Medintz I.L., Mauro J.M., Fisher B.R., Bawendi M.G., Mattoussi H., Fluorescence resonance energy transfer between quantum dot donors and dye-labeled protein acceptors, *J. Am. Chem. Soc.*, 2004, 126, 301-310
5. V.R. Hering, G. Gibson, R.I. Schumacher, A. Faljoni-Alario, M.J. Politi, Energy transfer between CdSe/ZnS core/shell quantum dots and fluorescent proteins, *Bioconj. Chem.* 2007, 18, 1705-1708
6. Y.S. Liu, Y. Sun, P.T. Vernier, C.H. Liang, S.Y.C. Chong, M.A. Gundersen, pH-sensitive photoluminescence of CdSe/ZnSe/ZnS quantum dots in human ovarian cancer cells, *J. Phys. Chem. C.*, 2007, 111, 2872-2878
7. C.P. Huang, Y.K. Li, T.M. Chen, A highly sensitive system for urea detection by using CdSe/ZnS core-shell quantum dots, *Biosens. Bioelectron.*, 2007, 22(8), 1835-1838
8. C.P. Huang, S.W. Liu, T.M. Chen, Y.K. Li, A new approach for quantitative determination of glucose by using CdSe/ZnS quantum dots, *Sens. Actuators B*, 2008, 130(1), 338-342
9. D. Du, S. Chen, D. Song, H. Li, X. Chen, Development of acetylcholinesterase biosensor based on CdTe quantum dots/gold nanoparticles modified chitosan microspheres interface, *Biosens. Bioelectron.*, 2008, 24, 475-479
10. L. Tang, Y. Zhu, X. Yang, J. Sun, C. Li, Self-assembled CNTs/CdS/dehydrogenase hybrid-based amperometric biosensor triggered by photovoltaic effect, *Biosens. Bioelectron.*, 2008, 24(2), 319–323
11. Z. Zhelev, R. Bakalova, H. Ohba, R. Jose, Y. Imai, Y. Baba, Uncoated, broad fluorescent, and size-homogeneous CdSe quantum dots for bioanalyses, *Anal. Chem.*, 2006, 78(1), 321–330
12. Z. Kaul, T. Yaguchi, S.C. Kaul, T. Hirano, R. Wadhwa, K. Taira, Mortalin imaging in normal and cancer cells with quantum dot immunoconjugates, *Cell Res.*, 2003, 13, 503-507

13. S.J. Rosenthal, I. Tomlinson, E.M. Adkins, S. Schroeter, S. Adams, L. Swafford, J. McBride, Y. Wang, L.J. DeFelice, R.D. Blakely, Targeting cell surface receptors with ligand-conjugated nanocrystals, *J. Am. Chem. Soc.*, 2002, 124, 4586-4594
14. J. Aldana, Y.A. Wang, X. Peng, Photochemical instability of CdSe nanocrystals coated by hydrophilic thiols, *J. Am. Chem. Soc.*, 2001, 123, 8844-8850
15. Q. Zhang, T. Xu, D. Butterfield, M.J. Misner, D.Y. Ryu, T. Emrick, T.P. Russell, Controlled placement of CdSe nanoparticles in diblock copolymer templates by electrophoretic deposition, *Nano Lett.*, 2005, 5, 357-361
16. H.S. Choi, W. Liu, P. Misra, E. Tanaka, J.P. Zimmer, B.I. Ipe, M.G. Bawendi, J.V. Frangioni, Renal clearance of quantum dots, *Nat. Biotechnol.*, 2007, 25(10), 1165-1170
17. B.K. Pong, B.L. Trout, J.Y. Lee, Modified ligand-exchange for efficient solubilisation of CdSe/ZnS quantum dots in water: a procedure guided by computational studies, *Langmuir*, 2008, 24, 5270-5276
18. M. Massey, W.R. Algar, U.J. Krull, Fluorescence resonance energy transfer (FRET) for DNA biosensors: FRET pairs and Forster distances for various dye-DNA conjugates, *Anal. Chim. Acta*, 2006, 568, 181-189
19. W.R. Algar and U.J. Krull, Adsorption and hybridization of oligonucleotides on mercaptoacetic acid-capped CdSe/ZnS quantum dots and quantum dot-oligonucleotide conjugates, *Langmuir* 2006, 22, 11346-11352
20. P. Jing, J. Zheng, M. Ikezawa, X. Liu, S. Lv, X. Kong, J. Zhao, Y. Masumoto, Temperature-dependent photoluminescence of CdSe-Core CdS/CdZnS/ZnS-multishell quantum dots, *J. Phys. Chem. C*, 2009, 113, 13545-13550

CHAPTER 5 – A PHOTOLUMINESCENT ACETYLCHOLINESTERASE-BASED BIOSENSOR

As seen in the previous Chapter, semiconducting quantum dots have been used in a wide variety of applications, as stable inorganic fluorophores [1,2], as immobilization platforms for biomolecules [3-5], for the construction of sensors and biosensors [6-9] to mention only a few of them. However, besides their obvious advantages, some of the semiconductor QDs have the drawback of being toxic, and thus less favourable for bio-applications [10]. This may be due to photochemical processes resulting in the irradiation of QDs under the aqueous aerobic conditions of in-vitro cell imaging [11], the process having as result the release of toxic free Cd^{2+} ions. However, in a recently published study [12], Graf and co-workers report on a 3-4 times lower release of toxic Cd^{2+} ions from CdSe/ZnS QDs doped silica colloids than those released from CdSe/ZnS QDs simply stabilized by organic ligands or biomolecules, result which indicates that coating the quantum dots delays this process and thus renders them suitable markers for in-vivo studies. In a paper published 3 years before the study of Graf and co-workers, silica-coated QDs showed no cytotoxic effects in cell lines investigated with concentration as high as 30 μM [13]. These results indicate that entrapment of the semiconductor QDs within silica provides the necessary protection from chemical degradation, reduce the degree of leaching of the toxic core material [14] and also present the advantages of hydrophilicity, biocompatibility, optical transparency and chemical stability.

In particular, QDs coated with silica shells have been widely investigated. Up until now, many methods have been reported to coat QDs with a silica shell through (a) Stöber-based approaches [15,16], (b) by reverse (water in oil) microemulsion method [17-20], or by (c) promoting silicification by enzymes, such as silicatein [21], or polysaccharides, such as chitosan [22]. Some groups have reported on immobilizing proteins onto silica coated quantum dots [23,24] the complex obtained being suitable for use in biolabelling and imaging. Of special interest are the experiments performed for encapsulating enzymes within a silica matrix. Sol-gel is a widely used method for immobilization of enzymes [25-27] but due to harsh processing conditions that result in a loss of enzyme activity, new, milder methods of silicification, namely biosilicification, that use more biologically compatible reaction conditions, have been studied [28]. By using this method, the complete entrapment of

the enzymes within the silica matrix has been confirmed, while, at the same time, managing to retain almost all of the initial activity of the enzyme. Recently, our group has studied the biosilicification of carbon nanofibers-immobilized enzymes, using a poly-L-lysine (PLL) templated silica matrix [29,30], proving that this approach is suitable for stabilizing enzymes and protect them from denaturation.

The aim of the present study was to develop a simple photoluminescent biosensor system for the detection of enzymatic reaction. In order to achieve this goal, the enzyme of choice was covalently immobilized onto the surface of highly luminescent core/shell semiconductor CdSe/ZnS quantum dots and the conjugates were further covered with poly-L-lysine (PLL) as template for the formation of bioinspired silica shell. This nanocomposite is used as a transduction and stabilization system for optical biosensor development. CdSe/ZnS quantum dots have been chosen as a signal transducer due to their excellent photoluminescence efficiency and stability while they are also used for the covalent immobilization of the enzyme. Poly-L-lysine is a positively charged homo-polypeptide which interacts electrostatically with DNA, red cell membrane and any negatively charged protein. In this case, it provides the template for the formation of biomimetically synthesized silica [31]. The pores of the poly-L-lysine templated silica matrix allow the transport of the substrate to the entrapped QD/enzyme conjugates and its subsequent conversion to products. The conjugation to the QDs and the entrapment inside the stable silica matrix is believed to increase the stability of this relatively unstable enzyme, protecting it from unfolding, denaturation and attack from proteases [29]. Also, the poly-L-lysine templated silica matrix is expected to protect the QDs from chemical degradation and leaching of the toxic core materials [12-14,32]. The catalytic reaction carried out by the enzyme was evaluated by monitoring the changes in the QDs' photoluminescence which are related to the changes of pH. These pH changes of the surrounding environment of the QDs are induced by the enzymatic reaction, and are associated with the analyte concentration in the solution. The work presented here is the first report on entrapment of QD/AChE conjugates into a poly-L-lysine (PLL) templated silica matrix and their use in photoluminescent biosensors.

In the present work, the enzyme Acetylcholinesterase from the fly *Drosophila melanogaster* (*Dm.* AChE) has been used, and for this reason, a few words about the enzymatic activity of this enzyme will follow. The covalent immobilization of the enzyme during the formation of the biomimetically synthesized silica is used here as a model, relatively unstable enzyme, as a proof of principle.

Acetylcholinesterase (AChE)

Acetylcholine-mediated neurotransmission [33] is fundamental for the proper function of the nervous system. Acetylcholine is a neurotransmitter that triggers neural responses, and its hydrolysis by acetylcholinesterase (AChE) is the fundamental step in the path to controlling and regulating the neural responses. The abrupt blockade of acetylcholine is lethal, and its gradual loss, as in Alzheimer's disease [34], multiple system atrophy [35] and other conditions [36], is associated with progressive deterioration of cognitive, autonomic and neuromuscular functions. Acetylcholinesterase hydrolyses and inactivates acetylcholine, thereby regulating the concentration of the transmitter at the synapse. The acetylcholine molecules are being synthesized in the presynaptic membrane through the transport of an acetyl group of the acetyl CoA to choline and retention by the synaptic vesicles of the presynaptic membrane. Upon arrival of a nervous impulse, acetylcholine is being released from the synaptic vesicles into the synaptic cleft and diffused to the post-synaptic membrane where it binds to special receptors (Figure 5.1).

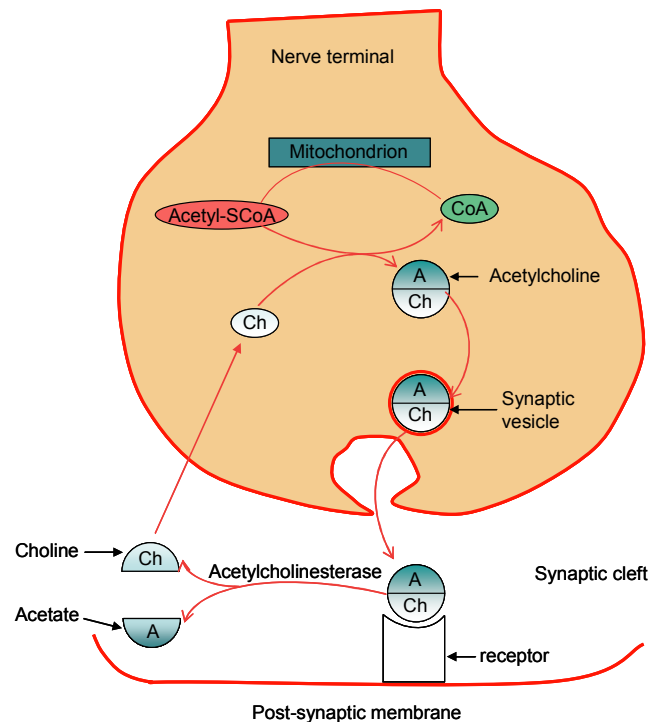


Figure 5.1. Schematic representation of the cholinergic synapse

This process alters the ionic permeability of the post-synaptic membrane, and results in a depolarization of the membrane, allowing for the transmission of electrical stimulation along the membrane of the second nerve cell. The role of acetylcholinesterase in the process

of neurotransmission is to hydrolyze acetylcholine in order to restore the polarization of the post-synaptic membrane. The rate by which acetylcholinesterase hydrolyzes acetylcholine is very fast (40msec), fact which allows for the rapid restoration of the membrane's excitability. Termination of activation is normally dependent on the dissociation of acetylcholine from the receptor and its subsequent diffusion and hydrolysis, except in diseases where acetylcholine levels are limiting or under AChE inhibition, conditions that increase the duration of receptor activation [37].

Acetylcholinesterase belongs to the family of α/β hydrolases and is found in many different forms such as monomer, dimer and tetramer. The crystalline structure of the enzyme varies with the source from which it originates, insects, nematodes, fish, reptiles, birds or mammals, but, regardless of their provenience, there are common structural features which are essential for the catalytic activity of the enzyme and found to be fundamentally similar [38-40].

Surprisingly for an enzyme with an extraordinarily rapid catalytic reaction, structural studies have revealed that its active site is buried in a 20 Å deep gorge which contains aromatic residues resulting in the channel being narrow at its entrance and wider at the bottom (Figure 5.2) [41].

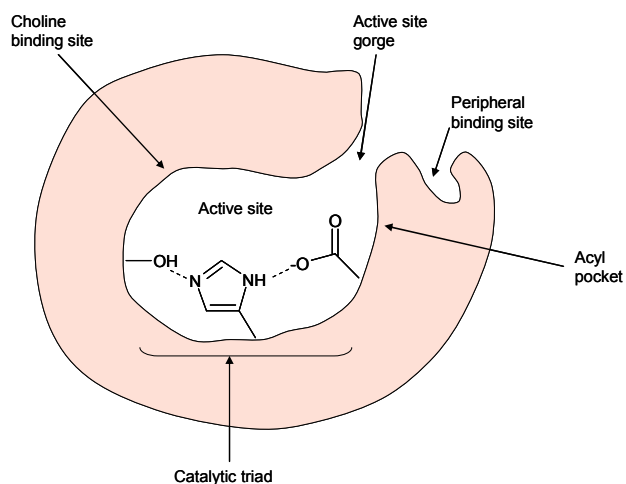


Figure 5.2. Structural features of the acetylcholinesterase

According to a recently developed kinetic model, the substrate and product molecules follow the same path [42]. The substrate molecule first binds to the peripheral site found at the entrance of the gorge [43]. This site facilitates the approach of the substrate to the catalytic center through electrostatic interactions, where it is hydrolyzed. The products escape the

gorge via the entrance. The active site gorge is too narrow to allow the crossing between a substrate molecule en route to the catalytic site and a product molecule en route to the exit. Consequently, at very high substrate concentrations, there is a traffic jam preventing the exit of the reaction product through the main entrance, resulting in inhibition [44].

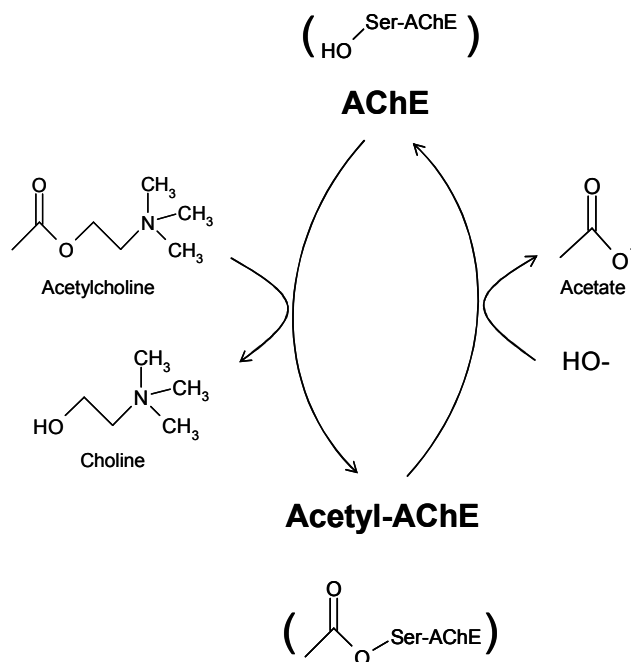


Figure 5.3. The acetylcholinesterase reaction

The catalytic site of the AChE contains a catalytic triad — serine, histidine and an acidic residue – as do the catalytic sites of the serine proteases. However, the acidic group in AChE is a glutamate, whereas in most other cases it is an aspartate residue. The nucleophilic nature of the carboxylate is transferred through the imidazole ring of histidine to the hydroxyl group of serine, allowing it to displace the choline moiety from the substrate, forming an acetyl–enzyme intermediate (Figure 5.3). A subsequent hydrolysis step frees the acetate group and regenerates the enzyme [45].

Detection method and assay conditions

The monitoring of an enzymatic reaction usually takes place by tracing its products. When these products are either bases, or acids, a change in the solution pH is observed, and thus, monitoring of the concentration of the enzyme's substrate through the pH changes is possible. The enzyme used in this study, acetylcholinesterase, hydrolyses the substrate acetylcholine producing choline and acetic acid as it is shown in the following scheme:



The surface of the CdSe/ZnS core-shell quantum dots used in these experiments is composed of mercaptoundecanoic acid (MUA) chains which are pH sensitive. In order to test the effect that the acetic acid produced by the enzymatic reaction would have on the quantum dots, we have added pure acetic acid to a solution of mercaptoundecanoic acid coated CdS/ZnS quantum dots. Their response is presented in Figure 5.4:

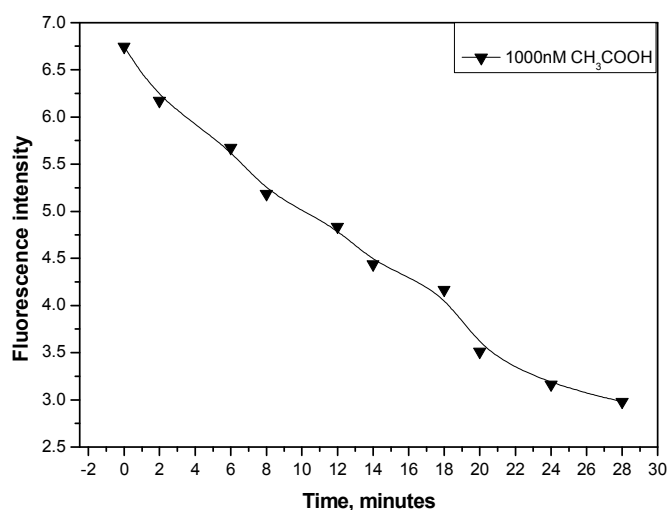


Figure 5.4. The photoluminescence response of the CdSe/ZnS quantum dots upon addition of acetic acid (excitation 470 nm)

We can clearly observe that the photoluminescence signal decreases dramatically within a few minutes after addition of the acetic acid to the quantum dots, indicating a fast response to the stimuli. This also indicates that a similar response should be expected for all the MUA-covered QDs systems to be further constructed and used in experiments, with their photoluminescence decreasing over time.

To study the effect that pH has on the photoluminescence intensity of the MUA-covered QDs, a series of solutions with different pH values (in the range 4.84 – 8.93) were prepared by adding various amounts of KOH (1.0 M) to a 2.0 mL MES buffered solution (1.0 mM, pH 4.55). For the assay, 10.0 μL of MUA-covered QDs were mixed with 990.0 μL of the pH solution and left to stabilize for 20 min before recording the photoluminescence spectra. All experiments were repeated in triplicate. As can be seen from Figure 5.5, there is a linear relationship between the pH value of the solution and the photoluminescence signal of the QDs for a pH range between 5.45 and 7.54. Knowing that the production of acetic acid during the enzymatic reaction will alter the pH of the immediate surroundings of the QDs causing a decrease in their fluorescence, and in order to ensure the highest possible photoluminescence sensitivity upon developing of the enzymatic reaction, together with a wide dynamic range, pH 7.0 was chosen for all buffer solutions, a value very close to the highest limit of the linear range.

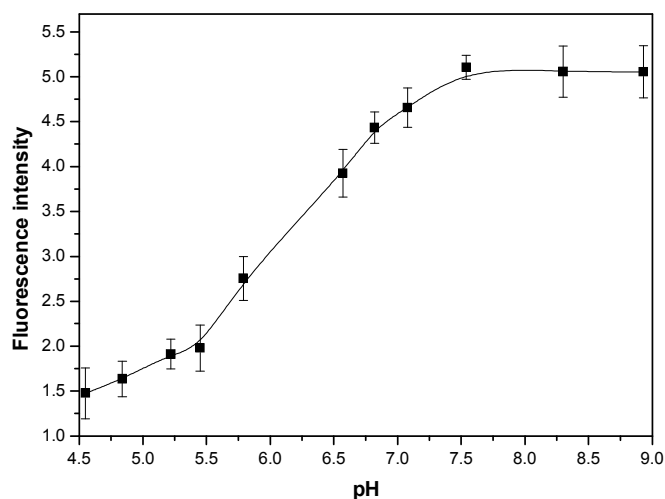


Figure 5.5. The photoluminescence signal of the CdSe/ZnS core/shell quantum dots (excitation 470 nm) recorded at different pH values

After determining the pH of the working solution to be used in all further experiments, we have proceeded with the conjugation of AChE onto the CdSe/ZnS quantum dots. A portion from the obtained bioconjugates was further subjected to entrapment into biomimetically synthesized silica.

Preparation of QD/AChE conjugates

The covalent immobilization of *Dm.* AChE on the carboxyl-covered QDs was performed through the coupling reaction of EDC and sulfo-NHS, the details of which have been described in Chapter 4. 1000.0 μL of EDC (2.0 mg/mL) and sulfo-NHS (6.0 mg/mL) stock solutions (prepared in phosphate buffer KH_2PO_4 , 25.0 mM, pH 7.0) were mixed together with a solution of QDs in phosphate buffer and the reaction mixture was allowed to stir for 2 hours at room temperature. Subsequently, 1000.0 μL of *Dm.* AChE (2.0 U/mL) stock solution were added and after other 2 hours of vortexing at room temperature, the mixture was placed at 4°C overnight. This step was found to be essential for the successful conjugation of the enzyme to the quantum dots. As a follow up, the QD/AChE conjugates were separated from any unbound enzyme still present in the mixture, by 3 rounds of centrifugation/washing (4000 rpm, 15 min) with phosphate buffer on a Millipore Amicon Ultra filter with a molecular weight cutoff of 100,000. At the end of the initial centrifugation cycle, the lower phase was checked for *Dm.* AChE activity according to Ellman's method [46], by comparing the initial activity of the enzyme (before conjugation) with the activity of the enzyme that remained free in solution after the conjugation experiment. This method is based on the enzymatic consumption of the substrate acetylthiocholine iodide with production of acetic acid and thiocholine. Subsequently, thiocholine reacts with the dithionitrobenzoic acid present in the Ellman reagent solution and produces the change of the solution's colour to yellow, due to the production of thionitrobenzoic acid. The change in colour is followed spectrophotometrically at 412 nm. From the slope of the absorbance curve as a function of time we then calculate the activity of the enzyme in units of $\text{Abs min}^{-1} \text{mL}^{-1}$. According to this method, only negligible AChE activity was detected in the lower phase, indicating that almost all of the enzyme was successfully conjugated to the surface of the CdSe/ZnS quantum dots.

Preparation of poly-L-lysine templated QD/AChE/PLL/silica nanocomposites

For the bio-inspired silicification reaction, a 1.0 mM PLL solution was added to the QD/AChE conjugates. The role of PLL is to produce a large number of amine groups around the conjugates, fact that facilitates the biosilicification process. After 30 min of vortexing at room temperature, the mixture was stored at 4°C overnight. The next day, a freshly prepared solution of silicic acid (fresh stock solution prepared by tetramethyl orthosilicate (TMOS) hydrolysis at a concentration of 1.0 M with 1.0 mM HCl solution) and nanopure H_2O were added, and after mixing in a vortex for approx 4 hours at room temperature, the nano-complexes were subjected to 4 rounds of centrifugation/washing with phosphate buffer, at

4000 rpm. The washed silica biomimetic composites were stored at 4°C in phosphate buffer for further use. Poly-L-lysine templated silica and AChE/PLL/silica nanocomposites were prepared according to a method recently published by our laboratory [29,30] by adding the corresponding amounts of phosphate buffer (for poly-L-lysine templated silica) and *Dm.* AChE (for AChE/PLL/silica nanocomposites) respectively. The isoelectric point of *Dm.* AChE is 5.0 [29], thus, at the pH where all experiments are performed (pH 7.0), the enzyme is negatively charged. The electrostatic interaction between the negatively charged enzyme and the positively charged poly-L-lysine template promotes the entrapment of the enzyme during biosilicification.

The schematic diagram for the development of the QD/AChE/PLL/silica nanocomposites is presented in Figure 5.6. In the first step, the enzyme acetylcholinesterase is covalently conjugated to the mercaptoundecanoic acid groups present on the surface of water soluble CdSe/ZnS quantum dots, through the coupling reaction of EDC and NHS. As a follow up, the QD/AChE conjugates were entrapped into the biomimetically synthesized silica matrix following a two step process: formation of a basic PLL template on top of which the biosilica is being formed. In this way, a solid matrix that completely entraps the QD/AChE conjugates is created. At the same time, the biomimetically synthesized silica matrix possesses pores that allow for the substrate to enter its cavities and reach the enzyme, thus allowing for the enzymatic reaction to take place. The catalytic reaction of AChE is followed by the photoluminescence changes of the CdSe/ZnS core/shell quantum dots.

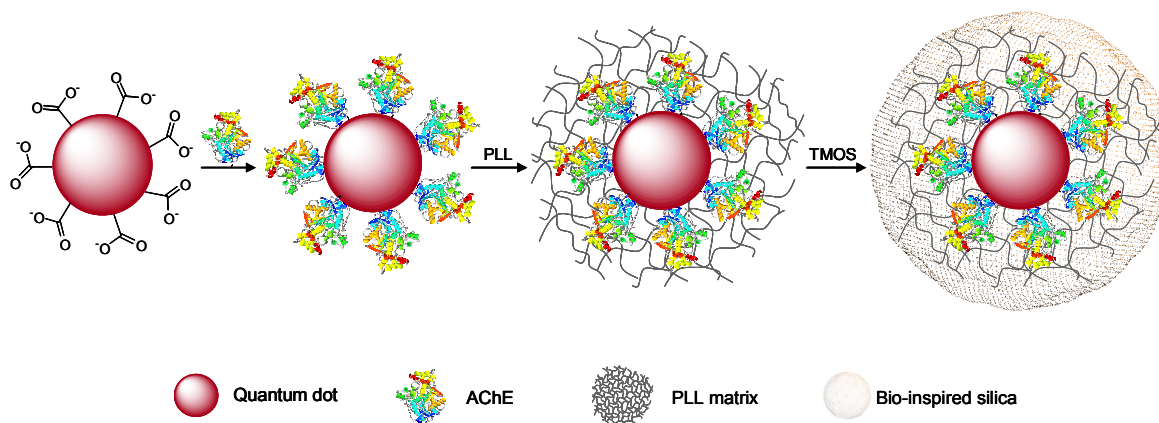


Figure 5.6. Schematic representation of the development of the QD/AChE/PLL/silica nanocomposites

Verification of successful conjugation and biosilicification by fluorescence measurements

In order to verify the successful conjugation of the enzyme to the surface of the QDs and the formation of the bio-inspired silica shell around the quantum dots/enzyme conjugates, fluorescence spectroscopy was employed. Fluorescence spectra have been recorded on an Aminco-Bowman series 2 luminescence spectrometer equipped with a continuous high power xenon lamp. All samples were analyzed at room temperature with excitation and emission slits set at 4 nm band-pass and a scan rate of 3 nm/s. Figure 5.7 presents the photoluminescence spectra of CdSe/ZnS QDs prior to any modification (solid line) and of the QD/AChE/PLL/silica nanocomposites (dashed line). It can be observed that the photoluminescence spectrum of the QDs entrapped into the bio-inspired silica does not show any significant shift in comparison to the bare QDs, which proves that the bioconjugation and encapsulation processes do not result in major changes of the QD' surface that would influence their photoluminescence.

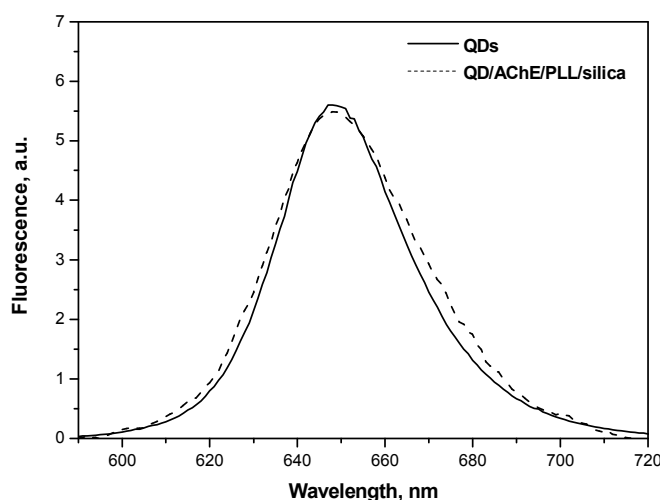


Figure 5.7. Photoluminescence spectra of CdSe/ZnS QDs prior to modifications (solid line) and of QD/AChE/PLL/silica nanocomposites (dashed line) (excitation 470 nm)

Determination of the QD/AChE/PLL/silica nanocomposite's morphology

The morphology of the formed QD/AChE/PLL/silica nanocomposites was determined by means of high resolution transmission electron microscopy (HR-TEM). Figure 5.8 represents the HR-TEM image of the mercaptoundecanoic acid-capped CdSe/ZnS QDs after entrapment into the bio-inspired silica matrix. The samples for HR-TEM analysis were prepared by evaporation of droplets placed on Formvar/Carbon coated TEM grids. The

solvent was allowed to evaporate under atmospheric conditions. As it can be seen from this image, the biosilicification process produced uniform structures which completely encapsulate and protect the QDs within the silica matrix without producing their aggregation. The formed poly-L-lysine templated silica nanocomposites are mainly spherical, with a size distribution from 45 to 85 nm in diameter (main population with an average diameter of 63 nm) while an average of 6 QDs are entrapped in each nanocomposite. Occasionally, biosilica structures that do not encapsulate QDs are also observed, this being a phenomenon frequently encountered in such processes.

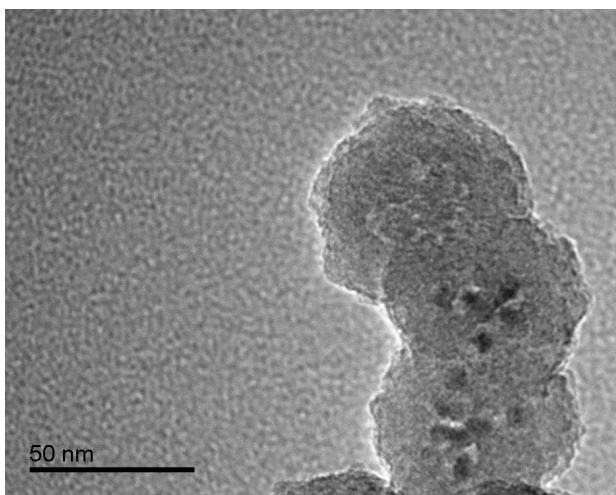


Figure 5.8. HR-TEM image of the semiconducting QDs after entrapment into the bio-inspired silica matrix

Verification of successful biosilicification by ATR-FT-IR measurements

The efficient entrapment of QD/AChE conjugates within the silica architecture was also examined by ATR-FT-IR spectroscopy. The infrared region of the light spectrum is very useful for analysis of organic compounds. Photon energies associated with the 2500 to 16000 nm range of the spectrum are not large enough to excite electrons, but may induce vibrational excitation of covalently bonded atoms and groups [47]. Covalent bonds can be stretched, bended, rotated around their axis, scissored, etc, all these motions being characteristic of their component atoms. Consequently, almost all organic compounds will absorb infrared radiation that corresponds to the energy of these vibrations, giving scientists a unique image of the molecules' structure.

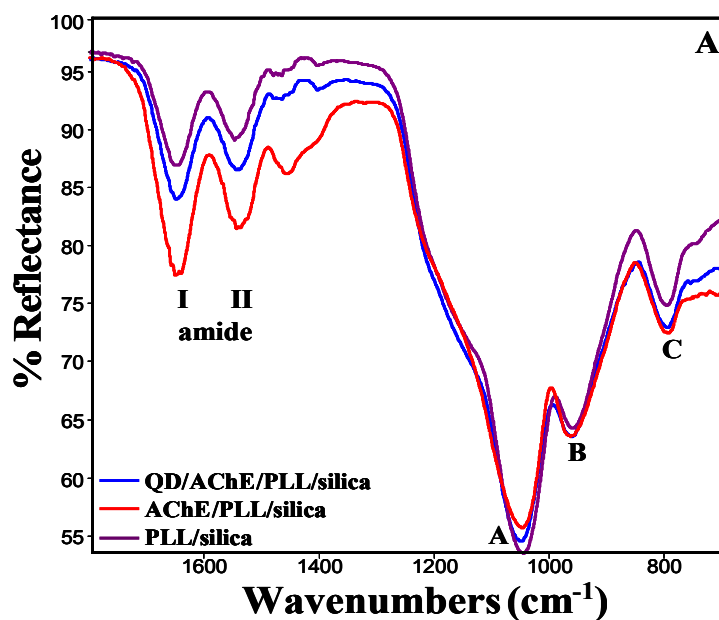


Figure 5.9. ATR-FT-IR spectra of bio-inspired silica nanocomposites: PLL/silica, AChE/PLL/silica and QD/AChE/PLL/silica

The spectrum of the poly-L-lysine templated QD/AChE/silica nanocomposites was recorded and subsequently compared to those of poly-L-lysine templated silica nanocomposites and of poly-L-lysine templated AChE/silica nanocomposites. The ATR-FT-IR spectra present the characteristic peaks of the amide I and amide II bands in the region 1400-1700 cm^{-1} as well as the peaks of biosilica, denoted A, B and C, in the region 760-1300 cm^{-1} (Figure 5.9).

Amide I and II vibrations of the polypeptide backbone are very sensitive to changes that might appear in the secondary conformations [48,49] and thus they are closely monitored. The shape of the amide I band (1620-1680 cm^{-1}) can provide information on the type (α -helix, β -sheets) and amount of secondary structure [50]. As can be seen from Figure 5.10, the amide I peak of all poly-L-lysine templated silica nanocomposites (PLL/silica, AChE/PLL/silica and QD/AChE/PLL/silica respectively) is shifted in comparison to the ones of the solid poly-L-lysine (1643.7 cm^{-1}) and that of the *Dm. AChE* (1642.2 cm^{-1}). Among these, the poly-L-lysine templated QD/AChE/silica nanocomposites display the highest amide I shift toward lower wavenumbers (1640.2 cm^{-1}) confirming the interaction of poly-L-lysine and protein residues with the biosilica network. These observed shifts of the amide I peak are due to electrostatic and/or hydrophobic interactions of poly-L-lysine and/or *Dm. AChE* with the silica matrix [51,52].

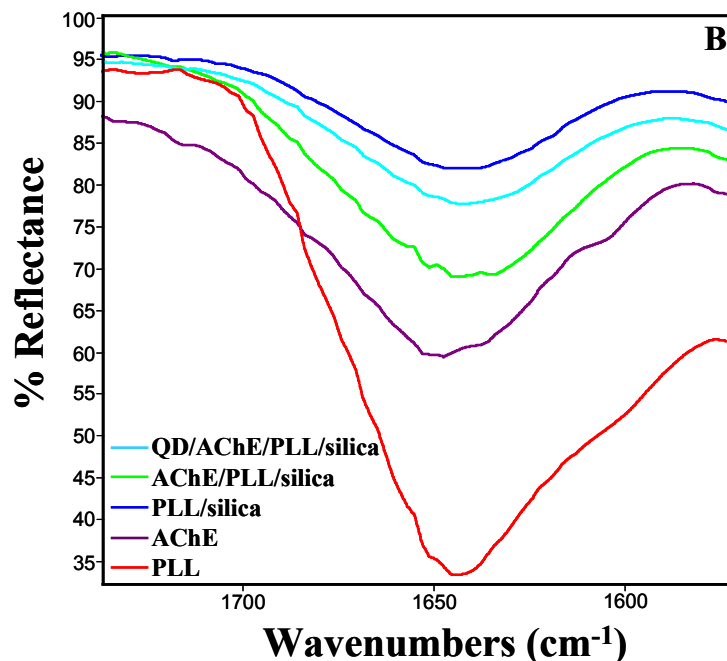


Figure 5.10. Amide I band of *Dm.* AChE, PLL and bio-inspired silica nanocomposites (PLL/silica, AChE/PLL/silica and QD/AChE/PLL/silica)

Si-O-Si asymmetrical and symmetrical stretching modes, respectively, give rise to silica peaks A and C, while peak B is attributed to Si-O stretching mode either as siloxane bridge (Si-O⁻) or as silanol group (Si-OH) [53-56]. The maximum of the main silica peak (A), for all poly-L-lysine templated silica nanocomposites, appears in the region 1039-1043 cm⁻¹ as compared to the corresponding silica peak that appears in the region 1070-1100 cm⁻¹ of other sol-gel silicas [57,58]. This shift can be attributed to the entrapment of AChE and of the QDs/AChE conjugates within the silica matrix, entrapment that affects the bond strength of neighboring Si-O-Si groups. The differences between the silica-based nanocomposites are visible, their ATR spectra recording a shift towards higher wavelengths from 1040.05 cm⁻¹ for the PLL/silica to 1041.5 cm⁻¹ for the AChE/PLL/silica and to 1042.94 cm⁻¹ for the QD/AChE/PLL/silica nanocomposites respectively. From these data it is concluded that the enzyme is indeed entrapped within the silica matrix, and that it also exists a close interaction of the surface functional groups of the protein with the QD/silica nanocomposite sites.

QD/AChE/PLL/silica based fluorescence assay

The response of the QD/AChE/PLL/silica nanocomposites to the substrate acetylcholine chloride was also evaluated. All measurements were performed by adding the substrate to a cuvette already containing the solution of QD/AChE/PLL/silica nanocomposites or QD/AChE conjugates respectively, and recording the photoluminescence intensity of the QDs for more than 20 minutes. Upon addition of substrate, the acetic acid produced by the enzymatic reaction lowered the pH of the surrounding environment of the QDs, which lead to the quenching of their photoluminescence. As a result, the higher the substrate concentration is, the higher the quantity of acetic acid to be produced and so the larger the decrease in the observed photoluminescence.

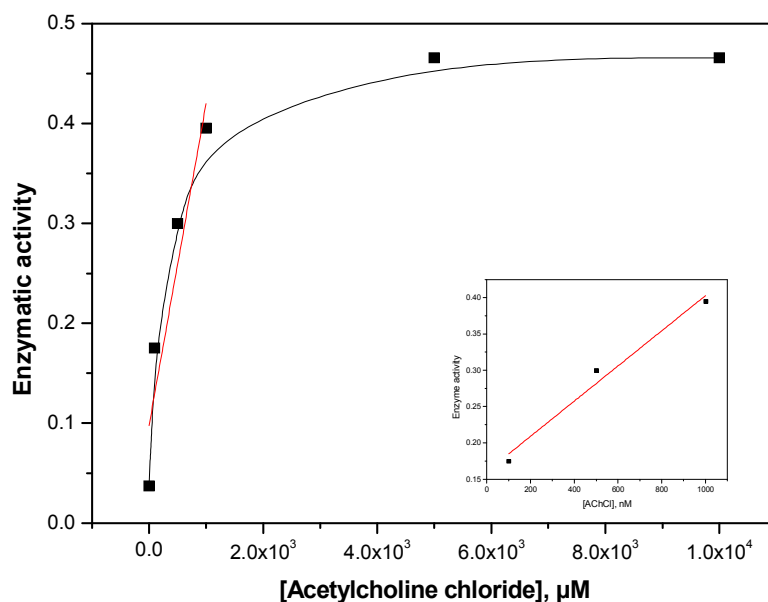


Figure 5.11. Calibration curve of the QD/AChE/PLL/silica biosensor.

The inset represents the linear range of response

Figure 5.11 shows the response of the QDs based system to a large scale of substrate concentrations and a linear relationship between the concentration of the substrate and the enzyme activity has been found in the range of 100 to 1000 μM (detailed in the inset) with a detection limit of 1 μM .

Storage stability assay

Subsequently, the stabilizing effect that the biomimetically synthesized silica has on the QD/AChE complex was evaluated, as compared to the free complex in solution. The storage stability was examined by repeated measurements of the response to the substrate over time. As it can be observed from Figure 5.12, 5 days from their production, the QD/AChE/PLL/silica nanocomposites present a remaining activity of 100%. The activity slowly decreases by time, but still remains at a level of 65% after 45 days of measurements. The activity of the QD/AChE composites not encapsulated into the biomimetically synthesized silica showed a considerable decrease of their activity to 50% after only 20 days. It is thus evident that the biomimetically synthesized silica provides an environment within which the relatively unstable *Dm.* AChE is stabilized.

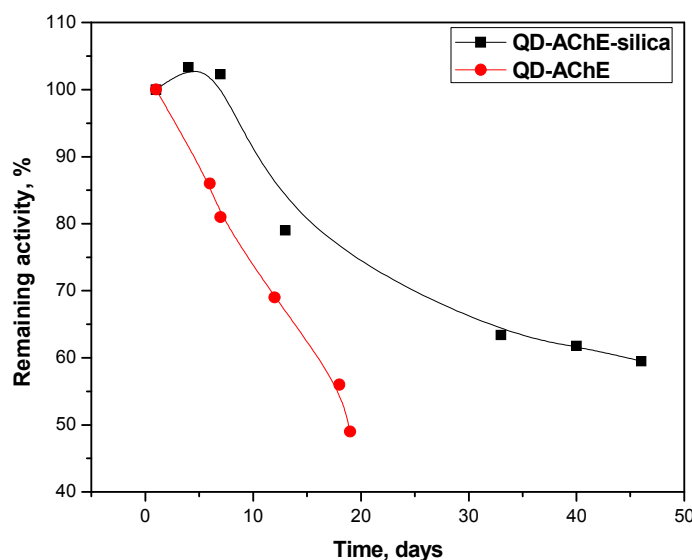


Figure 5.12. Stability study of the QD/AChE entrapped into the bio-inspired silica nanocomposites compared to the QD/AChE complex free in solution

Conclusions

From the presented results we can conclude that a new optical biosensor system based on water soluble semiconducting CdSe/ZnS QDs conjugated to *Dm.* AChE and entrapped into bio-inspired silica matrix based on poly-L-lysine was successfully constructed. The enzyme is successfully immobilized onto the QDs and then stabilized by the PLL capping and the subsequent formation of the outer nanoporous silica shell. It is shown that the poly-L-lysine

templated silica outer shell does not modify the optical properties of the quantum dots and at the same time the pores of the bio-inspired silica nanocomposites do not impede the transport of the substrate to the enzyme where the production of acid could be carried out and monitored by photoluminescence means. The bio-inspired silica nanocomposites provide protection of the sensitive QDs from the external environment while at the same time help the enzyme to be stabilized against unfolding or denaturation as proved by the storage stability experiments. The entrapment of QD/AChE conjugates into the bio-inspired silica nanocomposites is mentioned for the first time in literature and offers an optically active biosensor that was found to be suitable for monitoring low substrate concentrations in solution. The biodetection system proposed is shown to be stable with storage lifetime of more than 2 months. These QD based biosensors can provide stable and sensitive nano-biosensor platforms for the detection of the enzymatic activity.

It is important to note that even the very small QDs concentration used (1.96×10^{-6} mol/L) and the very small amount of enzyme incorporated into the biosensors (only 2U/mL in the initial solution) are sufficient to furnish a biosensor system with a reliable photoluminescence response. This suggests that using the system composed of the QD/AChE conjugates entrapped in the bio-inspired silica, AChE inhibitors could also be detected with good sensitivity.

References

1. W.C.W. Chan and S. Nie, Quantum dot bioconjugates for ultrasensitive nonisotopic detection, *Science*, 1998, 281, 2016–2018
2. Y.S. Liu, Y. Sun, P.T. Vernier, C.H. Liang, S.Y.C. Chong, M.A. Gundersen, pH-sensitive photoluminescence of CdSe/ZnSe/ZnS quantum dots in human ovarian cancer cells, *J. Phys. Chem. C.*, 2007, 111, 2872-2878
3. Z. Zhelev, R. Bakalova, H. Ohba, R. Jose, Y. Imai, Y. Baba, Uncoated, broad fluorescent, and size-homogeneous CdSe quantum dots for bioanalyses, *Anal. Chem.*, 2006, 78(1), 321–330
4. Z. Kaul, T. Yaguchi, S.C. Kaul, T. Hirano, R. Wadhwa, K. Taira, Mortalin imaging in normal and cancer cells with quantum dot immunoconjugates, *Cell Res.*, 2003, 13, 503-507
5. S.J. Rosenthal, I. Tomlinson, E.M. Adkins, S. Schroeter, S. Adams, L. Swafford, J. McBride, Y. Wang, L.J. DeFelice, R.D. Blakely, Targeting cell surface receptors with ligand-conjugated nanocrystals, *J. Am. Chem. Soc.*, 2002, 124, 4586-4594
6. C.P. Huang, Y.K. Li, T.M. Chen, A highly sensitive system for urea detection by using CdSe/ZnS core-shell quantum dots, *Biosens. Bioelectron.*, 2007, 22(8), 1835-1838
7. C.P. Huang, S.W. Liu, T.M. Chen, Y.K. Li, A new approach for quantitative determination of glucose by using CdSe/ZnS quantum dots, *Sens. Actuators B*, 2008, 130(1), 338-342
8. D. Du, S. Chen, D. Song, H. Li, X. Chen, Development of acetylcholinesterase biosensor based on CdTe quantum dots/gold nanoparticles modified chitosan microspheres interface, *Biosens. Bioelectron.*, 2008, 24, 475-479
9. L. Tang, Y. Zhu, X. Yang, J. Sun, C. Li, Self-assembled CNTs/CdS/dehydrogenase hybrid-based amperometric biosensor triggered by photovoltaic effect, *Biosens. Bioelectron.*, 2008, 24(2), 319–323
10. A.M. Derfus, W.C.W. Chen, S.N. Bhatia, Probing the cytotoxicity of semiconductor quantum dots, *Nano Lett.*, 2004, 4, 11-18
11. S.J. Cho, D. Maysinger, M. Jain, B. Röder, S. Hackbarth, F.M. Winnik, Long-term exposure to CdTe quantum dots causes functional impairments in live cells, *Langmuir*, 2007, 23, 1974-1980
12. C. Graf, S. Dembski, T. Kruger, U. Gbureck, A. Ewald, A. Bock, E. Ruhl, Photoactivation of CdSe/ZnS quantum dots embedded in silica colloids, *Small*, 2008, 4(9), 1516-1526

13. C. Kirchner, T. Liedl, S. Kudera, T. Pellegrino, A.M. Javier, H.E. Gaub, S. Stolzle, N. Fertig, W.J. Parak, Cytotoxicity of colloidal CdSe and CdSe/ZnS nanoparticles, *Nano Lett.*, 2005, 5, 331-338
14. T.J. Daou, L. Li, P. Reiss, V. Jossierand, I. Texier, Effect of poly(ethylene glycol) length on the in vivo behavior of coated quantum dots, *Langmuir*, 2009, 25, 3040-3044
15. M.A. Correa-Duarte, M. Giersig, L.M. Liz-Marzan, Stabilization of CdS semiconductor nanoparticles against photodegradation by a silica coating procedure, *Chem. Phys. Lett.*, 1998, 286(5-6), 497-501
16. A.L. Rogach, D. Nagesha, J.W. Ostrander, M. Giersig, N.A. Kotov, "Raisin bun"-type composite spheres of silica and semiconductor nanocrystals, *Chem. Mater.*, 2000, 12, 2676-2685
17. Y. Yang, L. Jing, X. Yu, D. Yan, M. Gao, Coating aqueous quantum dots with silica via reverse microemulsion method: toward size-controllable and robust fluorescent nanoparticles, *Chem. Mater.*, 2007, 19, 4123-4128
18. S.Y. Chang, L. Liu, S.A. Asher, Preparation and properties of tailored morphology, monodisperse colloidal silica-cadmium sulfide nanocomposites, *J. Am. Chem. Soc.*, 1994, 116, 6739-6744
19. S.T. Selvan, T.T. Tan, J.Y. Ying, Robust, non-cytotoxic, silica-coated CdSe quantum dots with efficient photoluminescence, *Adv. Mater.*, 2005, 17(13), 1620-1625
20. M. Darbandi, R. Thomann, T. Nann, Single quantum dots in silica spheres by microemulsion synthesis, *Chem. Mater.*, 2005, 17, 5720-5725
21. M.I. Shukoor, F. Natalio, H.A. Therese, M.N. Tahir, V. Ksenofontov, M. Panthöfer, M. Eberhardt, P. Theato, H.C. Schröder, W.E.G. Müller, W. Tremel, Fabrication of a silica coating on magnetic γ -Fe₂O₃ nanoparticles by an immobilized enzyme, *Chem. Mater.*, 2008, 20, 3567-3573
22. B. Leng, X. Chen, Z. Shao, W. Ming, Biomimetic synthesis of silica with chitosan-mediated morphology, *Small*, 2008, 4(6), 755-758
23. Q. Zhang, L. Zhang, B. Liu, X. Lu, J. Li, Assembly of quantum dots-mesoporous silicate hybrid material for protein immobilization and direct electrochemistry, *Biosens. Bioelectron.*, 2007, 23(5), 695-700
24. A. Wolcott, D. Gerion, M. Visconte, J. Sun, A. Schwartzberg, S. Chen, J.Z. Zhang, Silica-coated CdTe quantum dots functionalized with thiols for bioconjugation to IgG proteins, *J. Phys. Chem. B.*, 2006, 110(11), 5779-5789
25. D. Avnir, S. Braun, O. Lev, M. Ottolenghi, Enzymes and other proteins entrapped in sol-gel materials, *Chem. Mater.*, 1994, 6, 1605-1614

26. C. Lei, Y. Shin, J. Liu, E.J. Ackerman, Entrapping enzyme in a functionalized nanoporous support, *J. Am. Chem. Soc.*, 2002, 124, 11242-11243
27. J. Fan, J. Lei, L. Wang, C. Yu, B. Tu, D. Zhao, Rapid and high-capacity immobilization of enzymes based on mesoporous silicas with controlled morphologies, *Chem. Commun.*, 2003, 2140-2141
28. R.R. Naik, M.M. Tomczak, H.R. Luckarift, J.C. Spain, M.O. Stone, Entrapment of enzymes and nanoparticles using biomimetically synthesized silica, *Chem. Commun.*, 2004, 15, 1684 – 1685
29. V. Vamvakaki, M. Hatzimarinaki, N. Chaniotakis, Biomimetically Synthesized Silica-Carbon Nanofiber Architectures for the Development of Highly Stable Electrochemical Biosensor Systems, *Anal. Chem.*, 2008, 80, 5970-5975
30. M. Hatzimarinaki, V. Vamvakaki, N. Chaniotakis, Spectro-electrochemical studies of acetylcholinesterase in carbon nanofiber-bioinspired silica nanocomposites for biosensor development, *J. Mater. Chem.*, 2009, 19, 428–433
31. S.V. Patwardhan, N. Mukherjee, M. Steinitz-Kannan, S.J. Clarson, Bioinspired synthesis of new silica structures, *Chem. Commun.*, 2003, 10, 1122-1123
32. S. Dembski, C. Graf, T. Kruger, U. Gbureck, A. Ewald, A. Bock, E. Ruhl, Photoactivation of CdSe/ZnS Quantum Dots Embedded in Silica Colloids, *Small*, 2008, 4(9), 1516-1526
33. H.H. Dale, The action of certain esters and ethers of choline, and their relation to muscarine, *J. Pharmacol. Exp. Therap.*, 1914, 6, 147–190
34. C.I. Wright, C. Geula, M.M. Mesulam, Neurological cholinesterases in the normal brain and in Alzheimer's disease: relationship to plaques, tangles, and patterns of selective vulnerability, *Ann. Neurol*, 1993, 34, 373–384
35. R.J. Polinsky, K.V. Holmes, R.T. Brown, V. Weise, CSF acetylcholinesterase levels are reduced in multiple system atrophy with autonomic failure, *Neurology*, 1989, 39, 40–44
36. K. Ohno, A.G. Engel, J.M. Brengman, X.M. Shen, F. Heidenreich, A. Vincent, M. Milone, E. Tan, M. Demirci, P. Walsh, S. Nakano, I. Akiguchi, The spectrum of mutations causing end-plate acetylcholinesterase deficiency, *Ann. Neurol.*, 2000, 47, 162–170
37. A. Silver, A histochemical investigation of cholinesterases at neuromuscular junctions in mammalian and avian muscle, *J. Physiol. (Lond.)*, 1963, 169, 386–393
38. Y. Bourne, P. Taylor, P. Marchot, Acetylcholinesterase inhibition by fasciculon: crystal structure of the complex, *Cell*, 1995, 83, 503–512
39. M. Harel, G. Kryger, T.L. Rosenberry, W.D. Mallender, T. Lewis, R.J. Fletcher, J.M. Guss, I. Silman, J.L. Sussman, Three-dimensional structures of *Drosophila melanogaster*

- acetylcholinesterase and of its complexes with two potent inhibitors, *Protein Sci.*, 2000, 9, 1063–1072
40. G. Kryger, M. Harel, K. Giles, L. Toker, B. Velan, A. Lazar, C. Kronman, D. Barak, N. Ariel, A. Shafferman, I. Silman, J.L. Sussmana, Structures of recombinant native and E202Q mutant human acetylcholinesterase complexed with the snake-venom toxin fasciculin-II, *Acta Crystallogr. D Biol. Crystallogr.*, 2000, 56, 1385–1394
 41. F. Nachon, J. Stojan, D. Fournier, Insights into substrate and product traffic in the *Drosophila melanogaster* acetylcholinesterase active site gorge by enlarging a back channel, *FEBS Journal*, 2008, 275, 2659-2664
 42. J. Stojan, L. Brochier, C. Alies, J.P. Colletier, D. Fournier, Inhibition of *Drosophila melanogaster* acetylcholinesterase by high concentrations of substrate, *Eur. J. Biochem.*, 2004, 271, 1364–1371
 43. W.D. Mallender, T. Szegletes, T.L. Rosenberry, Acetylthiocholine binds to asp74 at the peripheral site of human acetylcholinesterase as the first step in the catalytic pathway, *Biochemistry*, 2000, 39, 7753–7763
 44. J.P. Colletier, D. Fournier, H.M. Greenblatt, J. Stojan, J.L. Sussman, G. Zaccai, I. Silman, M. Weik, Structural insights into substrate traffic and inhibition in acetylcholinesterase, *EMBO J*, 2006, 25, 2746–2756
 45. H. Soreq and S. Seidman, Acetylcholinesterase – new roles for an old actor, *Nature Reviews*, 2001, 2, 294-302
 46. G.L. Ellman, K.D. Courtney, V. Andres Jr., R.M. Featherstone, A new and rapid colorimetric determination of acetylcholinesterase activity, *Biochem. Pharm.*, 1961, 7, 88-95
 47. <http://www.cem.msu.edu/~reusch/VirtualText/Spectrpy/InfraRed/infrared.htm>
 48. S. Krimm and J. Bandekar, Vibrational spectroscopy and conformation of peptides, polypeptides and proteins, *Adv. Prot. Chem.*, 1986, 38, 181–364
 49. J. Bandekar, Amide modes and protein conformation, *Biochim. Biophys. Acta*, 1992, 1120, 123–143
 50. A. Barth and C. Zscherp, What vibrations tell us about proteins, *Q. Rev. Biophys.*, 2002, 35, 369-430
 51. S. Sotiropoulou and N.A. Chaniotakis, Tuning the sol–gel microenvironment for acetylcholinesterase encapsulation, *Biomater.*, 2005, 26, 6771–6779
 52. S. Wu, H. Ju, Y. Liu, Conductive mesocellular silica–carbon nanocomposite foams for immobilization, direct electrochemistry, and biosensing of proteins, *Adv. Func. Mater.*, 2007, 17, 585–592

53. R.M. Almeida, T.A. Guiton, C.G. Pantano, Characterization of silica gels by infrared reflection spectroscopy, *J. Non-Cryst. Sol.*, 1990, 121, 193–197
54. C.C. Perry, X. Li, D.N. Waters, Structural studies of gel phases-IV. An infrared reflectance and Fourier transform Raman study of silica and silica/titania gel glasses, *Spectrochim. Acta*, 1991, 47A, 1487–1494
55. P. Innocenzi, Infrared spectroscopy of sol–gel derived silica-based films: a spectromicrostructure overview, *J. Non-Cryst. Sol.*, 2003, 316, 309–319
56. A. Fidalgo, R. Cirimanna, L.M. Ilharco, M. Pagliaro, Role of the alkyl-alkoxide precursor on the structure and catalytic properties of hybrid sol-gel catalysts, *Chem. Mater.*, 2005, 17, 6686–6694
57. A. Bertoluzza, C. Fagnano, M.A. Morelli, V. Gottardi, M. Guglielmi, Raman and infrared spectra of silica gel evolving toward glass, *J. Non-Cryst. Solids*, 1982, 48, 117-128
58. J.R. Martinez, F. Ruiz, Y.V. Vorobiev, F. Perez-Robles, J. Gonzalez-Hernandez, Infrared spectroscopy analysis of the local atomic structure in silica prepared by sol-gel, *J. Chem. Phys.*, 1998, 109, 7511-7514

CHAPTER 6 – COLORIMETRIC DETECTION OF OLIGONUCLEOTIDES USING GOLD NANOPARTICLES

Due to its application in the diagnosis of hereditary diseases and of viral or bacterial infections, the detection of sequence-specific DNA represents a research area in continuous expansion. The first methods were based on detection of hybridization of probes that are either labelled, through the use of fluorescent markers [1] or other types of labels like tris-(1,10-phenanthroline)cobalt(III) perchlorate [2], or unlabeled probes [3]. Other methods rely on conjugation to an enzyme and the indirect detection of the enzymatically generated fluorescent, chemiluminescent, bioluminescent or colorimetric signal [4]. The past years though, have seen the development of new methods using the properties of nanomaterials, and more precisely gold nanoparticles, to generate an optical signal upon aggregation in solution [5-7].

The present work was focused on developing a colorimetric detection system for oligonucleotides from bacteria of the *Mycobacterium* class, using gold nanoparticles (Au NPs). Methods inspired from literature for conjugation of the oligonucleotides to the surface of the Au NPs have been tested, using a wide range of functional linkers and gold nanoparticles of different sizes. These methods have failed in producing the desired Au NPs – oligonucleotide conjugates, agglomeration and subsequent precipitation of the Au NPs from solution being observed in all cases. The conjugates were finally obtained when using pairs of thiol-modified oligonucleotides that have been designed as to align in a “tail-to-head” fashion onto a target polynucleotide. These conjugates were then subjected to hybridization experiments with the complementary strand of oligonucleotide, hybridization forcing the gold nanoparticles to come two by two in close proximity to one another and triggering a change in the solution colour from burgundy red to purple. The constructed Au NPs – oligonucleotide conjugates were proven to be stable, with a half life of at least two months.

Synthesis of colloidal gold nanoparticles

Gold nanoparticles used for experiments have been synthesized by the citrate reduction method and supplied to our Laboratory by our partner, Vinca Institute of Nuclear Sciences, from Belgrade, Serbia. Citrate reduction of gold chloride in water is known to produce nanosized gold particles with a narrow size distribution [8]. Briefly, a $\text{HAuCl}_4 \times 3\text{H}_2\text{O}$ solution is brought to boiling with vigorous stirring, inside of a round-bottomed flask equipped with a condenser. At boiling temperature, rapid addition of sodium citrate solutions of different concentrations, directly into the vortex of the solution, results in a colour change from pale yellow to burgundy red. Boiling is then continued for another 10 min to allow the complete formation of the gold colloids. The heating mantle is removed, and stirring continued for an additional time of 15 min. After synthesis, the colloidal dispersions were kept in the refrigerator, under dark and were stable for a very long period of time. Three different colloidal gold nanoparticles solutions, of different diameters, namely Au1-NPs, Au2-NPs and Au3-NPs, have been used in experiments.

Determination of Au NPs extinction coefficient

One of the most important parameters to be used in experiments is the Au NPs extinction coefficient and in order to determine their coefficient for all Au NPs solutions used, we have employed transmission electron microscopy (TEM) together with inductively coupled plasma mass spectrometry (ICP-MS) and absorbance spectroscopy measurements. ICP-MS is a method that combines the ion producing capacity of inductively coupled plasma with the ion separation and detection capacity of a mass spectrometer. This method is highly sensitive and capable of the determination of a wide range of metals and a few non-metals at concentrations below one part in 10^{12} (part per trillion).

In order to calculate the extinction coefficient of Au NPs solutions we need to know their concentrations. To calculate the exact concentration of a Au NP solution, we must calculate first the total number of gold atoms per gold nanoparticle. For this, transmission electron microscopy measurements have been used to determine the diameter of the colloidal Au NPs. The diameters of Au-NPs, as determined by TEM imaging were found to be: 9-12 nm for the Au1-NPs, 20-25 nm for the Au2-NPs and 25-28 nm for the Au3-NPs (Figure 6.1).

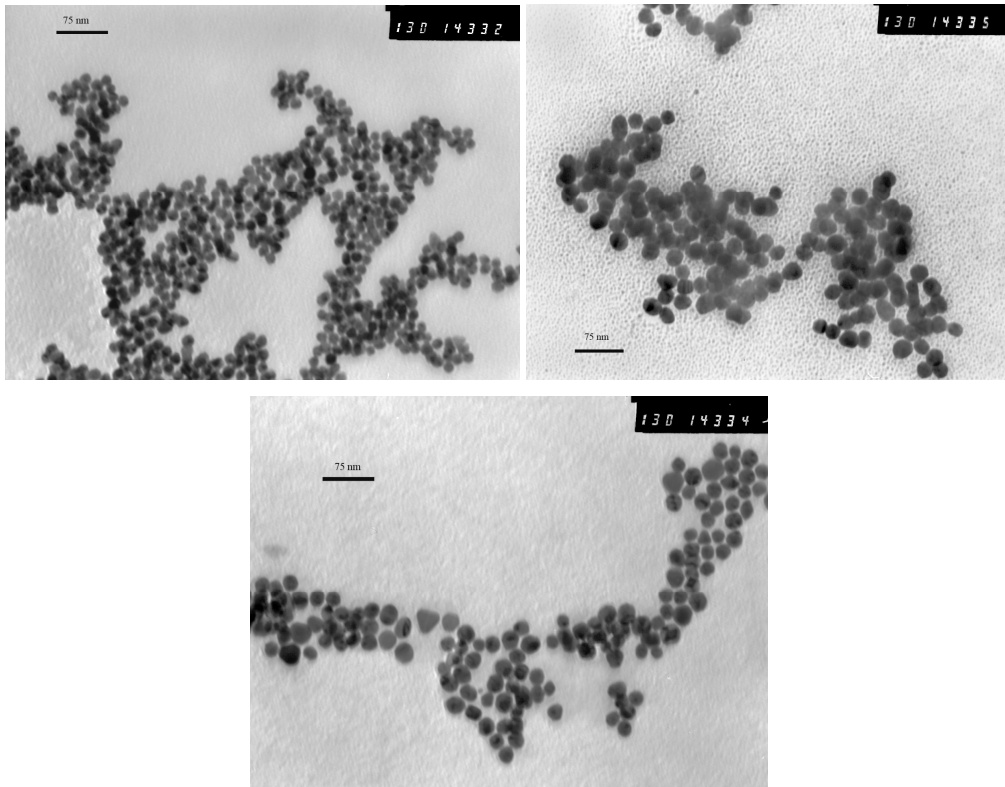


Figure 6.1. TEM images of the Au-NPs. a – Au1; b – Au2; c – Au3

Assuming a completely spherical shape of the Au NPs, and knowing their diameter as a result of the TEM measurements, we have used equation 6.1 to calculate the volume of a gold nanoparticle:

$$V_{AuNP} = \frac{4}{3} \cdot \pi \cdot r^3 \quad (\text{Eq. 6.1})$$

The number of gold atoms per nanoparticle was obtained from equation 6.2 upon using the results of equation 1 and the value of $1.69 \cdot 10^{-23} \text{ cm}^3$ for the volume of a single Au atom, as follows:

$$N^{\circ} \text{ atoms} / \text{nanoparticle} = \frac{V_{AuNP}}{V_{Auatom}} \quad (\text{Eq. 6.2})$$

As a follow up, the total number of Au atoms in solution was calculated using ICP-MS. Briefly, 50 μL of Au NPs solution were placed in a glass beaker to which 200 μL of aqua regia were added. The beakers were then placed on a hot plate and kept at 105°C for 12 hours

until the solvent evaporated completely. Subsequently, 50 μL of 5% HCl solution were added to the dried pellets in order to resuspend the Au atoms and the procedure was assisted with an ultrasonic bath. The solutions were then diluted 10.000 times and subjected to ICP-MS analysis.

Combining the ICP-MS results with the calculated values of the number of Au atoms per nanoparticle, the total concentration of the Au NPs solutions was calculated, according to equation 6.3:

$$C_{Au} = \frac{N_{total}}{N \cdot N_A} \quad (\text{Eq. 6.3})$$

where N_{total} is the total number of gold atoms
 N is the number of gold atoms per nanoparticle
 N_A is the Avogadro constant

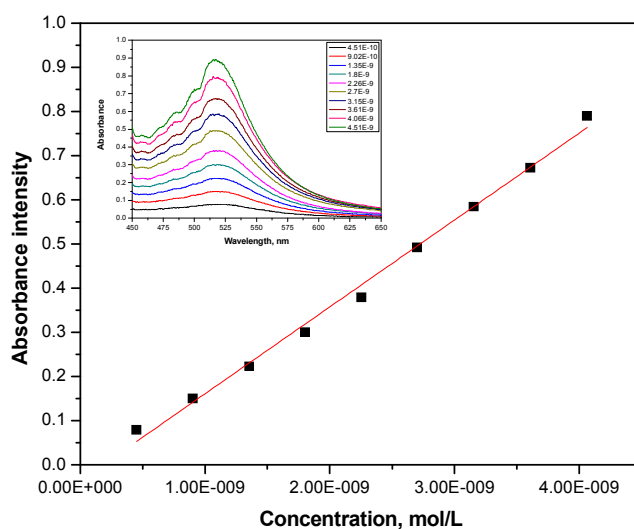


Figure 6.2. The peak intensity of the plasmon resonance band versus Au₃-NPs concentration. The inset represents the UV-vis absorption spectra at different relative concentrations

The final step in determining the Au NPs solutions extinction coefficients was to record their absorbance spectra. For this, all gold nanoparticles solutions have been diluted with deionised Milli-Q water prior to measurements. Figure 6.2 presents the experimental data of the peak intensity of the plasmon resonance band plotted versus the corresponding

concentration and fitted linearly for the Au₃-NPs solution. As we can observe, the calibration curve is linear with a correlation coefficient very close to 0.999. The inset represents the UV-vis absorption spectra at different relative concentrations.

The extinction coefficient of the Au NPs solutions was then determined based on the above data and using the Lambert-Beer law present in equation 6.4:

$$A = \varepsilon \cdot c \cdot l \quad (\text{Eq. 6.4})$$

where l = the length of the path length of 1 cm

ε = extinction coefficient

c = concentration (calculated from the ICP-MS data)

Table 6.1 summarizes the diameters, number of gold atoms per nanoparticle and the extinction coefficients of all gold nanoparticles solutions used for experiments.

Table 6.1. Au NPs physical characteristics.

Diameter, nm	Au NP volume, cm ³	Number Au atoms/surface of Au NP	Number Au atoms/Au NP	Extinction coefficient, M ⁻¹ cm ⁻¹
9-12	5.636*10 ⁻¹⁹	3925	3.335*10 ⁴	4.82*10 ⁷
20-25	4.71*10 ⁻¹⁸	16981.12	2.79*10 ⁵	3.26*10 ⁸
25-28	1.08*10 ⁻¹⁷	29467.33	0.64*10 ⁶	9.2*10 ⁸

Conjugation of gold nanoparticles with oligonucleotides, using a thiol-group-linker

In an initial approach, the modification of the Au NPs' surface with a series of linkers containing a thiol group at one end and a carboxyl or amine group at the other end was performed. The linkers bind with the thiol group to the surface of the Au NPs leaving the carboxyl- and amino- functionalities exposed to the outside and suitable for further conjugation to amino- and carboxyl-modified oligonucleotides through the EDC/NHS method. There are many papers reporting the successful conjugation of thiol linkers to the surface of spherical Au NPs and experiments were performed according to literature [8-12]. Much to our surprise, upon performing the conjugation experiments, we have observed that addition of the thiol linkers (carboxyl- or amino-modified at the other end) to the Au NPs

solutions always resulted in an immediate change of the solutions' colour from red to blue-black as demonstrated by Figure 6.3a. Also, this colour change was always accompanied by a red-shift of the maximum of the absorption peak from approx. 520 nm in the initial solution to around 650-700nm (Figure 6.3b). These changes are indicative of the formation of large Au NPs aggregates upon addition of the thiol linker. The aggregates then precipitate within the following 24 hours.

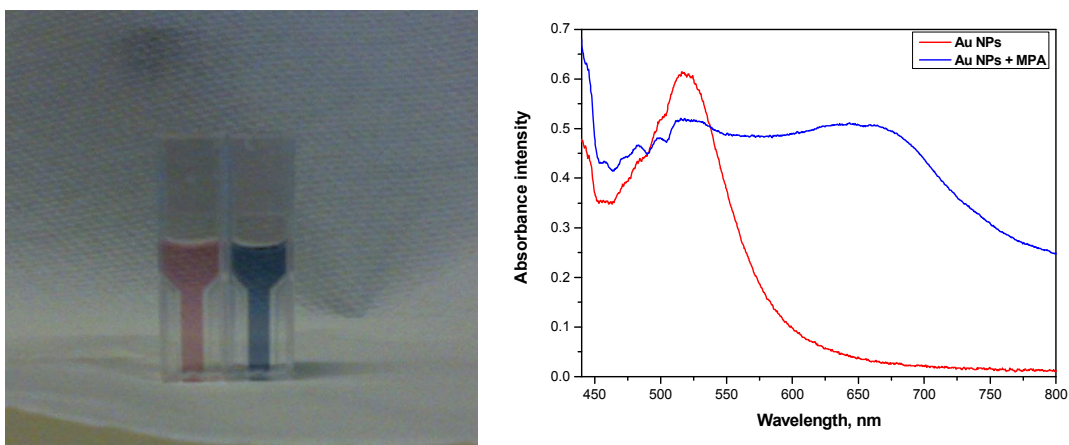


Figure 6.3. a) Au NPs solution before (red) and after (blue) addition of MPA;
b) Spectra of Au NPs solution before (solid line) and after (dashed line) addition of mercaptopropionic acid

Experiments using solutions of mercaptopropionic acid (MPA), mercaptosuccinic acid (MSA), cystamine (Cys) and dodecanethiol of different concentrations, prepared in different buffers and at different pH values have been performed. In all cases the solution colour turned blue-black followed by precipitation of all Au NPs in solution within 24 hours.

Conjugation of gold nanoparticles with thiol-modified oligonucleotides

In order to avoid the modification of Au NPs with thiol linkers (which proved to be unsuccessful), in the next step we have conducted their direct conjugation to thiol-modified oligonucleotides. The conjugation followed the methods described by Storhoff et al. [7], Reynolds et al. [6] and Hill and Mirkin [5], the multitude of literature reports covering the conjugation of Au NPs with thiol-modified oligonucleotides proving that this method is much more suitable when wanting to construct Au NPs with oligonucleotides on their surface. Conjugation of thiol-modified oligonucleotides to the surface of colloidal gold nanoparticles

can be monitored spectrophotometrically as it produces a small plasmon band shift towards higher wavelengths and a small decrease of its intensity which is associated with a decrease in particle concentration during the workup of the oligonucleotide-modified Au-NPs.

In our experiments, six 20-bases long *Mycobacterium* genus specific oligonucleotides modified either at the 3'- or at the 5'- end with thiol molecules and 15 adenine residues (thiol-oligos) were used for conjugation onto the surface of Au NPs. They were purchased in lyophilized state, from MWG Biotech GmbH and their modifiers, spacers and sequences are presented in Table 6.2. Stock solutions of all thiol-modified oligonucleotides were prepared in nanopure water to a concentration of 100 pmol/ μ L

Table 6.2: Modifiers, spacers and sequences of the oligonucleotides used for experiments.

Name	5' modifier	5' Spacer	Sequence	3' Spacer	3' modifier
Thiol-A1	Alkanethiol	AAA AAA AAA AAA AAA	GCA ACA CCG AAG TGA AGT CG		
Thiol-A2			TTC GTG CAG AAG GTC TGC AA	AAA AAA AAA AAA AAA	thiol
Thiol-B1	Alkanethiol	AAA AAA AAA AAA AAA	TGG ATA GTG GTT GCG AGC AT		
Thiol-B2			GGG GTG TGG TGT TTG AGT AT	AAA AAA AAA AAA AAA	thiol
Thiol-D1	Alkanethiol	AAA AAA AAA AAA AAA	GCG GAT TAG TAC CGT GAG GG		
Thiol-D2			TGA AAA GTA CCC CGG GAG GG	AAA AAA AAA AAA AAA	thiol

Complementary targets (100% complementary) have been purchased in lyophilized state from the Microchemistry Laboratory of FORTH, Crete, Greece and stock solutions were prepared in nanopure water to a concentration of 100 pmol/ μ L.

Oligonucleotide-modified gold nanoparticles were prepared by mixing 2.5 mL of Au NPs with 3.5 nmole of the thiol-modified oligonucleotide and keeping the mixture at dark for 12 hours, at room temperature. As a follow up, the solution was brought to 0.1 % Tween20 and kept for another hour in dark, at RT. This prevents the nanoparticle aggregation and adds to the efficiency of washing them in future steps [5]. To promote conjugation of Au-NPs with thiol-modified oligonucleotides, the solution was brought to 0.3 M NaCl using an aqueous 2 M NaCl solution, by six successive additions at one hour intervals. After another 12 hours standing at room temperature, the oligonucleotide-modified Au-NPs were subjected to centrifugation at 15000 rpm for 15 min in order to remove any possible unbound thiol-modified oligonucleotides. The red oily precipitate containing Au NPs – oligonucleotide

conjugates was washed two times with a washing buffer and finally redispersed in storage buffer according to the method of Hill and Mirkin.

Confirmation of conjugation by ATR-FT-IR spectroscopy

Chemical bonds exhibit a degree of movement, such as bending or stretching, in-plane or out-of plane. This movement occurs at specific frequencies corresponding to vibrational modes of energy levels. Energy from these bonds is absorbed in different regions of the infrared (IR) spectrum. This is the reason for which we have also followed the conjugation of thiol-modified oligonucleotides to Au NPs with ATR-FT-IR. Figure 6.4 presents the infrared spectra obtained from the Au NPs and the oligonucleotide-modified Au NPs. In order to record the ATR-FT-IR spectra, drops of the citrate – covered Au NPs and of the Au - oligo solutions have been placed on glass microscope slides and left overnight to dry. This method is efficient and most important, non-destructive.

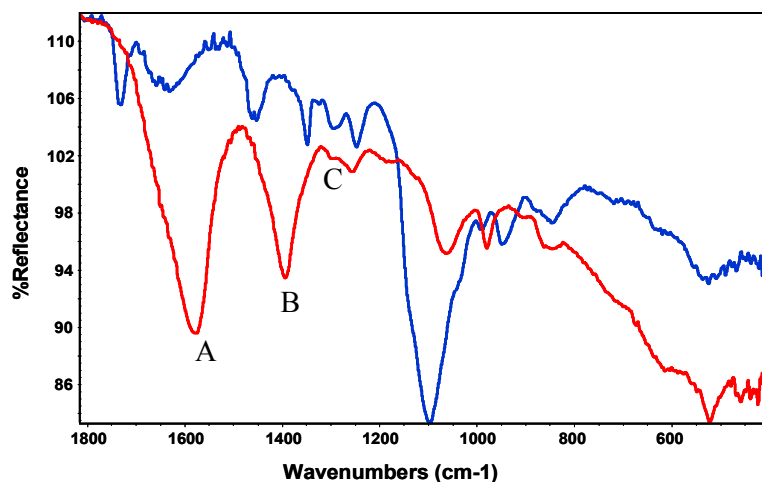


Figure 6.4. ATR-FT-IR spectra of citrate covered gold nanoparticles (red line) and of oligonucleotide-modified gold nanoparticles (blue line)

The ATR-FT-IR spectra of citrate – covered gold nanoparticles presents three characteristic citrate vibrational peaks, denoted A, B and C, that appear in the region of 1300-1600 cm^{-1} [13,14], more specifically peak A at 1577 cm^{-1} , peak B at 1400 cm^{-1} and a faint peak C at 1297 cm^{-1} (Figure 6.4 - red line). Upon modification with the thiol – modified oligonucleotides (Figure 6.4 - blue line), peak C is still slightly present, but the two main vibrational bands of the COO^- ion (peak A and peak B) disappear completely, fact proving the

almost complete removal of the surface citrate groups and their replacement by oligonucleotides.

Effect of oligonucleotide conjugation onto gold nanoparticles absorbance

Unmodified colloidal Au1 NPs (9-12 nm) and Au2 NPs (20-25 nm in diameter) are present as red coloured solutions with a plasmon band that peaks at 518 nm (Figure 6.5a and 6.5b). The Au3 NPs (25-28 nm in diameter) solution exhibits a dark red colour and a plasmon band at 520 nm (Figure 6.5c). The conjugation to thiol-modified oligonucleotides determined a slight change in colour that was not visible with the naked eye, but was confirmed by spectrophotometric measurements.

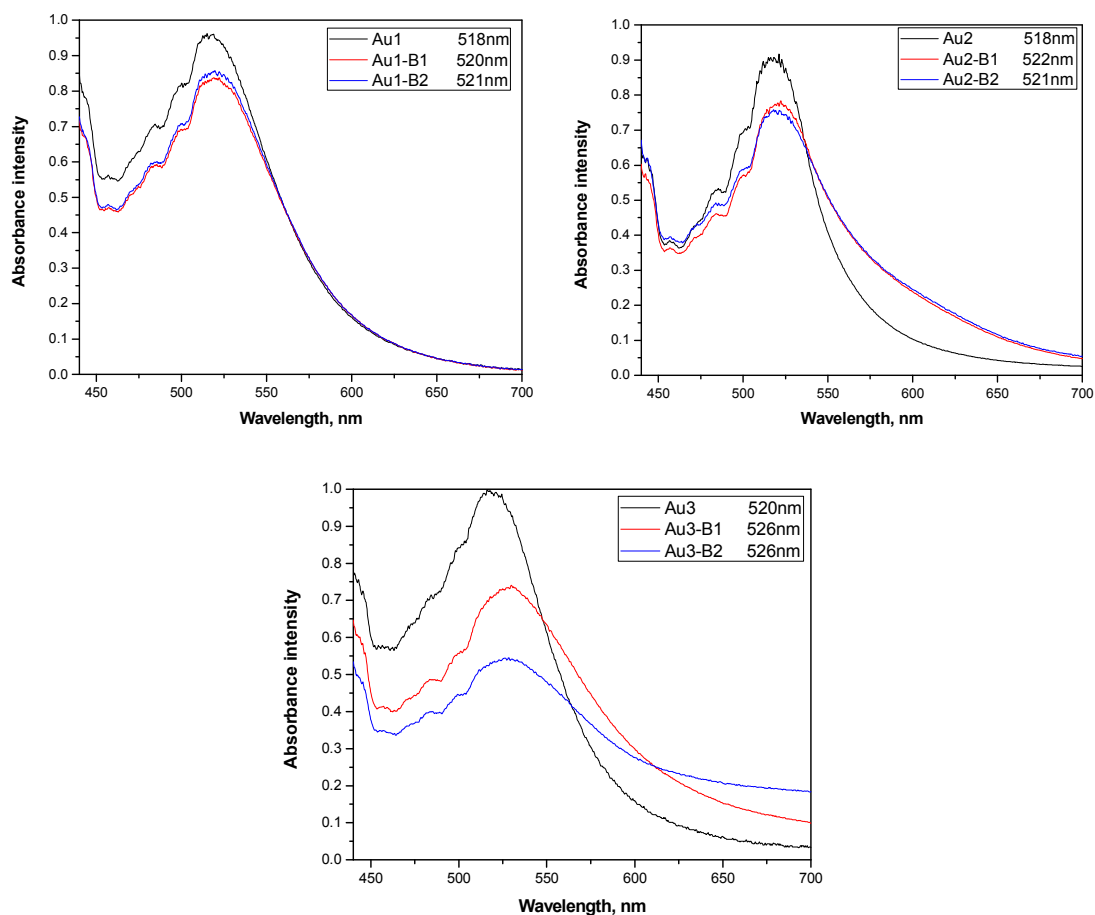


Figure 6.5. Spectra of different sized Au NPs before and after conjugation to thiol-modified oligonucleotides

As seen in Figure 6.5, upon completion of the conjugation experiments, the absorbance band shifts towards larger wavenumbers, shift that was not the same in all cases but depended on the Au-NPs diameter and on the linked thiol-modified oligonucleotides. In the case of the B1 – B2 pair of oligonucleotides, modification with the Au1 NPs resulted in a shift of 2 and respectively 3 nm (Figure 6.5a). Their conjugation to the surface of Au2 NPs produced a shift towards higher wavenumbers, of 4 and 3 nm, respectively (Figure 6.5b). Conjugation of the B1 – B2 pair of oligonucleotides with Au3 NPs produced a slightly higher shift of the absorbance peak, from the initial 520 nm to 526 nm (Figure 6.5c).

The Au NPs chemically modified with the 5'-alkanethiol-terminated 20-base oligonucleotides exhibited good stability even in solutions containing elevated salt concentrations (0.3 M NaCl), an environment that is incompatible with unmodified particles [5].

Hybridization of Au-thiol-oligo pairs with targets

In order to check if this system is suitable for detection of *Mycobacteria* DNA in solution, hybridization of the oligonucleotide modified Au NPs with the complementary targets was carried out. The oligonucleotides used in our experiments were designed in a manner that would allow them to align in a tail-to-head manner upon hybridization with the complementary strand, as evidenced by Figure 6.6.

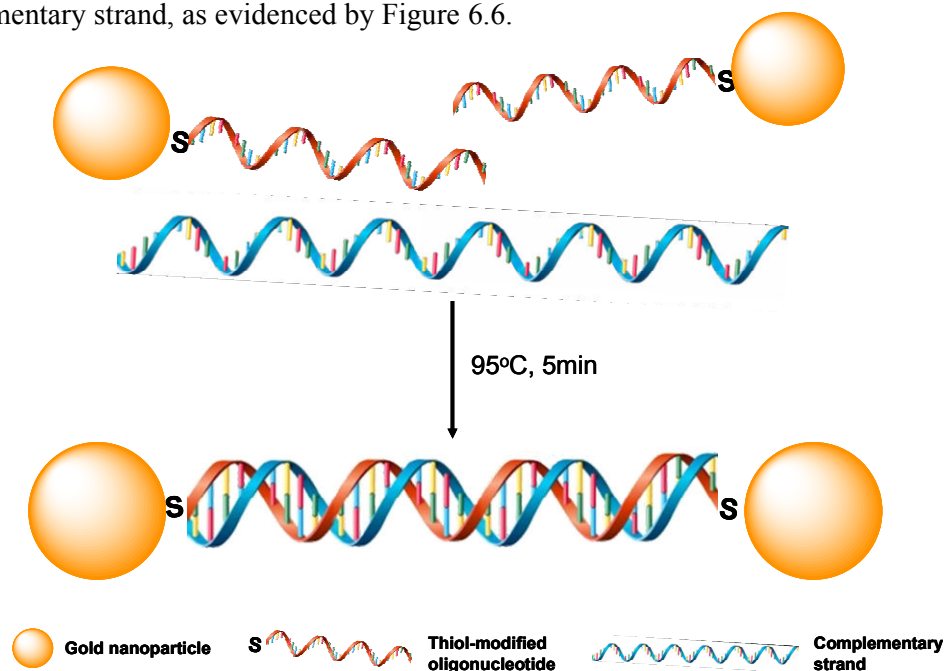


Figure 6.6. Schematic description of the hybridization experiment of Au NPs – oligonucleotide conjugates to the complementary oligonucleotide strand

For the hybridization experiment, 5 μL of the corresponding target were mixed with 120 μL of each Au-thiol-oligonucleotide pair (60 μL of the Au NP – oligo1 and 60 μL of the Au NP – oligo2 solutions) and to this, 300 μL of hybridization buffer were added. Incubation for 5 min at 95 $^{\circ}\text{C}$ and then slow cooling on the bench in order to reach room temperature followed. According to literature reports [7] hybridization with the complementary oligonucleotide strand brings the two Au NPs in close proximity, and the plasmon band registers a red shift and the solution colour changes from burgundy red to purple.

Confirmation of hybridization by ATR-FT-IR spectroscopy

The success of the hybridization experiment was proven by ATR-FT-IR measurements. An oligonucleotide is a single-strand DNA made up of various combinations of the four oligonucleotide bases (adenine, thymine, cytosine and guanine), each base being attached to the next one by a deoxyribose-phosphate backbone. When comparing the IR spectra of such molecules, differences in the bond dipole moment is vital, the asymmetrical distribution of electrons between atoms contributing to the energy absorbed. Figure 6.7 presents the ATR-FT-IR spectra of one pair of oligonucleotides used in our experiments. The main distinguishing wavenumbers owing to the presence of oligonucleotides on the surface of Au NPs are as follows: $\sim 1732\text{ cm}^{-1}$ (C=O from C), $\sim 1454\text{ cm}^{-1}$ (base and sugar vibrations from T), $\sim 1092\text{ cm}^{-1}$ (vsPO_2^- from A, G and T), $\sim 947\text{ cm}^{-1}$ (sugar-sugar phosphate vibrations from A and G) and $\sim 844\text{ cm}^{-1}$ (sugar/sugar phosphate vibrations from C) [15].

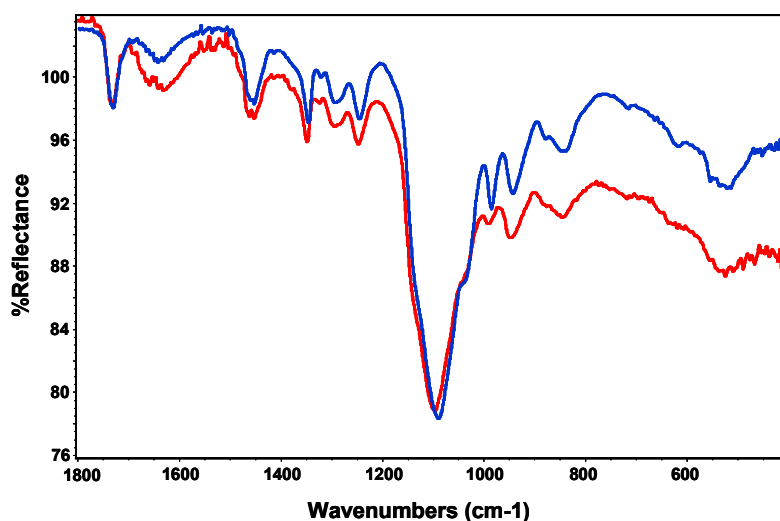


Figure 6.7. ATR-FT-IR spectra of Au₃ NPs conjugated to D1 oligonucleotide (blue line) and to D2 oligonucleotide (red line)

Chemical bonds associated with DNA absorb primarily in the 1750-760 cm^{-1} range. Conventionally, this is composed of two main portions: the double bond region (1750-1550 cm^{-1}) and the fingerprint region (1550-760 cm^{-1}). We can observe from Figure 6.8 the disappearance of the main vibrational peaks due to the presence of the single-strand oligonucleotide, and the appearance of some characteristic double-stranded DNA absorption bands: 1680-1640 cm^{-1} (carbonyl stretch), 1650-1620 cm^{-1} (NH_2), ~ 1580 cm^{-1} (NH bending and CN stretching), ~ 1217 cm^{-1} (asymmetric phosphate stretching vibrations), ~ 966 cm^{-1} (C-C stretching) and ~ 825 cm^{-1} (base residues out of plane) [15].

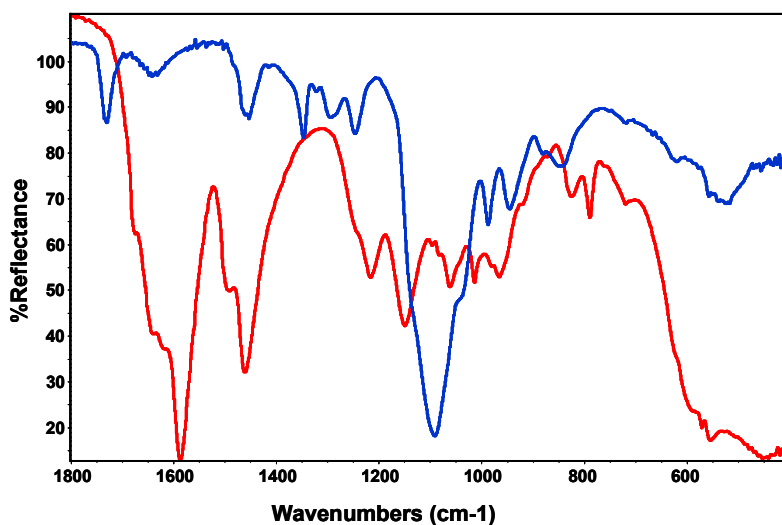


Figure 6.8. ATR-FT-IR spectra of Au₃ NPs conjugated to D1 oligonucleotide (blue line) and DNA-Au₃ NPs complex (red line)

All these factors are indicative of successful hybridization of the oligonucleotide-modified Au NPs to the complementary target oligonucleotide and formation of the DNA double strand.

Effect of DNA double strand formation onto gold nanoparticles absorbance

The hybridization experiment with the complementary targets has been carried out for all Au NPs sizes and oligonucleotide pairs.

The results were different depending on the size of the Au NPs used. The hybridization experiment conducted with the Au₁ NPs did not produce a shift of the plasmon band, the final solution absorbing at 521 nm. This was due to the fact that the 9-12 nm Au

NPs were too small in diameter as respect to the length of the formed double stranded DNA and thus could not come into proximity to one another and to result in a noticeable shift of the plasmon band towards higher wavelengths

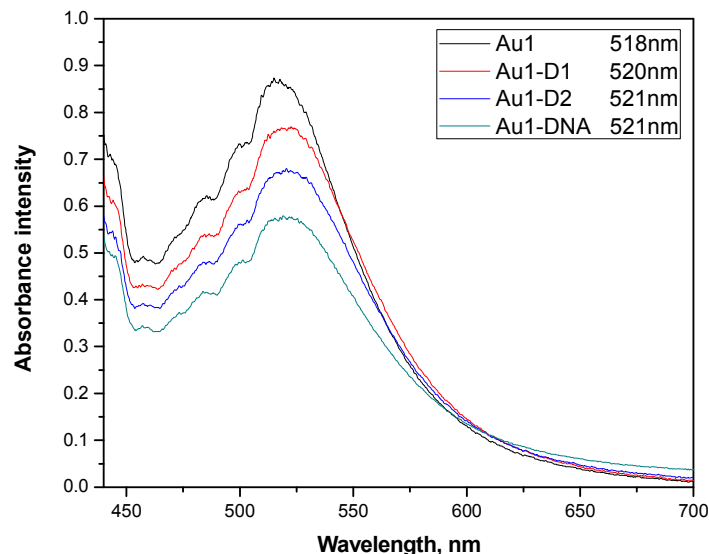


Figure 6.9. UV-vis spectra of bare Au1 NPs and of Au1 NPs – oligonucleotide before and after hybridization

Au2 NPs were also subjected to the hybridization experiment, the results not differing from the ones obtained with the Au1 NPs. The plasmon band red shifted to a merely 523 nm, proving that these Au NPs, even if 20-25 nm in diameter, do not possess the required dimension to produce a noticeable difference upon completion of the hybridization process.

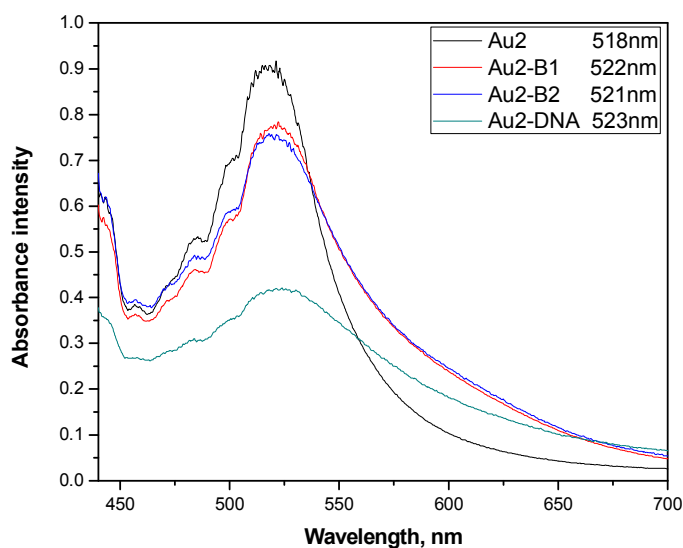


Figure 6.10. UV-vis spectra of bare Au2 NPs and of Au2 NPs – oligonucleotide before and after hybridization

When using the Au₃ NPs (25-28 nm) the expected result could finally be observed. Upon hybridization of the oligonucleotide pairs to the corresponding complementary targets, a colour shift observable with the naked eye was registered. Also, the plasmon band red shifted from 524 nm in the case of Au₃ NPs conjugated to oligonucleotide to a whopping 547 nm in the case of the Au₃ NPs – DNA complex. This fact demonstrated that the 25-28 nm nanoparticles represent the appropriate dimension of gold nanoparticles to be conjugated to 20 bases oligonucleotides. Their further hybridization with the complementary oligonucleotide strand brings the two Au NPs in close proximity, at a distance smaller than twice the diameter of one particle, proximity which produces the red shift of the plasmon band and the change in solution colour from burgundy red to purple.

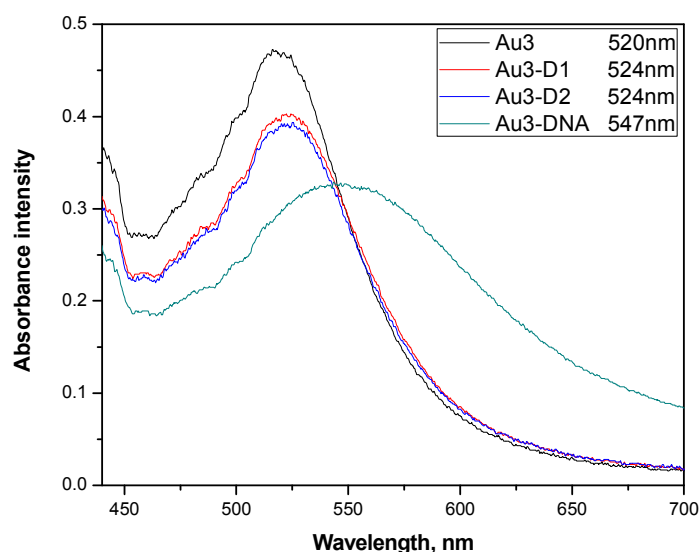


Figure 6.11. UV-Vis spectra of Au₃ NPs and of Au₃ NPs – oligonucleotide before and after hybridization

Storage stability of Au NPs – oligonucleotide conjugates

In order to check the conjugate's ability to withstand storage, the half-life of the conjugates was determined. The half life of a substance is the time it takes for that substance (for example a metabolite, drug, signalling molecule, radioactive nuclide, or other substance) to lose half of its pharmacologic, physiologic, or radiologic activity. In the case of Au NPs – oligonucleotide conjugates, half life represents the time it takes for the absorbance intensity to decrease to half of the initial value.

For the estimation of the half life of the Au NPs – oligonucleotides conjugates, the pair D1-D2 has been selected for the experiments. The respective oligonucleotides have been

conjugated to Au₃ NPs (25-28 nm in diameter) according to the procedure described above. The obtained conjugates have then been subjected to multiple absorbance readings over the course of more than 4 months and the results are presented in Figure 6.12.

As we can observe from the above graph, Au NPs conjugated to the oligonucleotide D2 is less stable than the Au₃ – D1 conjugates, having a pretty abrupt absorbance decreasing rate. The Au₃ – D2 conjugates reached their half life after a period of 67 days.

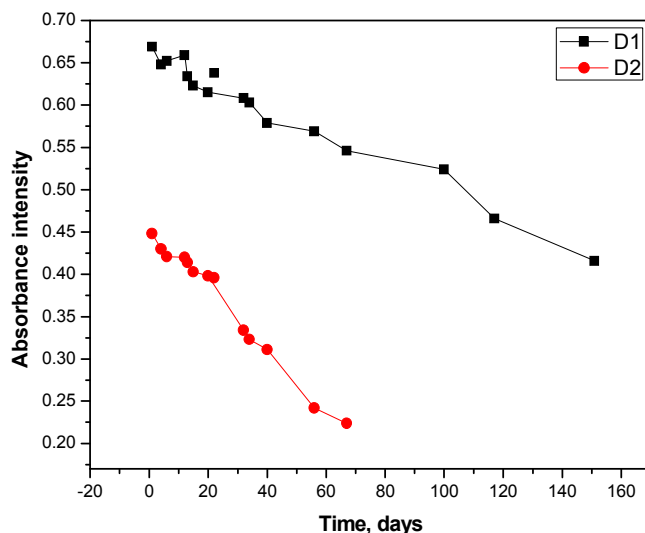


Figure 6.12. Half life estimation of the Au NPs – oligonucleotides conjugates

The conjugates with the oligonucleotide D1 proved to be more stable than its pair. They presented a slower absorbance decrease rate, reaching the half life after 150 days of absorbance measurements.

Conclusions

According to the presented data, conjugation of Au NPs to thiol-modified oligonucleotides is a reliable method for obtaining oligonucleotide-modified Au NPs. For developing a colorimetric DNA recognition method, careful consideration should be given to the choice of the Au NPs diameter as respect to the length of the oligonucleotide to be identified in solution. In our case, Au NPs with a diameter in the 25-28 nm range were proven suitable for the identification of *Mycobacteria* DNA targets. The oligonucleotide-modified Au NPs were stable, with at least 2 months life time.

References

1. H. Hakala, P. Heinonen, A. Iitia, H. Lonnberg, Detection of oligonucleotide hybridization on a single microparticle by time-resolved fluorometry: hybridization assays on polymer particles obtained by direct solid phase assembly of the oligonucleotide probes, *Bioconj. Chem.*, 1997, 8, 378-384
2. J. Wang, E. Palecek, P.E. Nielsen, G. Rivas, X. Cai, H. Shiraishi, N. Dontha, D. Luo, P.A.M. Farias, Peptide nucleic acid probes for sequence-specific DNA biosensors, *J. Am. Chem. Soc.*, 1996, 118, 7667-7670
3. K.A. Peterlinz, R.M. Georgiadis, T.M. Herne, M.J. Tarlov, Observation of hybridization and dehybridization of thiol-tethered DNA using two-color surface Plasmon resonance spectroscopy, *J. Am. Chem. Soc.*, 1997, 119, 3401-3402
4. E.S. Mansfield, J.M. Worley, S.E. McKenzie, S. Surrey, E. Rappaport, P. Fortina, Nucleic acid detection using non-radioactive labeling methods, *Mol. Cell. Probes* 1995, 9, 145-156
5. H.D. Hill and C.A. Mirkin, The bio-barcode assay for the detection of protein and nucleic acid targets using DTT-induced ligand exchange, *Nat. Protocols*, 2006, 1, 1-13
6. R.A. Reynolds III, C.A. Mirkin, R.L. Letsinger, Homogeneous, nanoparticle-based quantitative colorimetric detection of oligonucleotides, *J. Am. Chem. Soc.*, 2000, 122, 3795-3796
7. J.J. Storhoff, R. Elghanian, R.C. Mucic, C.A. Mirkin, R.L. Letsinger, One-pot colorimetric differentiation of polynucleotides with single base imperfections using gold nanoparticle probes, *J. Am. Chem. Soc.*, 1998, 120, 1959-1964
8. T. Zhu, K. Vasilev, M. Kreiter, S. Mittler, W. Knoll, Surface modification of citrate-reduced colloidal gold nanoparticles with 2-mercaptosuccinic acid, *Langmuir*, 2003, 19, 9518-9525
9. C.S. Weisbecker, M.V. Merritt, G.M. Whitesides, Molecular self-assembly of aliphatic thiols on gold colloids, *Langmuir*, 1996, 12, 3763-3772
10. K. Aslan and V.H. Perez-Luna, Surface modification of colloidal gold by chemisorption of alkanethiols in the presence of a nonionic surfactant, *Langmuir*, 2002, 18, 6059-6065
11. R.R. Bhattacharjee, T.K. Mandal, Polymer-mediated chain-like self-assembly of functionalized gold nanoparticles, *J. Coll. Int. Sci.*, 2007, 307, 288-295
12. X. Zhao, Y. Cai, T. Wang, Y. Shi, G. Jiang, Preparation of alkanethiolate-functionalized core/shell Fe₃O₄@Au nanoparticles and its interaction with several typical target molecules, *Anal. Chem.*, 2008, 80, 9091-9096

13. 35. S.M. Tsimbler, L.L. Shevchenko, V.V. Grigoreva, The IR absorption spectra of the tartrate and citrate complexes of nickel, cobalt and iron, *Zhurnal Prikladnoi Spektroskopii*, 1969, 11(3), 522-528
14. 36. C.L.Chu, P.H. Lin, Y.S. Dong, D.Y Guo, Influences of citric acid as a chelating reagent on the characteristics of nanophase hydroxyapatite powders fabricated by a sol-gel method, *J. Mater. Sci. Lett.*, 2002, 21, 1793-1795
15. J.G. Kelly, P.L. Martin-Hirsch, F.L. Martin, Discrimination of base differences in oligonucleotides using mid-infrared spectroscopy and multivariate analysis, *Anal. Chem.*, 2009, 81, 5314-5319

CHAPTER 7 – GOLD NANOPARTICLES AS BUILDING BLOCKS IN THE DEVELOPMENT OF ENZYMATIC BIOSENSORS

The activity and turnover rates of enzymes are important scientific and technological parameters and due to this, scientists have tried to combine metallic nanoparticles in general, and gold nanoparticles in particular, with different enzymes in order to develop nanoparticle – enzyme nano-bioconjugates to improve their behaviour, and at the same time monitor their enzymatic activity in real time. Some groups have developed methods to covalently conjugate enzymes like glucose oxidase [1], cytochrome *c* [2] or ribonuclease S [3] onto Au NPs, while others focused their research on the nonspecific attachment between the metal nanoparticles and different enzymes, as for example horseradish peroxidase [4,5], fungal protease [6], cytochrome *c* [7] or esterase [8].

Enzyme – Au NPs conjugates [1,9-12] have also been used as transducers in electrochemical biosensors. Unfortunately, the enzyme – metal nanoparticle bond is not always very stable, a fact that leads to the desorption of the enzyme from the surface of the nanoparticle so the system needs to be further protected. For this reason we propose coating the enzyme – metal nanoparticle composites with a biomimetically synthesized silica layer, a protective layer that offers mechanical and thermal stability [13]. The preparation of gold–silica core–shell nanoparticles has been studied by a number of groups [14-17] but the development of electrochemical biosensors based on biosilicated Au NPs – AChE complexes systems has yet to be documented.

In this work, we propose the construction of an acetylcholinesterase – gold nanoparticle – biosilica amperometric biosensor. The nanocomposite-based biosensor exploits the advantages of two different nanobiotechnologies: the Au NPs and the biomimetically synthesized silica. At first, the enzyme is immobilized onto the surface of Au NPs. Subsequently, the Au NPs – AChE nano-composites obtained are covered by poly-L-lysine (PLL) which acts as template in the formation of tetramethyl orthosilicate synthesized biosilica. The obtained enzyme doped nanocomposite material is deposited onto a Au electrode and allowed to dry. The gold nanoparticles play the important role of electron transducers from the enzyme to the electrode. In addition they act as a stabilizing platform, and together with the biosilica stabilize the acetylcholinesterase. UV-Vis and ATR-FT-IR

spectroscopy measurements were performed in order to confirm the immobilization of the enzyme onto the Au NPs' surface and the entrapment of the nano-composites into the biosilica matrix. The stabilizing effect that the Au NPs and biosilica have on the AChE is demonstrated by measuring the amperometric response of the system to the substrate acetylthiocholine chloride. The storage stability of the Au NPs – AChE – PLL – silica biosensor, in respect to the AChE and Au NPs – AChE biosensors has been studied and proved to be far more stable.

Preparation of Au NPs – AChE conjugates

The conjugation of the enzyme acetylcholinesterase to gold nanoparticles has been performed according to the well-known method of conjugating proteins to colloidal gold [18]. The colloidal gold nanoparticles' surface displays electrostatic and hydrophobic properties [18]. In order to reduce the electrostatic interactions and for the hydrophobic ones to prevail, the pH of the Au NPs stock solution should be adjusted to approx. 0.5 unit higher than the pI of the protein (pI of AChE from *E. eel* ~5.3) to be conjugated. This has been achieved by using 0.1 M HCl solution. In order to determine the concentration of AChE to be conjugated to the surface of the Au NPs, a series of dilutions of the enzyme have been realized. On top of them, Au NPs (stock solution) have been added and left to equilibrate for 10 minutes. Subsequently, NaCl is added and if there is not enough enzyme to stabilize the surface of the Au NPs, the colloids tend to aggregate and the solution colour changes from red to purple or blue. Through this method, the concentration of 80 U mL⁻¹ has been determined to be adequate for conjugation to Au NPs.

For the conjugation experiment, a 4900 µL aliquot of Au NPs is added on top of 100 µL from the AChE stock solution (80 U mL⁻¹) and allowed to react at room temperature for 10 min. Then 1% PEG is added to a final concentration of 0.04% and the solution is allowed to react for another 30 min. Finally the mixture is centrifuged at 6000 rpm for 60 min and before discarding, the clear supernatant is examined for AChE activity according to Ellman's method [19]. According to this method, only negligible AChE activity was detected, indicating that almost all enzyme was conjugated to the surface of the gold nanoparticles. The soft, red precipitate, containing the Au NPs – AChE conjugates is then re-suspended in 1.5 mL PBS containing 0.04% PEG. A small quantity of uncoated Au NPs precipitates as a hard metallic pellet.

Verification of successful conjugation by absorbance measurements

Initially, the conjugation of the enzyme onto the surface of the Au nanoparticles is verified using UV-Vis spectroscopy, and the results are presented in Figure 7.1. All gold nanoparticles solutions have been diluted with de-ionized Milli-Q water for absorbance measurements. If protein is successfully conjugated to Au NPs, a small red shift in the absorbance spectrum should be observed.

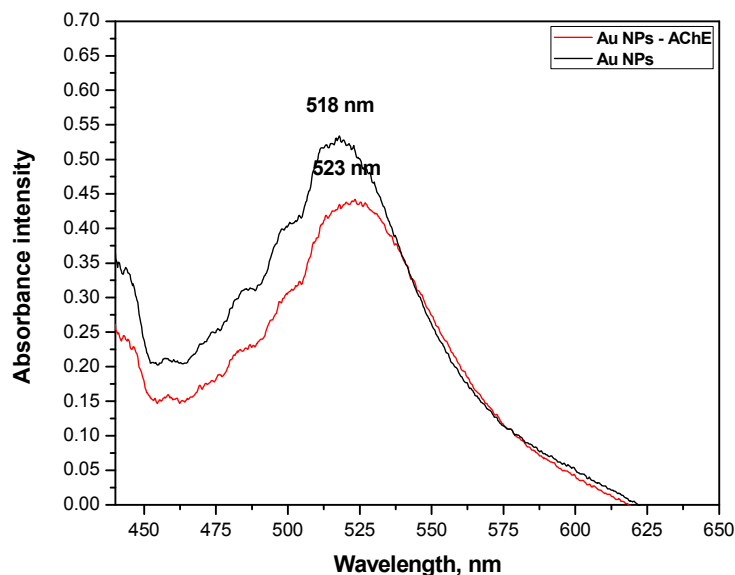


Figure 7.1. UV-vis spectra of citrate – covered Au NPs (black) and of Au NPs – AChE conjugates (red)

As we can observe, the surface plasmon band of the unmodified Au NPs covered with citrate moieties appears at 518 nm, while upon modification with the enzyme, the peak records a shift towards higher wavelengths, appearing now at 523 nm. The small decrease in the intensity of the plasmon band which accompanies the conjugation experiment is justified based on the decrease in particle concentration that occurs during the workup of the AChE modified Au NPs (present as a hard pellet after centrifugation of the conjugates).

Confirmation of successful conjugation by infrared spectrometry

The efficient conjugation of the enzyme onto the Au NPs was also verified using ATR-FT-IR spectroscopy. In order to record the ATR-FT-IR spectra, drops of the gold nanoparticles and gold nanoparticle – enzyme conjugates solutions have been placed directly onto the diamond and left overnight to dry. The spectrum of the acetylcholinesterase was

obtained using the freeze dried form of the enzyme. The spectrum of the Au – AChE conjugates was recorded and subsequently compared with the one of the citrate-covered Au NPs.

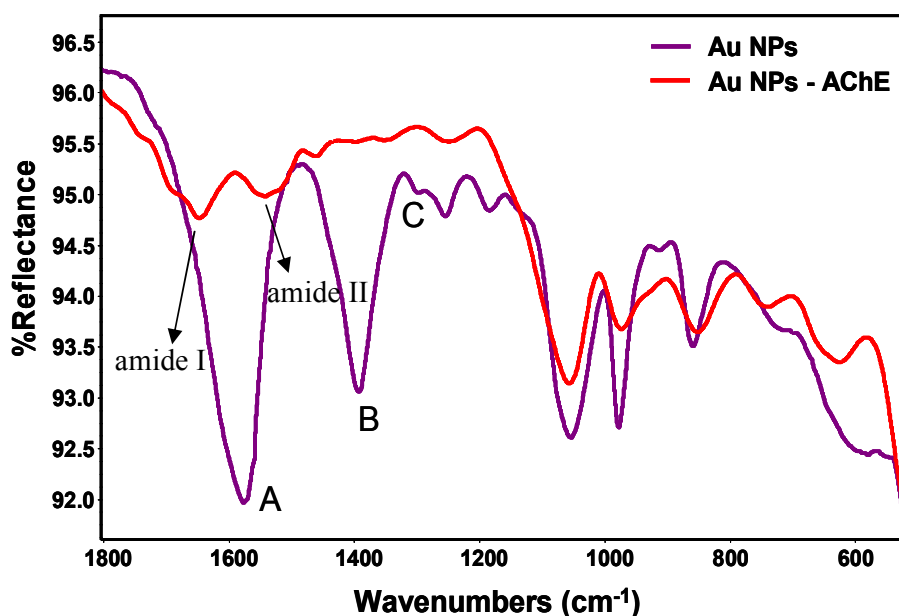


Figure 7.2. ATR-FT-IR spectra of citrate-covered Au NPs and Au NPs – AChE complexes

The most important peaks in the ATR-FT-IR spectra of citrate – covered gold nanoparticles are the vibrational citrate peaks denoted A, B and C, that appear in the region of 1300-1600 cm⁻¹ [20,21] (Figure 7.2). Upon modification of the surface of the Au NPs with the enzyme, the vibrational bands of the COO⁻ ion are no longer present. In addition, the amide I (~1640 cm⁻¹) and II (~1580 cm⁻¹) vibrations of the peptide backbone of the enzyme appear, indicating coverage of the Au NPs by the enzyme molecules.

After proving the conjugation of the AChE to the surface of gold nanoparticles, subsequent entrapment of the Au NPs – AChE bioconjugates into biomimetically synthesized silica has been performed.

Preparation of poly-L-lysine templated Au NPs – AChE – silica nanocomposites

For the bio-inspired silicification reaction, a 1.0 mM PLL solution is added to the Au NPs – AChE conjugates obtained previously, allowed to react for 30 min at room temperature and then stored for 12 hours at 4 °C. Subsequently, a freshly prepared solution of silicic acid

(obtained by hydrolyzing tetramethyl orthosilicate at a concentration of 1.0 M with 1.0 mM HCl for 30 minutes) and nanopure H₂O are added, and left to react for 3–4 h at room temperature. The final product is then subjected to four rounds of centrifugation/washing at 4800 rpm with 25.0 mM phosphate buffer, pH 7.0. The washed silica biomimetic composites were stored at 4°C in phosphate buffer for further use. Poly-L-lysine templated silica and AChE – PLL – silica nanocomposites were prepared as described in Chapter 5 by adding the corresponding amounts of phosphate buffer (for poly-L-lysine templated silica) and AChE stock solution (for AChE – PLL – silica nanocomposites) respectively [22,23], with the electrostatic interaction between the negatively charged enzyme and the positively charged poly-L-lysine template promoting the entrapment of the enzyme during biosilicification.

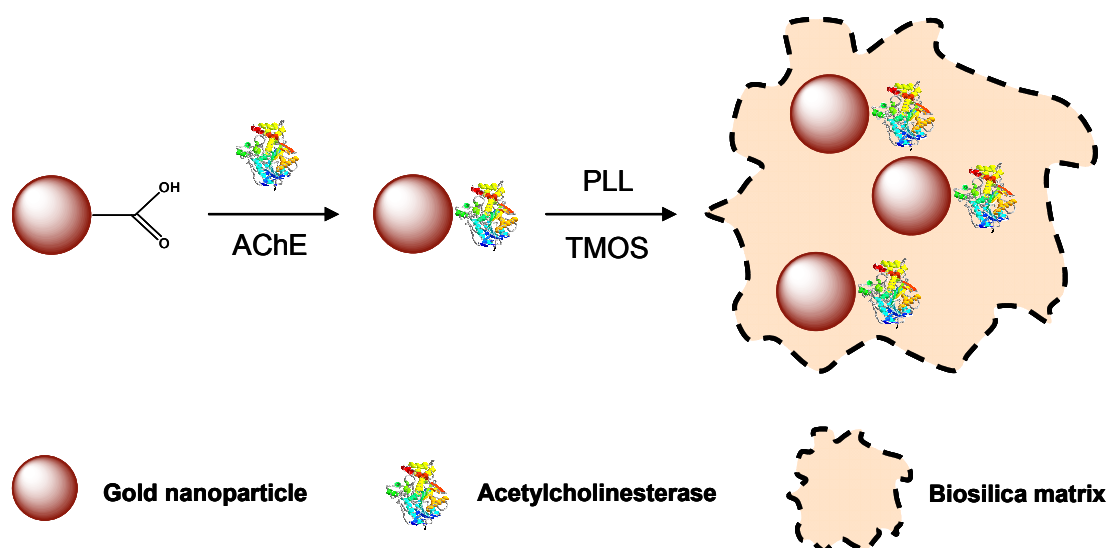


Figure 7.3. Schematic representation of the Au NPs – AChE – biosilica composites formation

Confirmation of successful biosilicification by infrared spectrometry

The success of the biosilicification experiments has been tested by ATR-FT-IR measurements. A silica shell entrapping different nanostructures [22-24] gives rise to three dominant peaks, S-A, S-B and S-C, that appear in the region 760-1300 cm⁻¹ (Figure 7.4). These peaks are attributed to the Si-O-Si asymmetrical (peak S-A) and symmetrical stretching modes (peak S-C) respectively, while peak S-B it is attributed to Si-O stretching mode either as siloxane bridge (Si-O⁻) or as silanol group (Si-OH) [25-28]. In the case of the Au NPs – AChE – silica nanocomposites, these peaks appear subsequent to biosilicification at 1042.6

cm^{-1} , 951.8 cm^{-1} and 789.5 cm^{-1} respectively, confirming the successful growth of a silica shell around the Au NPs – AChE complex.

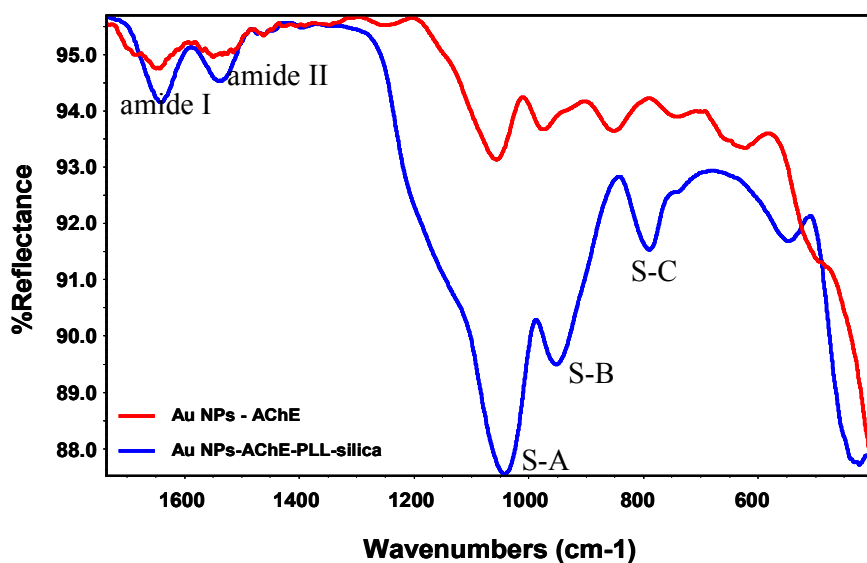


Figure 7.4. ATR-FT-IR spectra of the Au NPs – AChE complexes before and after entrapment into the biosilica matrix

The amide I and II bands of the peptides’ backbone represent the characteristic ATR-FT-IR peaks of a poly-peptide spectrum. As described earlier, they are very sensitive to any change that might appear in the secondary conformation of the peptide [29,30] and thus they are the peaks that indicate any change that takes place in the coordination sphere.

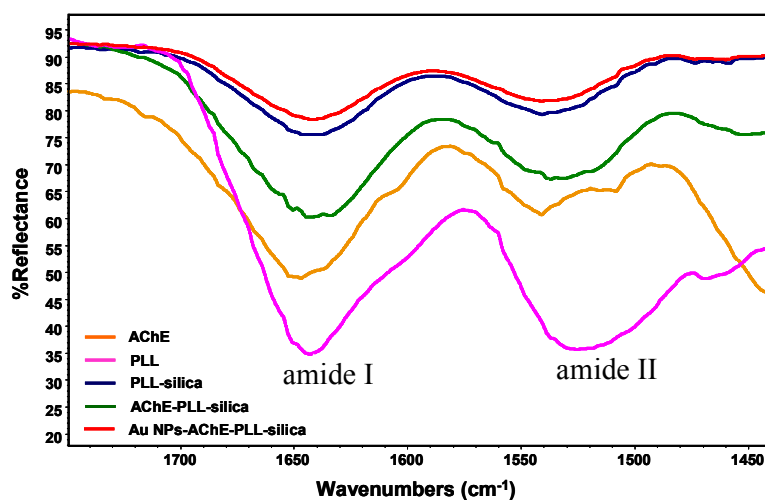


Figure 7.5. Amide I and II bands of AChE, PLL and bio-inspired silica nanocomposites (PLL - silica, AChE – PLL - silica and Au NPs – AChE – PLL - silica)

Figure 7.5 compares the ATR-FT-IR spectra of the AChE, poly-L-lysine, poly-L-lysine – silicate, AChE – poly-L-lysine – silicate and of the Au NPs – AChE – poly-L-lysine – silicate complexes. As it can be seen, the amide I band of the poly-L-lysine and AChE – poly-L-lysine intercalated in the silica network imposes a shift towards lower wavelengths as compared to their non-silicated forms. This shift is due to electrostatic or hydrophobic interactions with the silica matrix [31,32]. The largest shift towards lower wavelengths is registered by the Au NPs – AChE – PLL – silicate architecture, confirming that this protein residues - silica network interaction is the strongest.

Determination of the Au NPs – AChE – PLL - silica nanocomposite's morphology

The newly formed nanocomposites obtained by the biosilicification reaction were also characterized using HR-TEM, a micrograph being presented in Figure 7.6. The samples for HR-TEM analysis were prepared by evaporation of droplets placed on Formvar/Carbon coated TEM grids. The solvent was allowed to evaporate under atmospheric conditions. We can observe the formation of a nanoporous structure, spherically – shaped, that completely encapsulates several Au NPs – AChE conjugates. The biosilicification process offers a mild cover for the conjugates, does not produce the aggregation of the gold nanoparticles and creates a structure whose pores allow for the substrate to reach the enzyme and for the products to exit into the surrounding environment.

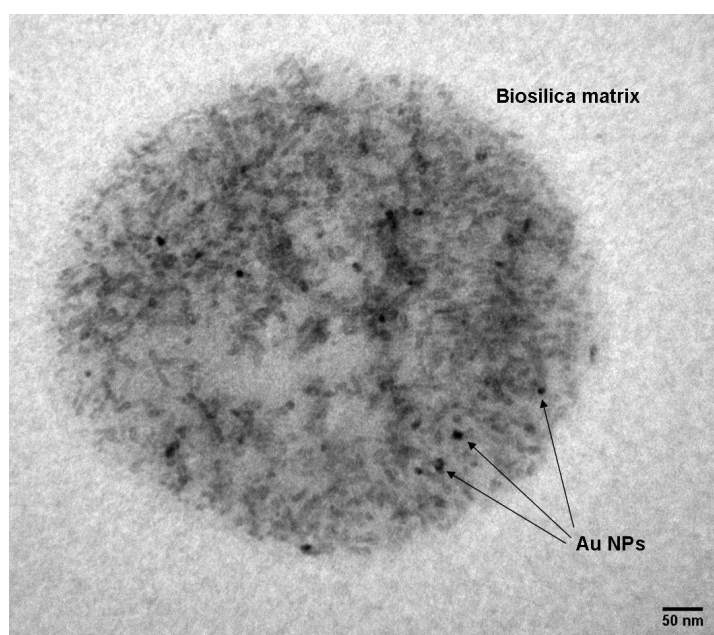


Figure 7.6. HR-TEM of the Au NPs – AChE – PLL – silica nanocomposites (bar = 50 nm)

Electrochemical assay conditions

For biosensor construction, Au NPs – AChE – PLL – silica conjugates, Au NPs – AChE conjugates and AChE solution respectively were placed onto the surface of 1 cm² polished gold electrodes and fixed with the help of a plasticized untreated regenerated cellulose membrane. The electrochemical measurements were obtained using a three-electrode cell that was completed using a silver/silver chloride double-junction reference electrode and a platinum counter electrode (surface 1 cm²). Prior to experiments, the gold electrodes were polished carefully with 1.0 and 0.05 μm alumina powder, thoroughly washed with nanopure water, and finally checked using cyclic voltammetry. All measurements were carried out in a phosphate buffer solution, 25 mM, pH 7.0, at room temperature. When not in use, the biosensors were stored in the refrigerator at 4°C.

Upon hydrolysis of the substrate acetylthiocholine by the enzyme acetylcholinesterase, thiocholine and acetic acid are produced. Thiocholine can be further oxidized on the surface of the working electrode generating a measurable signal (as shown in Figure 7.7). The influence of this signal may introduce a significant error to the measurements, and for this reason it must be carefully controlled during the evaluation of AChE-based biosensors.

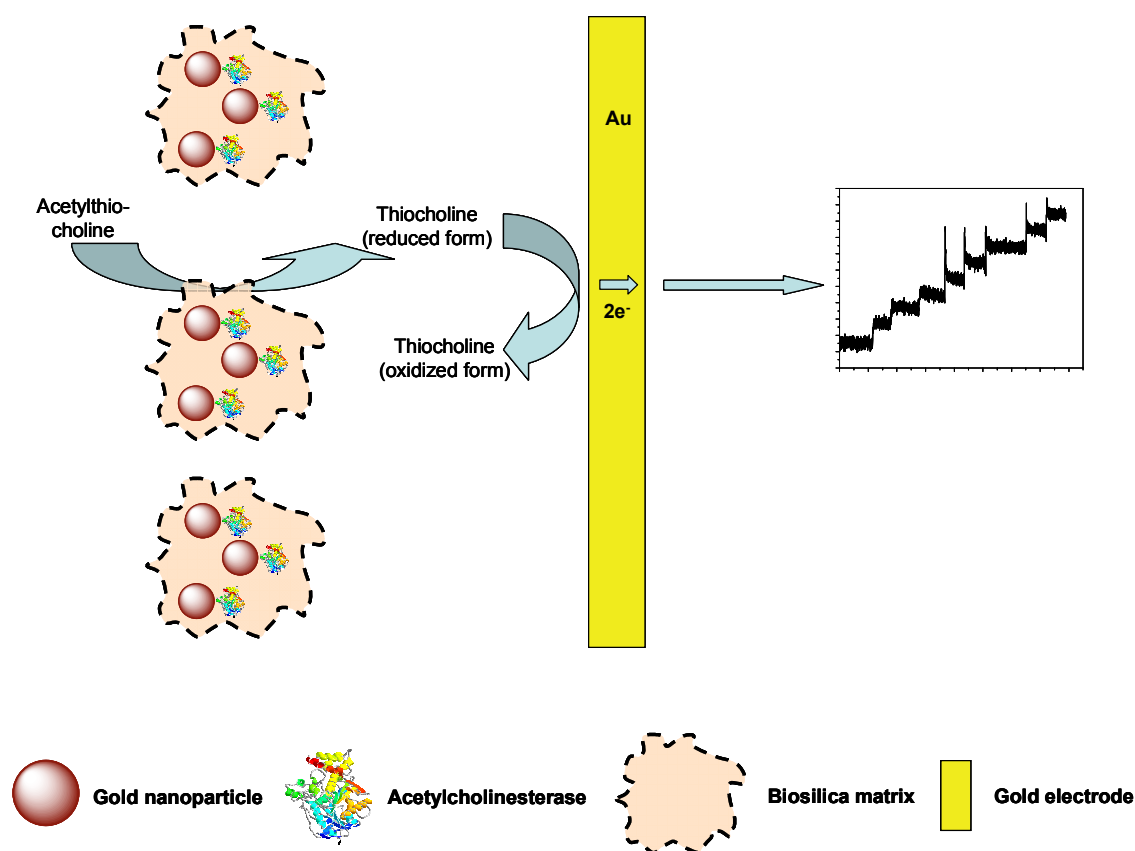


Figure 7.7. Schematic representation of the amperometric biosensor

Monitoring of the system's electrochemical response and storage stability study

The assay was performed by measuring the response of the Au NPs – AChE – PLL – silica biosensor to successive additions of the enzyme's substrate, acetylthiocholine chloride (100 mM stock solution), under continuous polarization at +300 mV.

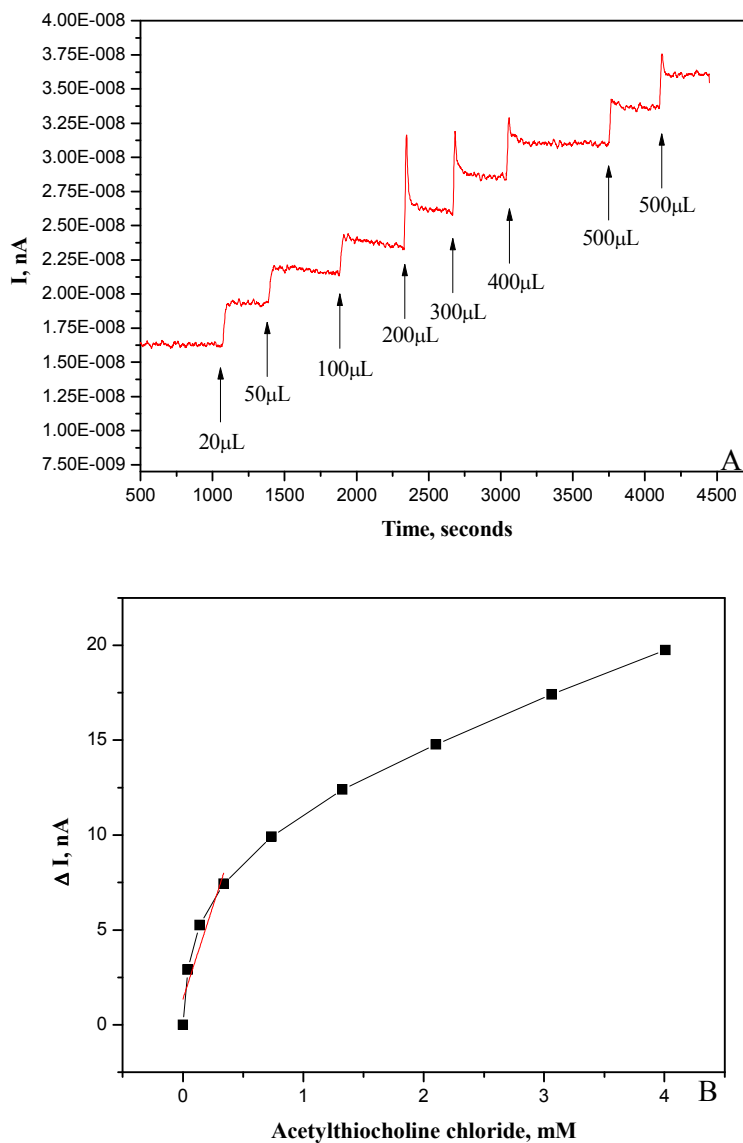


Figure 7.8. a) Amperometric response trace of the Au NPs – AChE – silica biosensor
b) Corresponding calibration curve (current vs. acetylthiocholine chloride concentration)

The successive additions of acetylthiocholine lead to an increase of the anodic current, which can be attributed to the decomposition of acetylthiocholine to thiocholine and its

further oxidation on the surface of the electrode. Through this reaction sequence, the sensitivity of the biosensor can be directly related to the enzyme activity [33].

The amperometric curve and the corresponding calibration curve of the Au NPs – AChE – PLL – silica biosensor are presented in Figure 7.8. Eight successive additions of the acetylthiocholine chloride substrate were performed, over a period of approx 60 minutes, under continuous polarization at +300 mV. The initial sensitivity of the nano-sensor was calculated to be 27.58 nA mM^{-1} and the response is linear to the concentration of the substrate in the range from 0.04 to 0.4 mM. The response time of the biosensor to the substrate was very fast, reaching the plateau in 0.5 minutes.

For comparison purposes, AChE and Au NPs – AChE biosensors have also been constructed and evaluated simultaneously. At different intervals, the calibration curves of the biosensors have been recorded. Between measurements, the biosensors were kept in phosphate buffer (25 mM, pH 7.0) at 4°C .

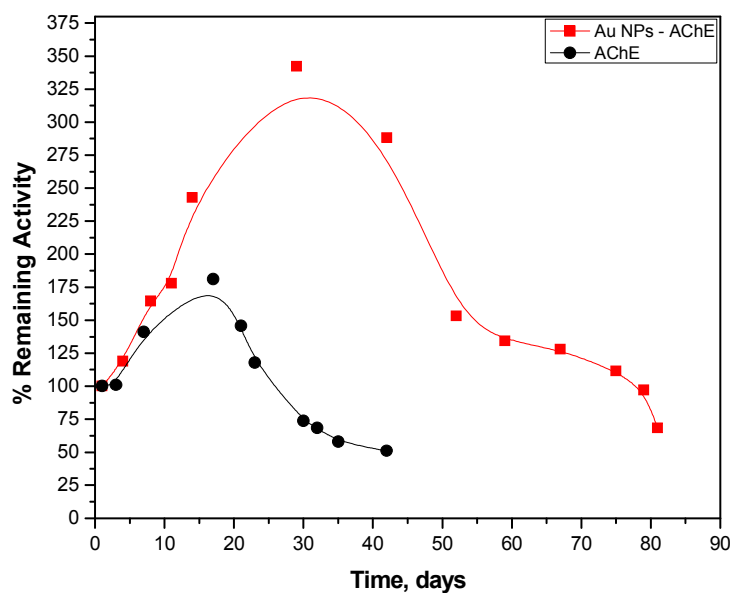


Figure 7.9. Storage stability of the Au NPs – AChE and AChE biosensors

The storage stability of all the biosensors was monitored under polarization at 25°C and +300 mV vs Ag/AgCl electrode for a period of 4 months in total. The initial increase observed in the biosensor sensitivity is a well-known phenomenon in biosensor systems, and is attributed to changes that appear in the enzyme's 3D structure inside the immobilization matrix when rehydration occurs [34].

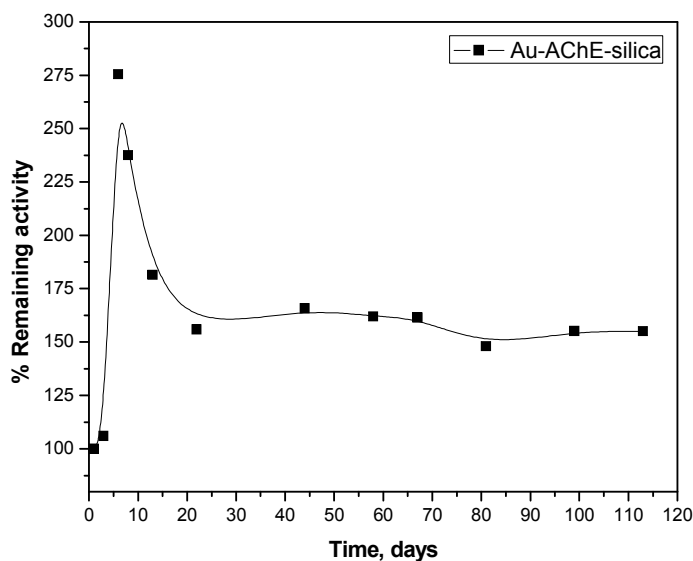


Figure 7.10. Storage stability of the Au NPs – AChE – PLL – silica biosensor

It is very interesting to observe that the Au NPs – AChE – PLL – silica biosensor provides excellent protection for the enzyme from denaturation, presenting a remaining activity of 155% after 113 days from its construction (Figure 7.9), while the Au NPs – AChE (red) and the AChE (black) biosensors showed a decrease of their activity to 50% after 85 and 42 days, respectively (Figure 7.10). The Au NPs prove that they are indeed suitable matrices for immobilization of enzymes but the combination of gold nanoparticles with biomimetically synthesized silica is shown to offer the enzyme a far more better protective environment.

Conclusions

From the data presented it can be concluded that immobilization of AChE onto gold nanoparticles and the further biosilicification of the nano-composites was found to be a very efficient method for the construction of sensitive amperometric biosensors. Both the Au NPs and the biosilica shell play the stabilizing role and constitute a protecting platform for the biomolecule, while the gold nanoparticles also provide the necessary conduction pathway as they assist the direct electron transfer between the enzyme and the surface of the electrode due to their high conductive properties. The proposed biosensor system is sensitive to very small substrate concentrations and very stable over time, since after 4 months of repeated measurements its activity was still at a very high level. It is also shown that the immobilization of the AChE onto the Au doped biosilica nano-composite provides both signal mediation and significant enzyme stabilization as compared to the existing AChE biosensors.

References

1. O. Lioubashevski, V.I. Chegel, F. Patolsky, E. Katz, I. Willner, Enzyme-catalyzed bio-pumping of electrons into Au-nanoparticles: a surface plasmon resonance and electrochemical study, *J. Am. Chem. Soc.*, 2004, 126, 7133-7143
2. M.E. Aubin-Tam and K. Hamad-Schifferli, Gold nanoparticle-cytochrome c complexes: the effect of nanoparticle ligand charge on protein structure, *Langmuir*, 2005, 21, 12080-12084
3. M.E. Aubin, D.G. Morales, K. Hamad-Schifferli, Labeling ribonuclease S with a 3 nm Au nanoparticle by two-step assembly, *Nano Lett.*, 2005, 5(3), 519-522
4. J.G. Stonehuerner, J. Zhao, J.P. O'Daly, A.L. Crumbliss, R.W. Henkens, Comparison of colloidal gold electrode fabrication methods: The preparation of a horseradish peroxidase enzyme electrode, *Biosens. Bioelectron.*, 1992, 7, 421-428
5. J. Jia, B. Wang, A. Wu, G. Cheng, Z. Li, S. Dong, A method to construct a third-generation horseradish peroxidase biosensor: self-assembling gold nanoparticles to three-dimensional sol-gel network, *Anal. Chem.*, 2002, 74, 2217-2223
6. A. Gole, C. Dash, C. Soman, S.R. Sainkar, M. Rao, M. Sastry, On the preparation, characterization, and enzymatic activity of fungal protease-gold colloid bioconjugates, *Bioconj. Chem.*, 2001, 12, 684-690
7. R.T. Tom and T. Pradeep, Interaction of azide ion with hemin and cytochrome *c* immobilized on Au and Ag nanoparticles, *Langmuir*, 2005, 21, 11896-11902
8. T.H. Ha, J.Y. Jeong, B.H. Chung, Immobilization of hexa-arginine tagged esterase onto carboxylated gold nanoparticles, *Chem. Commun.*, 2005, 31, 3959-3961
9. Y. Xiao, F. Patolsky, E. Katz, J.F. Hainfeld, I. Willner, "Plugging into enzymes": nanowiring of redox enzymes by a gold nanoparticle, *Science*, 2003, 299, 1877-1881
10. S. Zhang, N. Wang, H. Yu, Y. Niu, C. Sun, Covalent attachment of glucose oxidase to an Au electrode modified with gold nanoparticles for use as glucose biosensor, *Bioelectrochem.*, 2005, 67, 15-22
11. R.S.J. Alkasir, M. Ganesana, Y.H. Won, L. Stanciu, S. Andreescu, Enzyme functionalized nanoparticles for electrochemical biosensors: A comparative study with applications for the detection of bisphenol A, *Biosens. Bioelectron.*, 2010, 26, 43-49
12. Y. He, S. Zhang, X. Zhang, M. Baloda, A.S. Gurung, H. Xu, X. Zhang, G. Liu, Ultrasensitive nucleic acid biosensor based on enzyme-gold nanoparticle dual label and lateral flow strip biosensor, *Biosens. Bioelectron.*, 2011, 26, 2018-2024

13. J. Choma, A. Dziura, D. Jamiola, P. Nyga, M. Jaroniec, Preparation and properties of silica–gold core–shell particles, *Coll. Surf. A: Physicochem. Eng. Asp.*, 2011, 373, 167–171
14. M.M.Y. Chen, A. Katz, Synthesis and characterization of gold-silica nanoparticles incorporating a mercaptosilane core-shell interface, *Langmuir*, 2002, 18, 8566-8572
15. S. Cheng, Y. Wei, Q. Feng, K.Y. Qiu, J.B. Pang, S.A. Jansen, R. Yin, K. Ong, Facile synthesis of mesoporous gold-silica nanocomposite materials via sol-gel process with nonsurfactant templates, *Chem. Mater.*, 2003, 15, 1560-1566
16. S. Gu, J. Onishi, E. Mine, Y. Kobayashi, M. Konno, Preparation of multilayered gold–silica–polystyrene core–shell particles by seeded polymerization, *J. Coll. Int. Sci.*, 2004, 279, 284–287
17. H. Cong, R. Toftegaard, J. Arnbjerg, P.R. Ogilby, Silica-coated gold nanorods with a gold overcoat: controlling optical properties by controlling the dimensions of a gold-silica-gold layered nanoparticle, *Langmuir*, 2010, 26(6), 4188–4195
18. C. Oliver, in: L.C. Javois (Ed), *Methods in Molecular Biology*, Vol 115: Immunocytochemical Methods and Protocols, Humana Press Inc., Totowa, NJ, 1999, 331-334
19. G.L. Ellman, K.D. Courtney, V. Andres Jr., R.M. Featherstone, A new and rapid colorimetric determination of acetylcholinesterase activity, *Biochem. Pharm.*, 1961, 7, 88-95
20. S.M. Tsimbler, L.L. Shevchenko, V.V. Grigoreva, The IR absorption spectra of the tartrate and citrate complexes of nickel, cobalt and iron, *Zhurnal Prikladnoi Spektroskopii*, 1969, 11(3), 522-528
21. C.L.Chu, P.H. Lin, Y.S. Dong, D.Y Guo, Influences of citric acid as a chelating reagent on the characteristics of nanophase hydroxyapatite powders fabricated by a sol-gel method, *J. Mater. Sci. Lett.*, 2002, 21, 1793-1795
22. V. Vamvakaki, M. Hatzimarinaki, N. Chaniotakis, Biomimetically Synthesized Silica-Carbon Nanofiber Architectures for the Development of Highly Stable Electrochemical Biosensor Systems, *Anal. Chem.*, 2008, 80, 5970-5975
23. M. Hatzimarinaki, V. Vamvakaki, N. Chaniotakis, Spectro-electrochemical studies of acetylcholinesterase in carbon nanofiber-bioinspired silica nanocomposites for biosensor development, *J. Mater. Chem.*, 2009, 19, 428–433
24. R. Buiculescu, M. Hatzimarinaki, N. Chaniotakis, Biosilicated CdSe/ZnS quantum dots as photoluminescent transducers for acetylcholinesterase-based biosensors, *Anal. Bioanal. Chem.*, 2010, 398, 3015–3021

25. R.M. Almeida, T.A. Guiton, C.G. Pantano, Characterization of silica gels by infrared reflection spectroscopy, *J. Non-Cryst. Sol.*, 1990, 121, 193–197
26. C.C. Perry, X. Li, D.N. Waters, Structural studies of gel phases-IV. An infrared reflectance and Fourier transform Raman study of silica and silica/titania gel glasses, *Spectrochim. Acta*, 1991, 47A, 1487–1494
27. P. Innocenzi, Infrared spectroscopy of sol–gel derived silica-based films: a spectromicrostructure overview, *J. Non-Cryst. Sol.*, 2003, 316, 309–319
28. A. Fidalgo, R. Cirimanna, L.M. Ilharco, M. Pagliaro, Role of the alkyl-alkoxide precursor on the structure and catalytic properties of hybrid sol-gel catalysts, *Chem. Mater.*, 2005, 17, 6686–6694
29. S. Krimm and J. Bandekar, Vibrational spectroscopy and conformation of peptides, polypeptides and proteins, *Adv. Prot. Chem.*, 1986, 38, 181–364
30. J. Bandekar, Amide modes and protein conformation, *Biochim. Biophys. Acta*, 1992, 1120, 123–143
31. S. Sotiropoulou and N.A. Chaniotakis, Tuning the sol–gel microenvironment for acetylcholinesterase encapsulation, *Biomater.*, 2005, 26, 6771–6779
32. S. Wu, H. Ju, Y. Liu, Conductive mesocellular silica–carbon nanocomposite foams for immobilization, direct electrochemistry, and biosensing of proteins, *Adv. Func. Mater.*, 2007, 17, 585–592
33. J.J. Rippeth, T.D. Gibson, J.P. Hart, I.C. Hartley, G. Nelson, Flow-injection detector incorporating a screen-printed disposable amperometric biosensor for monitoring organophosphate pesticides, *Analyst*, 1997, 122, 1425–1430
34. G.F. Khan and W. Wernet, Design of enzyme electrodes for extended use and storage life, *Anal. Chem.*, 1997, 69(14), 2682–2687

PROSPECTIVE WORK

The results presented in this work confirm the fact that nanomaterials constitute suitable candidates for the construction of optical- and electrochemical-based biosensors and for the immobilization and stabilization of biomolecules. The biosensors used are easy to construct, present increased sensitivity, low detection limits and good storage stability offering stabilization to the biological molecule.

Nevertheless, further studies should be carried out in order to investigate all the properties and advantages that nanomaterials have to offer for the biosensors world. Further research into nanoparticle functionalization with different groups in order to obtain a wide range of functionalized nanomaterials should be undertaken. This would open the door for conjugation with numerous different biological molecules and to the development of new biosensor systems. The study of QDs conjugated to oligonucleotides, their physico-chemical properties and their response, upon hybridization, to the target will be continued in collaboration with the Microelectronics Group of FORTH Greece, a group of highly skilled physicists with background in semiconductor materials. A more detailed study on the behaviour of gold nanoparticles upon replacement of surface functional groups in order to fully understand the mechanisms that govern this process would also be interesting to perform. As far as encapsulation of nanomaterials into biosilica is concern, it is possible to improve the existing methodology in order to obtain more uniform structures that would encapsulate not more than one nanocrystal.

Of course, possible applications for nanomaterials and for nanomaterial – biomolecule conjugates are infinite, due to the large range of existing nanomaterials that can be synthesized and to the numerous advantages they offer in the sensors' field. Also, the multitude and the great structural diversity of the biomolecules existing in nature can provide us with new biosensor systems that will play an important role in the improvement of public health.

ACKNOWLEDGMENTS

The present PhD thesis was realized in the Analytical Chemistry Laboratory of the Chemistry Department, of the University of Crete.

I would like to give my thanks to my Coordinating Professor, Mr. N. Chaniotakis for his continuous support, guidance, and for the trust he offered to me from the first moment and throughout the duration of my PhD.

A special thank you I owe Mr. G. Konstantinidis for the ethical, economical and friendly support that he offered to me, without which I would have not be defending this PhD.

I would also like to thank all the members of my committee, Professors D. Ghanotakis, C. Katerinopoulos, P. Savvidis, N. Michalopoulos and K. Milios, for their valuable remarks and observations that contributed to the finalization of this PhD.

My warmest thank you and all my gratitude go to my parents that have given me their unconditioned love, trust and support throughout all these years.

I would like to thank Mrs. Mirjana Comor from the Vinca Institute of Nuclear Sciences, Belgrade, Serbia for providing the Au NPs and semiconductor QDs and Mrs. Sevasti Papadogiorgaki from the “Vassilis Galanopoulos” Electron Microscopy Laboratory and Mr. Manolis Kassotakis, for assistance with the transmission electron microscopy.

A special thank you goes to M. Fouskaki, V. Vamvakaki, N. Sofikiti, M. Hatzimarinaki, V. Stavyiannoudaki, M. Frasco and K. Perdikaki that are not only colleagues that transmitted their knowledge to me and with which I had a successful collaboration but also dear friends that always gave me their love.

Last, but not least, a warm thank you to all my friends (the ones I left home and the ones I found here) for their continuous love and support.

The present work is part of the European Commission programs NANOMYC (Contract No. 036812) and SANTS (Contract No.033254).

CURRICULUM VITAE

Studies

- Oct 2006 – present PhD student, Laboratory of Analytical Chemistry, Chemistry Department, University of Crete, under the supervision of Professor Nikos Chaniotakis,
- Thesis: “Development of optical and electrochemical biosensors based on gold metal nanoparticles and CdSe/ZnS quantum dots”
- 2004 – 2006 “Politehnica” University of Bucharest, Faculty of Industrial Chemistry
- M. Sc. in Biotechnology;
 - Thesis: “The extraction and characterization of some biologically active compounds from *Helleborus purpurascens* and the study of their effects on “*in vitro*” cell systems”
- 1999 – 2004 “Politehnica” University of Bucharest, Faculty of Industrial Chemistry
- B. Sc in Biochemical Engineering – among top 5%;
 - Thesis: “The extraction and characterization of some biological active compounds from *Equisetum arvense* and *Achillea millefolium*”
- 1995 – 1999 “Mihai Viteazul” High-School, Bucharest
- Mathematics-physics profile.

Work experience

- November 2004 – September 2006 “National Institute for Research and Development in Biological Sciences”, Bucharest
- Department of Cellular and Molecular Biology – research assistant.
- September 2003 – October 2004 “National Institute for Research and Development in Microtechnologies”, Bucharest
- Department of Biomedical and Environmental Applications - research assistant – part time
- July 2003 Practical training at “Antibiotice S.A.”, Iasi.
- July 2002 Practical training at the National Institute for Research and Development in Microbiology and Immunology “Cantacuzino”, Bucharest

Specialization courses

- January 2009 “SPM (Scanning Probe Microscopy) and AFM (Atomic Force Microscopy) applications in materials, polymers and biological samples”, Department of Chemistry, University of Crete, Iraklion, Crete, Greece
- July-August 2007 “Synthesis and Retrosynthesis in the Chemistry of Natural Products” SYNAPS, Erasmus Intensive Program, module 3 – Instrumental Analysis, Iraklion, Crete, Greece

Publications

1. “Carbon nanofiber-based nanocomposite membrane as a highly stable solid-state junction for reference electrodes, G.D. O’Neil, R. Buiculescu, S.P. Kounaves, N. Chaniotakis, accepted for publication in *Analytical Chemistry*”
2. “Gold nanoparticle – enzyme – biosilica architecture for the amperometric detection of enzymatic activity”, R. Buiculescu, N.A Chaniotakis, submitted to *Analytica Chimica Acta*
3. “Electrical behavior of multi-walled carbon nanotube network embedded in amorphous silicon nitride”, I. Stavarache, A.M. Lepadatu, V.S. Teodorescu, M.L. Ciurea, V. Iancu, M. Dragoman, G.Konstantinidis, R. Buiculescu, *Nanoscale Research Letters*, **2010**, 6(1), 88
4. “Biosilicated CdSe/ZnS Quantum Dots as Photoluminescent Transducers for Acetylcholinesterase-Based Biosensors”, R. Buiculescu, M. Hatzimarinaki, N.A. Chaniotakis, *Anal Bioanal Chem*, **2010**, 398, 3015–3021
5. “Negative differential resistance in GaN nanowire network”, M. Dragoman, G. Konstantinidis, A. Cismaru, D. Vasilache, A. Dinescu, D. Dragoman, D. Neculoiu, R. Buiculescu, G. Deligeorgis, A. P. Vajpeyi, and A. Georgakilas, *Appl. Phys. Lett.*, **2010**, 96, 053116
6. “Multiple negative resistances in trenched structures bridged with carbon nanotubes”, M. Dragoman, G. Konstantinidis, A. Kostopoulos, D. Dragoman, D. Neculoiu, R. Buiculescu, R. Plana, F. Coccetti, and H. Hartnagel, *Appl. Phys. Lett.*, **2008**, 93, 043117
7. “Evaluation of radioprotective capacity of green tea (*Camellia sinensis*) polyphenols”, O. Craciunescu, W. Buzgariu, R. Buiculescu, V. Coroiu, L. Moldovan, *Rom. Biol. Sci.*, **2005**, III(3-4), 20-27

8. “Methods of qualitative and quantitative analysis of the secondary polyphenolic metabolites”, L. Moldovan, F. Gatea, V. Alexandru, O. Craciunescu, R. Buiculescu, E. Gille, in “Experimental techniques in bioanalysis” Ed. Printech, Bucharest, **2004**, ISBN 973-718-132-8

Conference papers

1. “The optimization of oligonucleotide conjugation onto gold nanoparticles for biodetection”, R. Buiculescu, M. Čomor, N. A. Chaniotakis, Proc of International Semiconductor Conference – CAS, an IEEE event, Oct **2009**, pp 89-92, Sinaia, Romania
2. “The applications of carbon nanostructures and semiconductor materials in the development of biosensors”, M.F. Frasco, R. Buiculescu, V. Vamvakaki, N.A. Chaniotakis, Proc of International Semiconductor Conference – CAS, an IEEE event, Oct **2009**, pp 99-106, Sinaia, Romania
3. “Investigation of electrical properties of carbon nanotubes”, M.L. Ciurea, I. Stavarache, A.M. Lepadatu, V. Iancu, M. Dragoman, G. Konstantinidis, R. Buiculescu, Proc of International Semiconductor Conference – CAS, an IEEE event, Oct **2009**, pp 121-124, Sinaia, Romania
4. “RF NEMS based on carbon nanotubes and graphene”, M. Dragoman, G. Konstantinidis, D. Dragoman, D. Neculoiu, A. Cismaru, F. Coccetti, R. Plana, H. Harnagel, A. Kostopoulos, R. Buiculescu, Proc of International Semiconductor Conference – CAS, an IEEE event, Oct **2008**, pp 103-107, Sinaia, Romania
5. “Simple nanoelectromechanical systems for giga-applications”, M. Dragoman, G. Konstantinidis, D. Dragoman, D. Neculoiu, A. Cismaru, R. Plana, H. Harnagel, A. Kostopoulos, Raluca Buiculescu, MEMSWAVE **2008**, July 3-4, Fodele, Crete, Greece
6. “Antitumor activity of flavonoid like and polyphenol like active principles from *Azadirachta indica* on malignant gliomas *in vitro*”, W. Buzgariu, R. Buiculescu, F. Gatea, F. Brehar, The XXIIIth Annual Scientific Session of the National Society of Cellular Biology, June 9-12, **2005**, Sibiu, Romania
7. “Spectrophotometric and chromatographic characterization of *Helleborus purpurascens* extracts and their antitumor action”, R. Buiculescu, W. Buzgariu, F. Gatea, H. Berceanu, The XXIIIth Annual Scientific Session of the National Society of Cellular Biology, June 9-12, **2005**, Sibiu, Romania

Poster presentations

1. “Biosilicated CdSe/ZnS core/shell quantum dots as fluorescent transducers for acetylcholinesterase-based biosensors”, R. Buiculescu, Maria Hatzimarinaki, Nikos A. Chaniotakis, BIOSENSORS 2010, 20th Anniversary World Congress on Biosensors, May 26-28, **2010**, Glasgow, United Kingdom
2. “Covalent immobilization of glucose oxidase on gold nanoparticles for the development of electrochemical biosensor”, R. Buiculescu, M. Comor, G. Konstantinidis, N. Chaniotakis, International Semiconductor Conference – CAS, an IEEE event, Oct **2007**, Sinaia, Romania
3. “Experimental data on cell death mode induced by deuterated water in tumor cells”, W. Buzgariu, V. Coroiu, R. Buiculescu, G. Titescu, O. Zarnescu, Balkan Scientific Conference of Biology, May 19-21, **2005**, Plovdiv, Bulgaria

Faculty scientific communications

- R. Buiculescu – “The extraction of biologically active compounds from *Helleborus purpurascens* and their effects on cells” - annual student session, “Politehnica” University of Bucharest, May **2006** – first place
- R. Buiculescu – “The extraction and characterization of some biological active compounds from *Equisetum arvense* and *Achillea millefolium*“ – annual student session, “Politehnica” University of Bucharest, May **2004** – third place
- R. Buiculescu – “The synthesis of the cage complexes and their potential role in biology” – annual student session, “Politehnica” University of Bucharest, May **2000**

Professional competences

- Scanning Electron Microscopy (SEM)
- Transmission Electron Microscopy (TEM)
- Inductively Coupled Plasma Mass Spectrometry (ICP-MS)
- RAMAN and IR Spectroscopy
- Electrochemical methods (amperometry, cyclic voltammetry)
- UV-Vis and fluorescence spectrometry
- Thin layer chromatography (TLC)

- High performance liquid chromatography (HPLC)
- Electrophoresis and zymography
- Giemsa and hematoxylin-eosin staining
- MTT-citotoxicity

Other competences

- Computer skills: Windows, MS Office
- Volunteer in the technical team at the International Conference “Micromechanics Europe” (MME 2002), Sinaia – Romania, October, 2002 and at the International Semiconductor Conference, CAS 2005, Sinaia, Romania
- Participant in the organization of two International Conferences (International Semiconductor Conference, CAS 2003, Sinaia, Romania and International Semiconductor Conference, CAS 2004, Sinaia, Romania) and two International Workshops (“European networking in micro- and nanotechnologies as bridge between West and East”, 28-29 September, 2003, Sinaia, Romania, and “1st NanoForum Workshop: Nanomaterials and Applications”, 5-7 October, 2003, Sinaia, Romania)

Foreign languages

- English: fluent
- Greek: good
- French: fair
- German: basic knowledge